VOL. 711 NO. 2 22 SEPTEMBER 1995
THIS ISSUE COMPLETES VOL. 711

JOURNAL OF CHROMATOGRAPHY A
INCLUDING ELECTROPHORESIS AND OTHER SEPARATION METHODS

ELSEVIER

JOURNAL OF CHROMATOGRAPHY A

INCLUDING ELECTROPHORESIS AND OTHER SEPARATION METHODS

Scope. The *Journal of Chromatography A* publishes papers on all aspects of **chromatography, electrophoresis** and related methods. Contributions consist mainly of research papers dealing with chromatographic theory, instrumental developments and their applications. In the *Symposium volumes*, which are under separate editorship, proceedings of symposia on chromatography, electrophoresis and related methods are published. *Journal of Chromatography B: Biomedical Applications* —This journal, which is under separate editorship, deals with the following aspects: developments in and applications of chromatographic and electrophoretic techniques related to clinical diagnosis or alterations during medical treatment; screening and profiling of body fluids or tissues related to the analysis of active substances and to metabolic disorders; drug level monitoring and pharmacokinetic studies; clinical toxicology; forensic medicine; veterinary medicine; occupational medicine; results from basic medical research with direct consequences in clinical practice.

Submission of Papers. The preferred medium of submission is on disk with accompanying manuscript (see *Electronic manuscripts* in the Instructions to Authors, which can be obtained from the publisher, Elsevier Science B.V., P.O. Box 330, 1000 AH Amsterdam, Netherlands). Manuscripts (in English; *four* copies are required) should be submitted to: Editorial Office of *Journal of Chromatography A*, P.O. Box 681, 1000 AR Amsterdam, Netherlands, Telefax (+31-20) 485 2304, or to: The Editor of *Journal of Chromatography B: Biomedical Applications*, P.O. Box 681, 1000 AR Amsterdam, Netherlands. Review articles are invited or proposed in writing to the Editors who welcome suggestions for subjects. An outline of the proposed review should first be forwarded to the Editors for preliminary discussion prior to preparation. Submission of an article is understood to imply that the article is original and unpublished and is not being considered for publication elsewhere. For copyright regulations, see below.

Publication information. *Journal of Chromatography A* (ISSN 0021-9673): for 1995 Vols. 683–714 are scheduled for publication. *Journal of Chromatography B: Biomedical Applications* (ISSN 0378-4347): for 1995 Vols. 663–674 are scheduled for publication. Subscription prices for *Journal of Chromatography A*, *Journal of Chromatography B: Biomedical Applications* or a combined subscription are available upon request from the publisher. Subscriptions are accepted on a prepaid basis only and are entered on a calendar year basis. Issues are sent by surface mail except to the following countries where air delivery via SAL is ensured: Argentina, Australia, Brazil, Canada, China, Hong Kong, India, Israel, Japan, Malaysia, Mexico, New Zealand, Pakistan, Singapore, South Africa, South Korea, Taiwan, Thailand, USA. For all other countries airmail rates are available upon request. Claims for missing issues must be made within six months of our publication (mailing) date. Please address all your requests regarding orders and subscription queries to: Elsevier Science B.V., Journal Department, P.O. Box 211, 1000 AE Amsterdam, Netherlands. Tel.: (+31-20) 485 3642; Fax: (+31-20) 485 3598. Customers in the USA and Canada wishing information on this and other Elsevier journals, please contact Journal Information Center, Elsevier Science Inc., 655 Avenue of the Americas, New York, NY 10010, USA, Tel. (+1-212) 633 3750, Telefax (+1-212) 633 3764.

Abstracts/Contents Lists published in Analytical Abstracts, Biochemical Abstracts, Biological Abstracts, Chemical Abstracts, Chemical Titles, Chromatography Abstracts, Current Awareness in Biological Sciences (CABS), Current Contents/Life Sciences, Current Contents/Physical, Chemical & Earth Sciences, Deep-Sea Research/Part B: Oceanographic Literature Review, Excerpta Medica, Index Medicus, Mass Spectrometry Bulletin, PASCAL-CNRS, Referativnyi Zhurnal, Research Alert and Science Citation Index.

US Mailing Notice. *Journal of Chromatography A* (ISSN 0021-9673) is published weekly (total 52 issues) by Elsevier Science B.V., (Sara Burgerhartstraat 25, P.O. Box 211, 1000 AE Amsterdam, Netherlands). Annual subscription price in the USA US$ 5389.00 (US$ price valid in North, Central and South America only) including air speed delivery. Second class postage paid at Jamaica, NY 11431. **USA POSTMASTERS**: Send address changes to *Journal of Chromatography A*, Publications Expediting, Inc., 200 Meacham Avenue, Elmont, NY 11003. Airfreight and mailing in the USA by Publications Expediting.

See inside back cover for Publication Schedule, Information for Authors and information on Advertisements.

0021-9673/95/$09.50

Printed in the Netherlands

CONTENTS

(Abstracts/Contents Lists published in Analytical Abstracts, Biochemical Abstracts, Biological Abstracts, Chemical Abstracts, Chemical Titles, Chromatography Abstracts, Current Awareness in Biological Sciences (CABS), Current Contents/Life Sciences, Current Contents/Physical, Chemical & Earth Sciences, Deep-Sea Research/Part B: Oceanographic Literature Review, Excerpta Medica, Index Medicus, Mass Spectrometry Bulletin, PASCAL-CNRS, Referativnyi Zhurnal, Research Alert and Science Citation Index)

REGULAR PAPERS

Column Liquid Chromatography

Electrophoresis

(Continued overleaf)

Contents (continued)

SHORT COMMUNICATIONS

Electrophoresis

ELSEVIER

Journal of Chromatography A, 711 (1995) 235–245

JOURNAL OF CHROMATOGRAPHY A

Liquid chromatography–time-of-flight mass spectrometry with continuous-flow matrix-assisted laser desorption ionization

Davinder S. Nagra, Liang Li*

Department of Chemistry, University of Alberta, Edmonton, Alb. T6G 2G2, Canada

First received 11 April 1995; revised manuscript received 8 June 1995; accepted 9 June 1995

Abstract

Matrix-assisted laser desorption ionization (MALDI) mass spectrometry has been combined with liquid chromatography (LC) by using a continuous-flow sample inlet system. The on-line interface consists of two major components: a three-port mixing tee for post-column matrix addition and a flow probe for introducing the solution directly into a time-of-flight mass spectrometer. In the experiment, the LC effluent and the matrix solution flow into the mixing tee through two separate ports. The resulting mixture is directed to the flow probe for MALDI. Both conventional LC and microbore LC have been successfully interfaced to MALDI for on-line detection of proteins. It is demonstrated that the interface does not degrade the chromatographic performance significantly. With microbore LC, LC–MALDI can be performed with total-sample injection in the low-picomole region. An example is also given to illustrate the application of on-line LC–MALDI for peak identification in a protein mixture separation.

1. Introduction

Matrix-assisted laser desorption ionization (MALDI) mass spectrometry along with electrospray ionization has become an increasingly important method for biological macromolecule characterization. The MALDI technique has a wide applicability and is remarkably tolerant to buffers, salts, and other additives in the sample [1,2]. However, compared with electrospray, MALDI is difficult to interface to solution-based separation methods, such as liquid chromatography (LC) and capillary electrophoresis (CE), for mixture analysis [2]. While MALDI can be used for analyzing simple mixtures directly, it is still highly desirable and often required to perform sample clean-up and fractionation by chromatographic methods. There are reports of off-line combination of LC and CE with MALDI mass spectrometry [3–8]. In these techniques, the effluents are collected onto either a rotating disk or an array of collecting cups. The matrix solution is then added to the sample and MALDI can be performed in a way similar to conventional static MALDI experiments. In an attempt to introduce solutions directly into a MALDI mass spectrometer, Murray and Russell recently developed an elegant system in which an aerosol beam is formed from the protein samples and the matrix solution [9,10]. These aerosols are subsequently transferred to a time-of-flight mass spectrometer. MALDI is performed from the aerosol particle surfaces. Although the detection sensitivity is demonstrated to be about 100

* Corresponding author.

0021-9673/95/$09.50
SSDI 0021-9673(95)00658-3

nmol with a mass resolution of 5–10, samples can be continuously introduced into a TOF-MS at 1 ml/min and the technique has been recently used for LC detection [10].

We have developed a continuous-flow matrix-assisted laser desorption ionization (CF-MALDI) technique for introducing solutions directly into a conventional MALDI–TOF-MS system [11]. This technique uses a flow probe to continuously flow the sample and a liquid matrix, 3-nitrobenzyl alcohol (3-NBA), for MALDI. In this earlier work [11], a frit-type flow probe was used to deliver the sample and matrix at a flow-rate of 1–5 μl/min through a capillary tube and onto the probe surface, upon which laser desorption/ionization was carried out. Detection sensitivity of hundreds of picomoles was demonstrated. The use of 3-NBA liquid matrix was found to be very important in achieving reproducible signals under the flow conditions [11].

In this report, we describe the design of a much improved flow probe for CF-MALDI. With this new probe, CF-MALDI can be used for the detection of proteins with an injection of low picomoles of samples in flow injection experiments. Furthermore, we report the development of an interface for combining conventional as well as microbore LC to CF-MALDI for protein analysis. The interface consists of a three-port mixing tee, similar to that employed in continuous-flow fast-atom bombardment for coupling LC [12]. The effluent from the liquid chromatography system is directed to one port of the mixing tee. The second port is connected to a syringe pump which continuously feeds in the MALDI liquid matrix, 3-NBA, in a diluted solution. In this manner the LC effluent is allowed to mix with the liquid matrix. The resulting mixture flows out of the third port and through a flow probe to a TOF mass spectrometer for MALDI. One major advantage of this post-column matrix addition method is that since no matrix is added to the elution solvent, there is no need to change the LC separation process. In addition, flow-rates for LC separation and matrix introduction can be independently changed and optimized for speed and ion detection sensitivity.

2. Experimental

2.1. Probe design consideration

In MALDI, a small amount of sample in the low-picomole to femtomole range, loaded onto a solid probe, often yields a mass spectrum with a good signal-to-background ratio (static MALDI). The detection limit achieved with the MALDI technique depends on several factors, including ionization efficiency, detection efficiency, and the sample loading procedure. From a technical point of view, the major difference between static MALDI and CF-MALDI is the sample loading procedure. In both cases only a small area of the sample is subject to laser desorption, since the laser beam is normally focused onto a spot size of less than 500 μm in diameter. Thus, the question of how one loads the sample into a small, confined area on the probe becomes important in determining the overall detection limit of a MALDI system. In CF-MALDI, the sample is either injected or dissolved into a carrier solvent containing 3-nitrobenzyl alcohol, and flows continuously over the probe surface. Consequently, it is expected that the detection limit of the CF-MALDI method is affected by the size of the area of the probe surface in which the solution diffuses. Diffusion of the sample solution into a large area on the probe surface would result in a high detection limit. We note that other parameters may also play a role in determining the overall sensitivity, such as the degree of sample adsorption onto the capillary tube or to other parts of the probe with which the sample solution makes a direct contact.

In order to obtain better detection sensitivity with CF-MALDI it is thus necessary to maximize the ratio between the area of the sample being desorbed and the total area of the sample diffused on the probe. There are two major ways of achieving this goal. First, an increase in the laser beam size would allow a larger sample area to be desorbed. However, we found that an increase in the beam size above 0.5 mm in diameter does not enhance the signal-to-background ratio sig-

nificantly [11]. An alternative way to maximize the ratio is to decrease the sample probe area. This would allow the sample to flow in a more confined region on the probe surface. The new flow probe described below is geared towards this latter strategy. In addition, the stainless steel frit used in our previous design has been eliminated.

2.2. Design of the new probe

Fig. 1 shows the design of the new flow probe along with the ionization region of the time-of-flight mass spectrometer. A silica capillary tube (100 μm I.D., 360 μm O.D.) (Polymicro Technologies, Phoenix, AZ, USA) is inserted into a 1.27 cm O.D. and 0.635 cm I.D. stainless steel tube and extends from the injector to the probe tip. For electrical insulation the end section of the probe is made of vespel (~2.5 cm long, 2.8 mm O.D.). At the vespel tip a piece of kapton (2.8 mm diameter), with a small hole pierced through the center, is mounted. The use of the kapton sheet improves the flow stability, possibly due to the improvement of surface properties such as the surface flatness over the vespel material. The capillary tube is fitted to the hole in the kapton and is placed no more than 1 mm above the surface. The hole will allow the capillary to slide back and forth but it is not big enough to allow backflow of the liquid. A piece of filter paper is wrapped several times around the probe tip to absorb the excess liquid. The flow probe is inserted into the TOF mass spectrometer between the repeller and extraction plates via a custom-built solid probe lock.

2.3. Mixing tee for LC–CF-MALDI

Fig. 2 shows the schematic diagram of the 3-port mixing tee. It is constructed from a stainless steel 1.59-mm Swagelok tee. The tee is connected to the MALDI flow probe through a transfer tube. This tube is made of stainless steel and has 1.59 mm O.D. and 127 μm I.D. with both ends enlarged. The total length of the tube is 5 cm. In the experiment, the LC effluent from either a micro-LC column or a conventional LC with a sample splitter (see below) flows through a 30 μm I.D., 360 μm O.D. capillary tube to the transfer tube. In order to mix the effluent with the matrix solution, this sample capillary tube is inserted into one end of the transfer tube (500 μm I.D. and about 1 cm depth) and placed about 50–150 μm away from the recessed edge of the transfer tube (see Fig. 2). The liquid matrix solution is pumped through the space between the transfer tube (500 μm I.D.) and the sample tube (360 μm O.D.). At the other end of the transfer tube, a hole with 370 μm I.D. and a

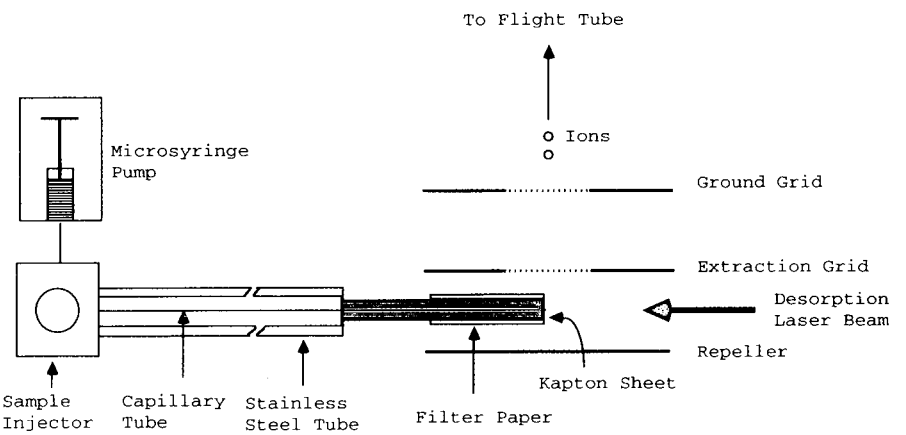

Fig. 1. Schematic of the flow probe used for continuous-flow matrix-assisted laser desorption. Drawing is not to scale. The dimensions of the major components are given in the text.

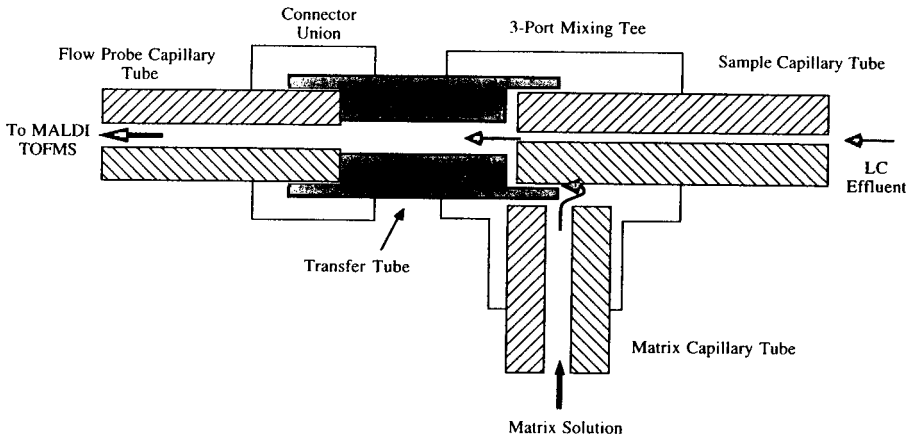

Fig. 2. Schematic of the 3-port mixing tee used for CF-MALDI with post-column matrix addition. Drawing is not to scale.

depth of 1 cm has been drilled to fit to the flow probe capillary tube (100 μm I.D. × 360 μm O.D. × 45 cm) snugly. The mixed solution then flows to the tip surface of the flow probe, at which point MALDI is carried out. Note that different tube I.D.s are used in the interface assembly. This arrangement seems to create a sufficient amount of turbulence in the transfer tube, resulting in better sample/matrix mixing and stable ion signals.

For delivering the matrix solution, a syringe pump (Harvard Apparatus, Model 11, Southnatick, MA, USA) is used. The solution consists of 15% of 0.1% trifluoroacetic acid (TFA), 45% ethylene glycol, 25% 1-propanol, and 15% 3-nitrobenzyl alcohol (all by volume). The flow-rate is generally fixed at 5 μl/min. The LC effluent or sample flow-rate is normally in the range of 1–5 μl/min.

2.4. Conventional LC with CF-MALDI

Fig. 3 shows the overall schematic of the LC system and the interface. A Shimadzu LC-600 dual pump system is used for solvent delivery. For protein separation, a Vydac 25 cm × 2.1 mm I.D. Protein and Peptide C_{18} column is used. A Rheodyne Model 7125 injection valve with a 20-μl internal loop is used for sample injection. The LC separation is carried out at a flow-rate of 0.5 ml/min. In order to achieve a sample flow-rate of 1–5 μl/min prior to matrix addition, the LC effluent is split by a tee using two Swagelok metering valves connected in parallel. This combination of a fine and coarse metering valve gives reproducible and fine flow-rate control of the LC effluent entering the mixing tee.

2.5. Micro-column LC with CF-MALDI

Fig. 4 shows the schematic of the micro-column LC/MALDI system. The LC system consists of a Shimadzu LC-600 dual pump and a home-built solvent splitter. The latter is used to obtain a flow-rate compatible for the micro-column LC separation. The solvent splitter consists of a tee connected to a parallel combination of a coarse and fine metering valve, allowing a controllable flow-rate of 1–10 μl/min for the LC separations. The micro-column (LC Packings, Fusica C_{18}, 5 cm × 320 μm I.D.) is connected directly to a Valco sample injector (60 nl) with finger tight fittings. For MALDI detection, the end of the capillary column is connected to the 3-port mixing tee through a short transfer tube, as shown in Fig. 4.

2.6. Time-of-flight mass spectrometer

A Jordan's reflectron time-of-flight mass spectrometer (R.M. Jordan co., Grass Valley, CA, USA) is used for the CF-MALDI experiments

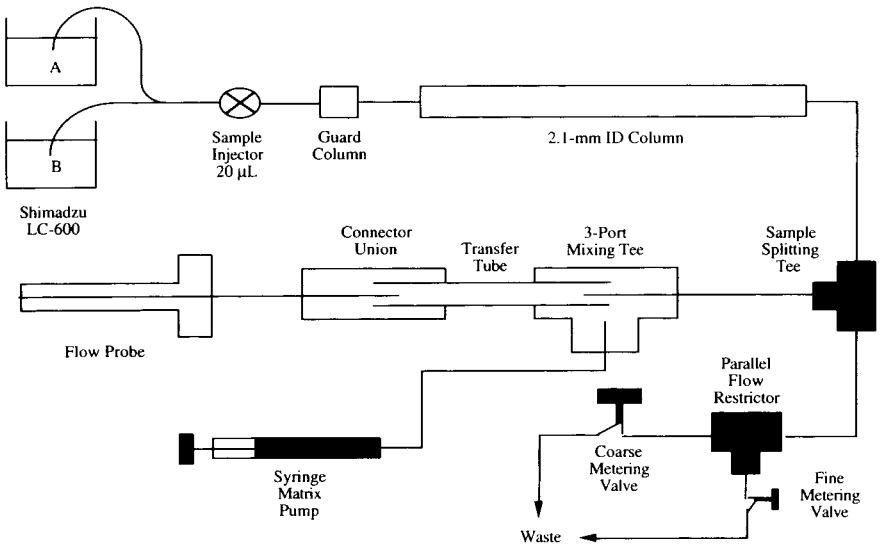

Fig. 3. Schematic of the conventional LC–MALDI system.

reported here. This angular reflectron system, designed primarily for multiphoton ionization of small molecules, has been described previously in detail [13–15]. The reflector can withstand up to 5 kV reflecting voltage. Thus, the present design of the reflector is suitable for reflecting relatively low mass ions. However, for ions with molecular masses above 5000 it is generally found that a voltage much higher than 5 kV is required to achieve good detection sensitivity. Therefore, for the CF-MALDI experiments reported here, the reflectron system is operated in a linear mode. As shown in Fig. 1, the flow probe is placed in between the repeller and the

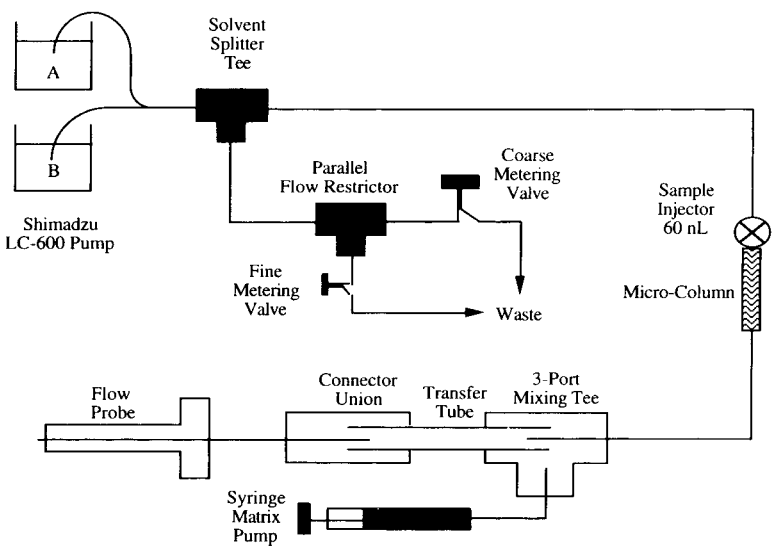

Fig. 4. Schematic of the micro-column LC–MALDI system.

extraction grid. The ions generated from the MALDI process expand in a direction orthogonal to the flight path.

The TOF mass spectrometer is mounted vertically in a six-port cross pumped by a 6-inch diffusion pump (Varian Associates, Lexington, MA, USA). The 1-m flight tube is pumped by a 4-inch diffusion pump (Varian). The pressure in the flight tube is usually below $9 \cdot 10^{-4}$ Pa during operation. A Bayard–Alpert ion gauge with Varian's multi-gauge controller is used for the pressure measurement. It is worth noting that the vacuum pressure reading can sometimes be used as an indication concerning the stability of the continuous flow. A stable flow would result in an almost constant reading or only minor fluctuations in the vacuum pressure.

2.7. Laser desorption and data processing

A frequency quadrupled Nd:YAG laser (GCR-3, Spectra-Physics, CA, USA) which generates 266 nm radiation is used for performing MALDI. The laser is operated at 10 Hz repetition rate. A convex lens (300-mm focal length) is used to focus the laser beam to a ~ 0.5 mm diameter spot on the flow probe. The spot size is estimated by examining the dark image created on a thermal-sensitive paper, which is placed on the probe using double sided tape, after the paper has been briefly exposed to the laser beam. The laser power density used varies from 10^6 to 10^7 W/cm^2. The laser power is measured with an Ophir Model 10A-MED-AN laser power/energy meter (Diamond Ophir Optics, Wilmington, MA, USA).

The mass spectrum generated by the laser desorption process is recorded with a LeCroy 9400A digital oscilloscope. The analog signal is preamplified 25 × before being fed into the oscilloscope. Data produced on the oscilloscope are then transferred in real time to a PC via General Purpose Interface Bus (GPIB). The PC is a generic 486DX33 machine with a 210-MByte hard drive and 4 MBytes of RAM. The data transfer and data analysis software is developed in-house. Details of the functions of the data system and its performance for chromatography–time-of-flight mass spectrometry have been reported elsewhere [16]. In brief, the data system is capable of transferring and storing transients up to 20k data points at a repetition rate of greater than 10 Hz from the oscilloscope to the PC via GPIB. After storing all the mass spectra in the PC, either a selected-ion or a total-ion chromatogram can be established. Both the mass spectrum and the chromatogram can be saved into a text disk file for use by other commercial software packages for further processing such as mass spectral averaging.

All samples are purchased from Sigma and Aldrich (St. Louis, MO, USA). Protein sample solutions are prepared in 0.1% aqueous TFA.

3. Results and discussion

With the new flow probe for performing CF-MALDI experiments, it is found that flow injection analysis (FIA) can be readily performed. Using the experimental setup shown in Fig. 1 for FIA without the mixing tee, protein samples can be introduced into the matrix flow with the use of a 60-nl sample injector. The microsyringe pump delivers the matrix solution through a capillary tube. This solution consists of 95% ethanol (25%), 0.1% TFA (25%), ethanediol (35%), 3-NBA (15%), and trypsinogen ($6 \cdot 10^{-6}$ M). Trypsinogen is added to the mobile phase and is continuously introduced into the probe for the purpose of optimizing the flow conditions. We note that during the initial development of CF-MALDI, the use of the standard can greatly assist the optimization of the flow conditions. During the course of the experiment, the ion signals in the molecular ion region of trypsinogen is carefully monitored to ensure that experimental conditions such as laser power are not significantly changed. Fig. 5 shows the ion profile of five repeated injections of 3 picomoles of horse heart cytochrome c (M_r 12 361) along with the ion profile from repeated injections of 9 picomoles. The ion profile is obtained by integrating the molecular-ion peak area of each mass spectrum collected and summing 10 peak areas to generate one data point in the ion profile. As

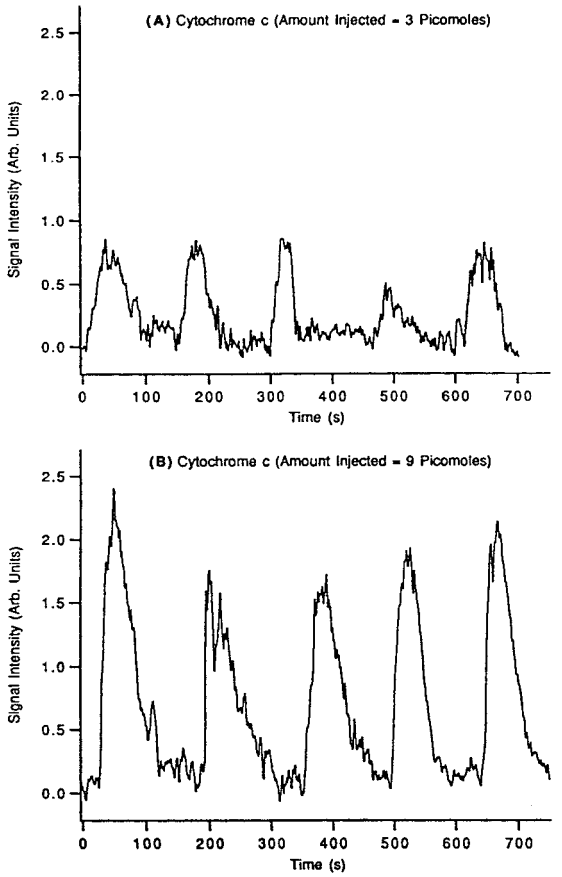

Fig. 5. Flow injection ion profiles of repeated injections of different amounts of horse heart cytochrome c: (A) 3 picomoles and (B) 9 picomoles, without the use of the mixing tee.

Fig. 5 illustrates, the peak areas are dependent on the concentration of the protein injected. We find that under the same experimental conditions (i.e., using the same laser power, same gain for the detector, etc.), a linear calibration can be obtained with the injection of cytochrome c at an amount ranging from 1 to 12 picomoles. Higher concentration requires the reduction of laser power to prevent signal saturation, in order to extend the dynamic range of the technique. This is consistent with the results reported by using static MALDI [17].

In order to examine the effect of the addition of the mixing tee on the performance of CF-

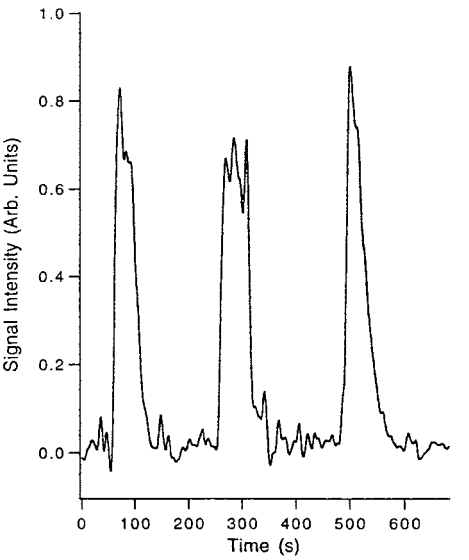

Fig. 6. Flow injection ion profiles obtained from 3 repeat injections of 10 picomoles of cytochrome c with the use of the mixing tee.

MALDI, FIA is first carried out. The experimental setup for FIA is similar to that used for micro-column LC detection as shown in Fig. 4. In FIA, the LC column is not used. Fig. 6 shows three repeat injections of 10 pmol cytochrome c. In this case, the mobile phase solvent contains 60% water and 40% acetonitrile. The peak shapes shown in Fig. 6 are almost the same as those obtained without a 3-port mixing tee as shown in Fig. 5. This indicates that the mixing tee does not introduce a significant amount of dead volume. By examining the ion signal reproducibility, it appears that the injected sample is well mixed with the matrix solution in the tee. By alternately injecting different samples, we do not observe any cross-over ion signals, indicating the absence of memory effect in the interface. It should be pointed out that the current design of the mixing tee has evolved from several earlier attempts. We find that the optimization of the tube diameters and the manner in which the matrix solution is guided to the transfer tube is critical in achieving stable and reproducible results. For example, doubling the I.D. of the

transfer tube would result in larger peak tailing in the FIA ion profile. This can be attributed to the increase of dead volume in the transfer tube.

This mixing tee is then used to combine LC separation with MALDI. In using a conventional 2.1-cm column for protein separation, the flow-rate used is relatively high, i.e., 0.5 ml/min. Since the flow probe can only accept a flow-rate of 1–10 μl/min for stable operation, the LC effluent has to be split. The experimental arrangement shown in Fig. 3 is very easy to set up and we find it to be quite convenient in combining conventional LC with MALDI. Fig. 7A shows the ion chromatogram of a simple mixture containing horse heart cytochrome c and chicken egg white lysozyme obtained by LC–MALDI. In this case, binary gradient elution is used for separation. Pump A contains 0.1% aqueous TFA, while pump B delivers acetonitrile–water (90:10) containing 0.1% TFA. A gradient was performed from an initial 40% solvent B to 65% solvent B in 5 min. From 5 to 8 min the gradient was increased to 70%, and subsequently held thereafter. A 5-nmol injection of each protein was made, with about 0.2% split to the MALDI mass spectrometer. Thus, about 10 pmol of each protein was actually used for producing the ion chromatogram shown in Fig. 7A. We note that, although the rest of the sample was split to the waste in this experiment, it should be possible to recover the sample either directly or after flowing through a UV detector in a real sample application.

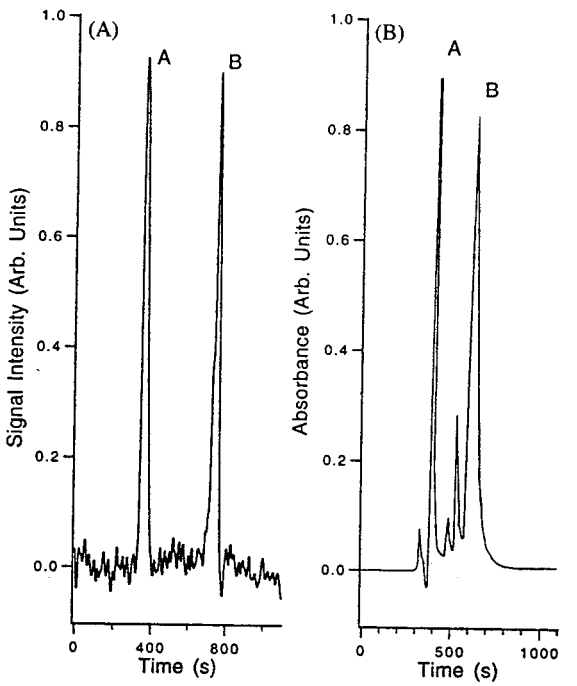

Fig. 7. (A) Ion chromatogram of LC separation of a mixture of horse heart cytochrome c and chicken egg white lysozyme by using a conventional 2.1 mm I.D. column. The total sample injected is 5 nmol each with a 0.2% sample split ratio to MS. (B) UV chromatogram (242 nm) of the same mixture.

Fig. 7A clearly shows that the two proteins are well separated. For comparison, a UV chromatogram of the same mixture obtained by using a conventional LC–UV detection system is shown in Fig. 7B. Since the UV chromatogram was not obtained on-line with the CF-MALDI results, a strict comparison cannot be made. Nevertheless, based on peak shapes and widths, the LC interface for CF-MALDI does not introduce a significant amount of peak broadening or distortion to the LC separation. Note that there are several other small peaks observed in the UV chromatogram. These peaks are not detected in LC–MALDI. They are very likely from low-molecular-mass species present in the sample ($M_r <$ 1000). Since the background signals are quite strong in CF-MALDI in the region with $m/z <$ 1000, these small ions are not resolved from the background signals.

A representative mass spectrum of cytochrome c is shown in Fig. 8. The resolution of the mass spectrum shown in Fig. 8 is 16 FWHM (full width at half maximum) for cytochrome c. With external calibration, the calculated mass for cytochrome c is 12 325. Compared with the known molecular mass of cytochrome c (12 361), the mass measurement error is about 0.29% in this case. Similar results are obtained for other proteins separated by LC. In light of the fact that the current mass spectrometric system is not fully optimized for high-resolution MALDI, these results are quite encouraging.

We also find that the resolution obtained with CF-MALDI is not degraded when compared with static MALDI in this TOF-MS instrument. Therefore, the resolution of CF-MALDI is very

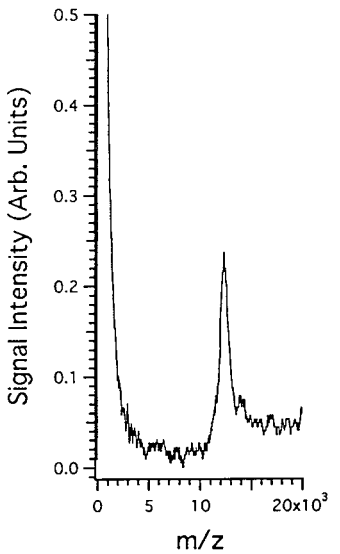

Fig. 8. Mass spectrum cytochrome c obtained at the LC peak shown in Fig. 7.

much related to the design of the mass spectrometer. One of the major reasons of observing low resolution in this TOF-MS system is related to the orientation of the sample probe with respect to the flight tube. In our experimental setup for CF-MALDI, the ions are extracted in an orthogonal configuration with constant voltages applied to the repeller and extraction grid. This configuration allows us to flow the liquid into the ionization region of the TOF without electric breakdown. However, with this configuration, even using a very small laser beam size, one would expect some ion spatial distribution, which would result in poor mass resolution. The development of high-resolution TOF-MS for CF-MALDI is currently underway. Preliminary results indicate that parallel ion extraction provides 5 to 10 times enhancement in mass resolution as well as detection sensitivity [18]. Mass resolution in the range of 100 to 250 and mass measurement error in the range of 0.02% to 0.12% have been obtained for small peptides for CF-MALDI [18]. A full account of this work will be reported in the future.

While LC separation is convenient to perform with a conventional LC system, CF-MALDI–TOF-MS requires a high sample split ratio, on the order of 500, in order to avoid overloading the mass spectrometer with excess solvent. We thus explored the possibility of using microbore-LC for separation. With slight modifications the methodology applied to the conventional column LC was also applied to the micro-column LC as shown in Fig. 4. The 3-NBA matrix solution is added to the mixing tee after the column separation, and the entire sample mixture is introduced through the flow probe and onto the probe surface. Fig. 9A shows the MALDI–TOF-MS ion chromatogram of a mixture of cytochrome c (9 pmol) and lysozyme (8 pmol) separated by micro-column LC. The separation is carried out using isocratic conditions [60% solvent A containing 0.1% TFA and 40% solvent B consisting of acetonitrile–water (90:10) containing 0.1% TFA]. Peak A in Fig. 9A is from cytochrome c and peak B from lysozyme. The chromatogram of the same mixture using a UV detector replacing the MALDI–TOF-MS is shown in Fig. 9B for comparison. To obtain the UV chromatogram a piece of capillary tubing (50

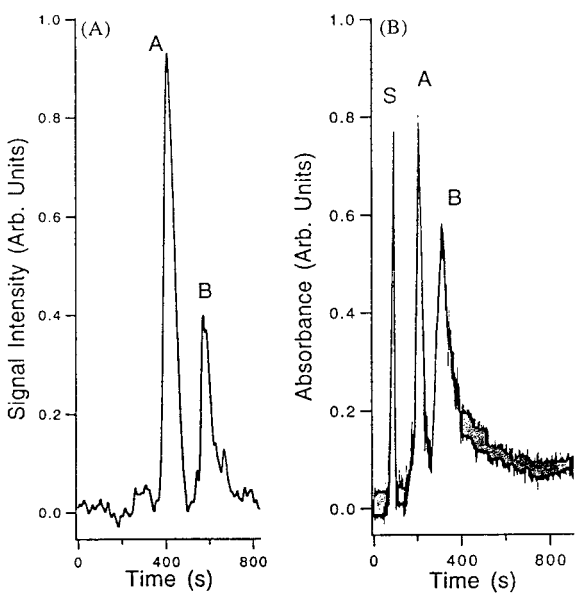

Fig. 9. (A) Ion chromatogram of LC separation of a mixture of horse heart cytochrome c and chicken egg white lysozyme by using a micro-column. The injected sample consists of 9 pmol cytochrome c and 8 pmol lysozyme. (B) UV chromatogram (214 nm) of the same mixture.

μm I.D. × 360 μm O.D. × 60 cm) was connected to the outlet of the LC capillary column, and the other end of the capillary positioned into a 214 nm UV detector (Waters Quanta 4000 capillary electrophoresis). At a point 7 cm from the capillary end a 1-cm portion of the polyimide coating was burnt away to yield a clear quartz surface. Peak S in this UV chromatogram is from the solvent and peaks A and B from cytochrome c and lysozyme, respectively. The comparison of these two chromatograms shown in Fig. 9 shows a small loss in resolution in the ion chromatogram, particularly for peak A. However, the ion chromatogram still retains good overall chromatographic integrity.

A unique application of LC–MALDI is shown in Fig. 10 for the separation of three proteins: horse heart cytochrome c, chicken egg white lysozyme, and horse heart myoglobin on a reversed-phase LC column. The separation is performed with a linear gradient (65%A/35%B to 15%A/85%B in 20 min), where eluent A is

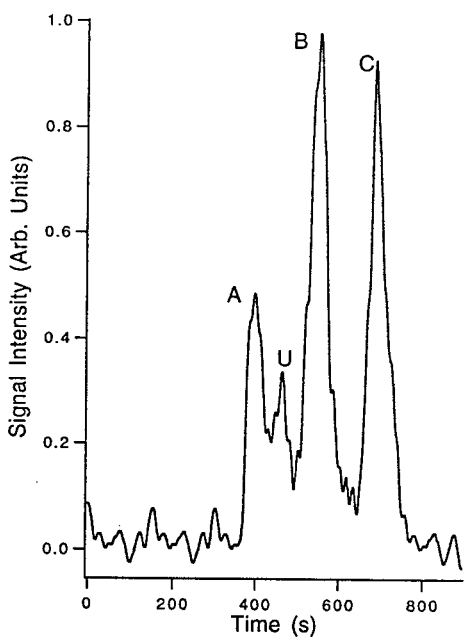

Fig. 10. Ion chromatogram of a mixture of horse heart cytochrome c, chicken egg white lysozyme, and horse heart myoglobin with conventional LC separation and MALDI–TOF-MS detection. The chromatogram represents 5 nmol injection each with 0.2% split to MS.

0.1% TFA and eluent B is 0.1% TFA in acetonitrile–H_2O (90:10). The flow-rate is 0.5 ml/min. In the ion chromatogram shown in Fig. 10, peak A is from cytochrome c, and peak B is from lysozyme and peak C is from myoglobin. Under the solution and separation conditions used here, an unexpected peak (peak U) is also observed. The mass spectra obtained during the elution of this peak are the same as those of cytochrome c. This suggests that other forms of cytochrome c have been generated during the course of sample preparation and LC separation.

The peaks A and U may belong to cytochrome c with different degrees of folding. Proteins can alter their conformational structures under non-physiological conditions, such as in acidic solutions or in a column [19]. For example, lysozyme remains folded at 20°C under the acidic condition whereas apo-cytochrome c is unfolded with differing degrees depending on the ionic strength of the protein solution [20,21]. This uncertainty can often create artifacts in the chromatographic trace with a conventional detector. Recently, it was shown that on-line UV spectroscopy using photodiode-array detector in conjunction with temperature studies can be quite useful in confirming whether any additional peaks in protein separation are due to protein itself or to impurities [19]. However, for unknown sample separation, peak identification in UV chromatography would still be difficult. On the other hand, with the use of MALDI for LC detection as illustrated in Fig. 10, the mass spectra provide an additional dimension for identification.

In conclusion, we have developed an on-line LC–MALDI system for protein analysis. We envision that the ability of separating and identifying structurally closely related species by this on-line method should be very useful in protein chemistry. We are exploring the applications of this technique for real-world biological sample analysis. In addition, the on-line technique may provide unique advantages over other LC–MS methods such as electrospray ionization MS in the area of tandem MS for peptide sequencing where MALDI can generate singularly charged species that can be dissociated via collisional-

induced dissociation (CID) to produce full sequencing information, as well as in the area of combining size-exclusion chromatography with MS for industrial polymer analysis. We plan to extend this work to a sector tandem MS instrument for high energy CID experiment with LC–CF-MALDI.

On the instrumental development of LC–MALDI, our future work will mainly concentrate on improving the mass resolution and mass measurement accuracy. To this end, we are developing a second generation time-of-flight mass spectrometric system for high-resolution CF-MALDI. This new instrument will incorporate parallel ion extraction, instead of the orthogonal configuration used in this work. In addition, we will incorporate a time-lag focusing technique for ion extraction. In a linear instrument with static MALDI, we have recently shown that mass resolution in the range of 3000 to 6000 can be obtained with time-lag focusing [22]. With this high resolution, isotopically resolved mass spectra are observed for peptides with masses up to 3000. For proteins such as cytochrome c and myoglobin, mass resolution up to 1200 can be obtained. In view of these new developments, the prospect for developing a high-performance on-line LC–CF-MALDI–TOF-MS is good. With this improved instrument, we will then compare the performance of the LC–CF-MALDI–MS technique with the well-established LC–electrospray ionization mass spectrometry for analytical applications.

Acknowledgements

We are grateful to Dr. Jean-Pierre Salzmann of LC Packings (San Francisco, CA, USA) for many helpful discussions and for loan of the capillary LC equipment. We are also grateful to Professor N.J. Dovichi of the University of Alberta for loan of the capillary LC and electrophoresis UV detector. This work was supported in part by the Natural Sciences and Engineering Research Council of Canada.

References

[1] M. Karas, D. Bachmann and F. Hillenkamp, Int. J. Mass Spectrom. Ion Proc., 78 (1987) 53.
[2] F. Hillenkamp, M. Karas, R.C. Beavis and B.T. Chait, Anal. Chem., 63 (1991) 1193A and references cited therein.
[3] C.R. Blakley, M.L. Vestal, A. Verentchikov and Y.P. Wang, in Proceedings of the 42nd ASMS Conference on Mass Spectrometry and Allied Topics, Chicago, IL, May 29–June 3, 1994, p. 1045.
[4] T. Keough, R. Takigiku, M.P. Lacey and M. Purdon, Anal. Chem., 64 (1992) 1594.
[5] J.A. Castoro, R.W. Chiu, C.A. Monnig and C.L. Wilkins, J. Am. Chem. Soc., 114 (1992) 109.
[6] P.A. van Veelen, U.R. Tjaden, J. van der Greef, A. Ingendoh and F. Hillenkamp, J. Chromatogr., 647 (1993) 367.
[7] W.M.A. Niessen, U.R. Tjaden and J. van der Greef, J. Chromatogr., 636 (1993) 3.
[8] W. Weinmann, C.E. Parker, L.J. Deterding, D.I. Papac, J. Hoyes, M. Przybylski and K.B. Tomer, J. Chromatogr. A, 680 (1994) 353.
[9] K.K. Murray and D.H. Russell, Anal. Chem., 65 (1993) 2534.
[10] K.K. Murray, T.M. Lewis, M.D. Beeson and D.H. Russell, Anal. Chem., 66 (1994) 1601.
[11] L. Li, A.P.L. Wang and L.D. Coulson, Anal. Chem., 65 (1993) 493.
[12] P. Kokkonen, W.M.A. Niessen, U.R. Tjaden and J. van Der Greef, J. Chromatogr., 474 (1989) 59.
[13] L. Li, A.M. Hogg, A.P.L. Wang, Y.Y. Zhang and D.S. Nagra, Anal. Chem., 63 (1991) 974.
[14] D.S. Nagra, J.Y. Zhang and L. Li, Anal. Chem., 63 (1991) 2188.
[15] A.P.L. Wang and L. Li, Appl. Spectrosc., 45 (1991) 969.
[16] L.D. Coulson, D.S. Nagra, X.J. Guo, R.M. Whittal and L. Li, Appl. Spectrosc., 48 (1994) 1125.
[17] R.W. Nelson, M.A. McLean and T.W. Hutchens, Anal. Chem., 66 (1994) 1408.
[18] R.W. Whittal, D.S. Nagra and L. Li, in Proceedings of the 42nd American Society for Mass Spectrometry Conference on Mass Spectrometry and Allied Topics, Chicago, IL, May 29–June 3, 1994, p. 985.
[19] S.L. Wu and B.L. Karger, in C.T. Mant and R.S. Hodges (Editors), High-Performance Liquid Chromatography of Peptides and Proteins: Separation, Analysis, and Conformation, CRC Press, Boca Raton, FL, 1991, p. 613.
[20] D.F. Nicoli and G. Benedek, Biopolymers, 15 (1976) 2421.
[21] K. Gast, G. Damaschun, H. Damaschun, R. Misselwitz, D. Zirwer and V.A. Bychkova, in S.E. Harding, D.B. Sattelle and V.A. Bloomfield (Editors), Laser Light Scattering in Biochemistry, The Royal Society of Chemistry, Cambridge, 1992, p. 209.
[22] R.M. Whittal and L. Li, Anal. Chem., 67 (1995) 1950.

ELSEVIER

Journal of Chromatography A, 711 (1995) 247–255

JOURNAL OF CHROMATOGRAPHY A

Uniform-sized polymer-based separation media prepared using vinyl methacrylate as a cross-linking agent Possible powerful adsorbent for solid-phase extraction of halogenated organic solvents in an aqueous environment

Ken Hosoya*, Yoko Kageyama, Kimihiro Yoshizako, Kazuhiro Kimata, Takeo Araki, Nobuo Tanaka

Department of Polymer Science and Engineering, Kyoto Institute of Technology, Matsugasaki, Sakyo-ku, Kyoto 606, Japan

First received 21 February 1995; revised manuscript received 19 April 1995; accepted 19 April 1995

Abstract

Uniform-sized macroporous polymer-based separation media were prepared through a typical two-step swelling method utilizing vinyl methacrylate or other ordinary cross-linking agents to investigate their properties as packing materials in HPLC. A simple and less hydrophobic cross-linking agent, vinyl methacrylate, afforded stable macroporous packing materials unexpectedly affording the largest retention volume towards hydrophobic solutes in reversed-phase liquid chromatography with good column efficiency. The retention ability towards seven halogenated organic solvents from chloroform to tetrachloroethylene was found to be much higher than that with a typical hydrophobic polymer-based packing material, poly(styrene–divinylbenzene) particles, and also a typical C_{18} silica-based hydrophobic station phase.

1. Introduction

With growing needs for the recovery and/or analyses of environmental organic pollutants such as halogenated organic solvents, various strategies to simplify the pretreatment of environmental samples have been developed [1–3]. Generally, concentration of organic pollutants from aqueous media is necessary because of the low solubility of such compounds in an aqueous phase [4,5]. Recovery of organic pollutants by reversed-phase liquid chromatography (RPLC) using solid-phase extraction has frequently been utilized for pretreatment [1,2,4,5].

From its retention properties in RPLC, a C_{18} stationary phase is one of the most effective adsorbents and various types of C_{18} packing materials are commercially available for utilization in solid-phase extractions. Hydrophobic compounds are effectively concentrated from aqueous media with a C_{18} stationary phase followed by easy recovery of the concentrated compounds by a subsequent flow of an organic solvent such as methanol [1].

Of the available adsorbents for the recovery and analysis of halogenated organic solvents such as chloroform or tetrachloroethylene, a polymer-

* Corresponding author.

0021-9673/95/$09.50
SSDI 0021-9673(95)00493-9

based packing material is more effective than a silica-based packing material [6]. Fig. 1 shows a comparison of separation selectivity towards seven common halogenated organic solvents between a typical monomeric C_{18} packing material and two ordinary polymer-based packing materials, poly(methyl methacrylate–ethylene dimethacrylate) beads (MMA–EDMA) and poly(styrene–divinylbenzene) beads (ST–DVB) [7].

Although MMA–EDMA is considered to be relatively hydrophilic packing material in RPLC, the k' values for the four trihalogenated methanes utilized (chloroform to bromoform) are larger than those with the C_{18} stationary phase. This means that MMA–EDMA affords a higher concentration ratio than the C_{18} stationary phase for the four solutes employed.

Both of the polymer-based packing materials utilized here can separate the four trihalogenated methanes, which cannot be separated with the C_{18} stationary phase, whereas the C_{18} stationary phase easily separates the four trihalogenated methanes from a trihalogenated ethane, which cannot be readily achieved with the polymer-based packing materials. Moreover, the C_{18} stationary phase can hardly separate trichloroethane and trichloroethylene, whereas ST–DVB can easily separate these two compounds, having different molecular planarities. These different separation selectivities between silica- and polymer-based packing materials are of interest for effecting different types of separations such as group separation or isomer separation. Polymer-based separation media are good for isomer separations, and we have been trying to prepare new media or adsorbents to extend their potential utility.

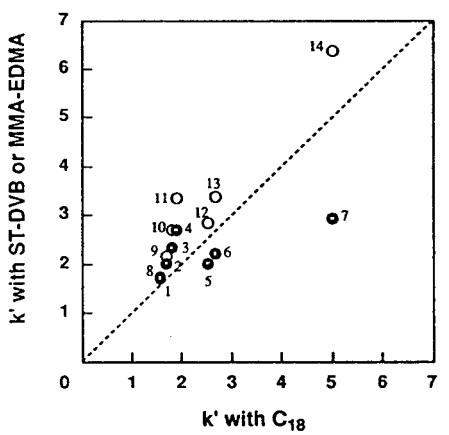

Fig. 1. Separation selectivities towards halogenated organic solvent on ordinary polymer-based packing materials compared with monomeric C_{18} packing material. Solute Nos. 1–7: ● = poly(methyl methacrylate–ethylene dimethacrylate) packing material (MMA–EDMA) versus C_{18} packing material. Solute Nos. 8–14: ○ = poly(styrene–divinylbenzene) packing material (ST–DVB) versus C_{18} packing material. Solutes: 1 = chloroform; 2 = bromodichloromethane; 3 = dibromochloromethane; 4 = bromoform; 5 = 1,1,1-trichloroethane; 6 = trichloroethylene; 7 = tetrachloroethylene; 8 = chloroform; 9 = bromodichloromethane; 10 = dibromochloromethane; 11 = bromoform; 12 = 1,1,1-trichloroethane; 13 = trichloroethylene; 14 = tetrachloroethylene. Chromatographic conditions: mobile phase, 60% aqueous acetonitrile; flow-rate, 0.8 ml/min; detection, UV at 205 nm.

Most synthetic polymer-based separation media have been prepared utilizing a few limited cross-linking agents, which would affect their chromatographic properties. As utliized for the preparation of MMA–EDMA and ST–DVB, relatively reactive ethylene dimethacrylate and divinylbenzene (Fig. 2) are alternatively utilized for the preparation of majority of synthetic hydrophobic polymer-based HPLC packing materials. Therefore, when the copolymerization reactivity between the cross-linking agents and

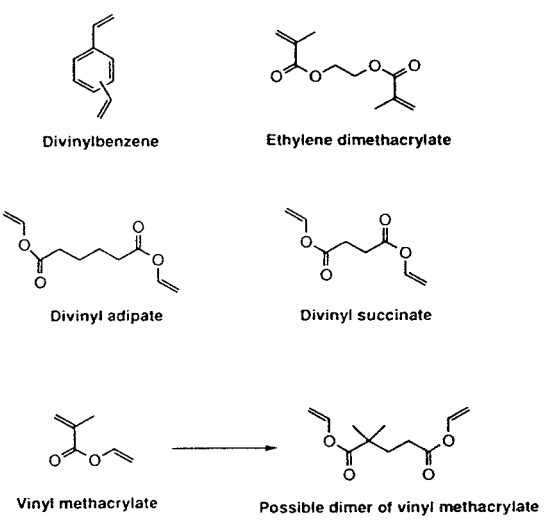

Fig. 2. Structures of cross-linking agents.

comonomers to be incorporated is not well matched, the macroporous copolymer beads obtained will become chemically and/or physically heterogeneous [8]. In severe cases, no comonomers are incorporated in the cross-linked structure owing to the badly mismatched copolymerization [9].

In order to alleviate possible mismatching of the copolymerization of reactive ethylene dimethacrylate or divinylbenzene with less reactive comonomers, we recently prepared macroporous polymer beads utilizing different types of cross-linking agents having lower polymerization reactivities [10]. Divinyl adipate (Fig. 2) was found to show interesting retention properties, but the polymer beads obtained were all unstable gel-type beads, probably owing to the flexible structure and swelling in an aqueous acetonitrile mobile phase, leading to high column pressure drops.

Although the divinyl succinate utilized previously [10] (Fig. 2) afforded stable macroporous beads, the retention properties (hydrophobicity) were not suitable for the purpose to be discussed here, because the hydrophobicity of the beads was lower than that of beads prepared utilizing ethylene dimethacrylate as the cross-linking agent.

In this work, we utilized vinyl methacrylate (Fig. 2) as a cross-linking agent, to overcome the disadvantages encountered when using divinyl adipate and divinyl succinate. Vinyl methacrylate is one of the simplest cross-linking agents, but one of the possible dimers that might be formed by the faster reaction between methacrylate groups compared with vinyl alcohol groups would have an intermediate structure between divinyl succinate and divinyl adipate, with the possibility of overcoming the disadvantages of both of those beads.

2. Experimental

2.1. Materials

Divinyl succinate and vinyl *p-tert.*-butylbenzoate were gifts from Fuso Chemical Industry (Osaka, Japan) and divinyl adipate and vinyl methacrylate were gifts from ShinEtsu Vinyl Acetate (Osaka, Japan). Ethylene dimethacrylate and methyl methacrylate were purchased from Tokyo Chemical Industry (Tokyo, Japan) and Wako (Osaka, Japan), respectively. All the monomers were purified by general distillation techniques in vacuo to remove the polymerization inhibitors. Benzoyl peroxide as a radical initiator was purchased from Nacalai Tesque (Kyoto, Japan) and utilized as received.

2.2. Two-step swelling and polymerization method

Uniformly sized polystyrene seed particles as shape templates were prepared through an emulsifier-free emulsion polymerization and purified by the previously reported method [11]. The size of the seed particle was ca. 1 μm in diameter.

The preparation of uniformly sized macroporous polymer beads by a two-step swelling and polymerization method was carried out as follows. An aqueous dispersion of the uniformly sized polystyrene seed particles (9.5×10^{-2} g/ml) (1.4 ml) was admixed with a microemulsion prepared from 0.95 ml of dibutyl phthalate as activating solvent [12], 0.085 g of benzoyl peroxide, 0.04 g of sodium dodecyl sulfate and 10 ml of distilled water by sonication. This first swelling step was carried out at room temperature while stirring at 125 rpm. Completion of the first swelling step was determined as the vanishing point of micro oil droplets in the microemulsion observed using an optical microscope.

A dispersion of 10 ml of cross-linking agent (or 8 ml of cross-linking agent and 2 ml of comonomer) and 10 ml of cyclohexanol as a parogenic solvent in 90 ml of water containing 1.92 g of poly(vinyl alcohol) (degree of polymerization = 500, saponification value = 86.5–89 mol-%) as a dispersion stabilizer was added to the dispersion of swollen particles. Swelling was carried out at room temperature for 12 h while stirring at 125 rpm.

After the second swelling step was completed, the polymerization procedure was started at 70°C under an argon atmosphere with slow stirring.

After 24 h, the dispersion of polymerized beads was poured into 250 ml of water to remove the poly(vinyl alcohol) suspension stabilizer and the supernatant was discarded after sedimentation of the beads.

The polymer beads were redispersed in methanol and the supernatant was again discarded after sedimentation. This procedure was repeated three times in methanol and twice in tetrahydrofuran (THF), then the polymer beads were filtered on a membrane filter, washed with THF and acetone and dried at room temperature to determine the chemical yields of the beads.

The prepared beads were packed into a stainless-steel column (100 mm × 4.6 mm I.D.) by a slurry technique, using aqueous acetonitrile as the slurry medium, to evaluate their chromatographic characteristics.

2.3. Chromatography

All the chromatographic solvents were purchased from Nacalai Tesque and used as received. HPLC was performed with a Jasco 880-PU Intelligent HPLC pump equipped with a Rheodyne Model 7125 valve loop injector and a Jasco UVIDEC-100-III UV detector set at 254 or 205 nm. Chromatography was carried out at 30 ± 0.5°C and a Shimadzu C-R4A recorder was utilized.

2.4. BET measurements

BET measurements on the prepared beads were carried out at Fuso Chemical Industry (Fukuchiyama, Japan).

3. Results and discussion

3.1. Physical properties of the beads

The physical data for the prepared beads are summarized in Table 1. The beads prepared through homopolymerization of each cross-linking agent were obtained in good chemical yields. As mentioned in the Introduction, the specific surface area of DVAP is severely limited by BET measurement, whereas the pore volume measured by size-exclusion chromatography (SEC) in tetrahydrofuran (THF) resembles those of EDMA and DVSA. This means that DVAP has a gel-type structure which cannot retain a porous structure under the dry conditions required for

Table 1
Properties of the prepared packing materials

Cross-linking agent	Comonomer	Abbreviation	Yield (%)	C (%)[a] (calcd.)	SA[b] (m^2/g)	Pressure[c] (MPa)	Pore volume[d] (ml/g)
Ethylene dimethacrylate	No	EDMA	99	59.48 (60.59)	376.6	2.4	0.656
Divinyl succinate	No	DVSA	98	55.68 (56.47)	204.7	2.7	0.627
Divinyl adipate	No	DVAP	95	60.07 (60.59)	4.7	4.0	0.664
Vinyl methacrylate	No	VMA	95	64.17 (64.27)	300.8	4.4	0.548
Vinyl methacrylate	Methyl methacrylate	VMA–MMA	79	63.14 (63.41)	15.9	4.4	0.540
Vinyl methacrylate	Vinyl *p-tert.*-butylbenzoate	VMA–VPTBBA	93	66.16 (66.70)	320.4	3.4	0.565

[a] Measured by elemental analyses.
[b] SA = specific surface area measured by the BET method.
[c] Pressure = column pressure drop observed in 60% aqueous acetonitrile at 0.8 ml/min. Column size: 100 mm × 4.6 mm I.D.
[d] Measured by SEC in tetrahydrofuran.

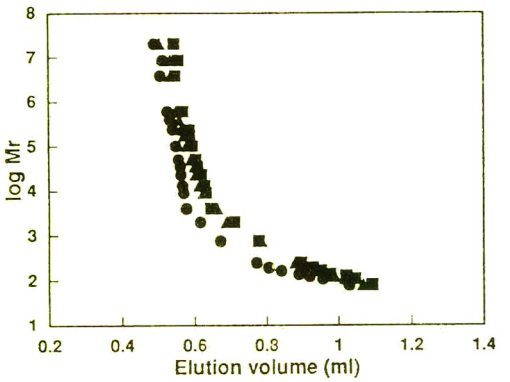

Fig. 3. Calibration graphs for the beads prepared using vinyl methacrylate as cross-linking agent. ■ = VMA; ● = VMA–MMA; ▲ = VMA–VPTBBA. Chromatographic conditions: mobile phase, tetrahydrofuran; flow-rate, 0.5 ml/min; detection, UV at 254 nm; samples, polystyrene standards and alkylbenzenes.

BET measurements. In fact, the calibration graph for DVAP in THF indicated that DVAP has only small pores, which is a typical property of gel-type beads [13].

BET measurements indicated that VMA has a large specific surface area, and a broad pore size distribution is observed from the calibration graph obtained by SEC in THF, as depicted in Fig. 3. These observations suggest that VMA has a stable porous structure, hence the preparation of macroporous beads utilizing vinyl methacrylate overcomes the problem with DVAP mentioned above.

The size monodispersity of VMA appears excellent, as demonstrated in Fig. 4. Whereas DVSA and DVAP show warped shapes (Fig. 4), owing to their relatively slow polymerization rate [14], the shape of VMA is spherical. In detail,

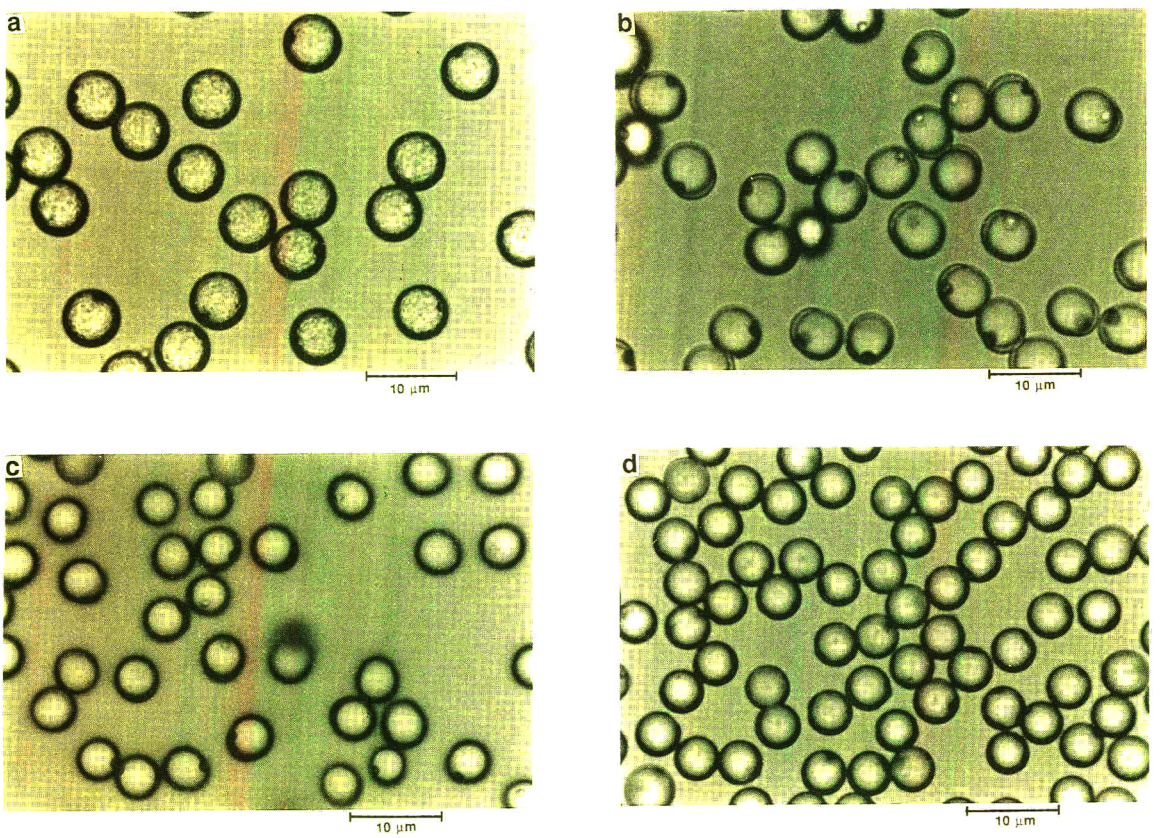

Fig. 4. Optical micrographs of the prepared beads: (a) EDMA; (b) DVSA; (c) DVAP; (d) VMA.

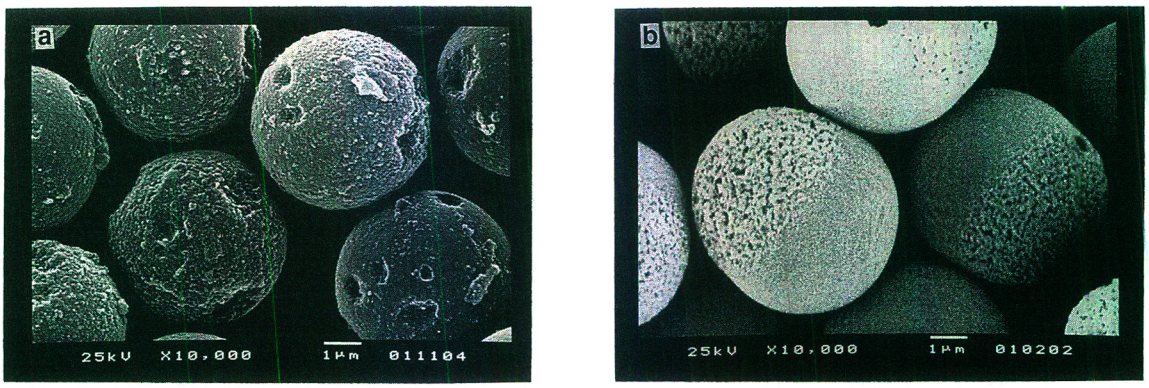

Fig. 5. Scanning electron micrographs of (a) VMA and (b) DVSA.

the scanning electron micrograph of VMA (Fig. 5) exhibits a very rough surface with a few pits and the particle size of the beads obtained is smaller (4.7 μm) than the calculated size of the final particles in the swelling process (5 μm). Moreover, Table 1 also shows that VMA is obtained with a slightly smaller pore volume than other beads. Since the chemical yield of VMA is good and the observed carbon content of VMA is comparable to the calculated value, these reductions in the particle size and pore volume mean that part of the porogenic solvent is somehow lost from the swollen particles during the polymerization step [15]. On the basis of the data obtained, the amount of the porogenic solvent left in a swollen or polymerizing particle is calculated to be 83 vol.-% of the amount introduced. This percentage is equivalent to the decrease in the particle size and the pore volume of the final beads. Although the observed decrease in particle size affords a comparatively higher column pressure drop which is similar to that of gel-type DVAP, the pressure drop was very stable, and the prepared VMA is stable enough to be utilized as a column packing material for HPLC.

Table 2
Chromatographic properties of the beads

Packing material	$k'_{monomer}$ on C_{18} [a]	$\alpha(CH_2)$ [b]	$\alpha(T/O^c)$
EDMA	3.63	1.24	1.30
DVSA	1.74	1.17	2.12
DVAP	4.47	1.23	2.26
VMA	2.75	1.32	1.30

[a] k' of each monomer on C_{18} column in 60% aqueous methanol (UV detection at 205 nm).
[b] $k'_{pentylbenzene}/k'_{butylbenzene}$ on each packing material in 60% aqueous acetonitrile.
[c] $k'_{triphenylene}/k'_{o\text{-}terphenyl}$ in 60% aqueous acetonitrile.

Copolymerization of vinyl methacrylate with methyl methacrylate affords (VMA–MMA) a lower yield with a much smaller specific surface area compared with those of VMA, while that with vinyl *p-tert.*-butylbenzoate (VMA–VPTBBA) results in a good yield with a large specific surface area (Table 1). Generally, the addition of a monovinyl comonomer decreases the specific surface area of the macroporous beads through a decrease in the volume in the small pore regions compared with those prepared by homopolymerization of a divinyl monomer cross-linking agent [13]. However, the calibration graphs measured in THF (Fig. 3) on three packing materials (VMA, VMA–MMA and VMA–VPTBBA) indicate that VMA–MMA involves more micropores, while the pore volume is just equal to that of VMA, as found in Table 1. Since the polymerization reactivity of methyl methacrylate is relatively high, this should disturb the formation of a stable cross-linked structure by vinyl methacrylate, having a relatively slow polymerization reactivity. Therefore, the large decrease in specific surface area found in VMA–MMA is due to the formation of a gel-type structure.

On the other hand, copolymerization with the less reactive comonomer vinyl *p-tert.*-butylbenzoate [9] afforded stable macroporous beads with a good yield and a large specific surface area. Since no stable macroporous beads were obtained by copolymerization of divinyl adipate and vinyl *p-tert.*-butylbenzoate or with methyl methacrylate, vinyl methacrylate increases the possible combination of copolymerizations which can afford stable macroporous beads.

3.2. Chromatographic properties of the beads

When the chromatographic separation selectivities of DVSA and DVAP are compared with those of EDMA in the RPLC mode, both DVSA and DVAP show different separation selectivities, as depicted in Fig. 6, where flat aromatic solutes (nos. 7–11) such as pyrene or triphenylene are preferably retained with DVSA and DVAP compared with alkylbenzenes (Nos. 1–6). These tendencies with DVSA and DVAP indicate relatively large α(T/O) ($k'_{\text{triphenylene}}/k'_{o\text{-terphenyl}}$) values, which is usually utilized as a parameter to show molecular recognition of the stationary phase toward flat solutes [16], compared with that with EDMA, as summarized in Table 2. The reason why these differences occur is not clear, but a different polymerization process, including cyclization, might be a possible reason for the effect on the cross-linked structures [14].

As mentioned in the Introduction, DVSA affords smaller retention volumes for the solutes used, probably owing to the lower carbon content of the monomer, which would reduce the hydrophobicity of the stationary phase in RPLC. The k' value of divinyl succinate monomer measured with a C_{18} stationary phase is the smallest for all the cross-linking agents. On the other hand, DVAP shows much larger retention volumes than EDMA. In this case, the k' value of divinyl adipate monomer is 1.2 times larger than that of ethylene dimethacrylate monomer, in spite of the identical carbon contents. This clearly means that both the hydrophobicity of the monomer and the carbon content play an important role in affecting the retention volume of the polymer beads in RPLC.

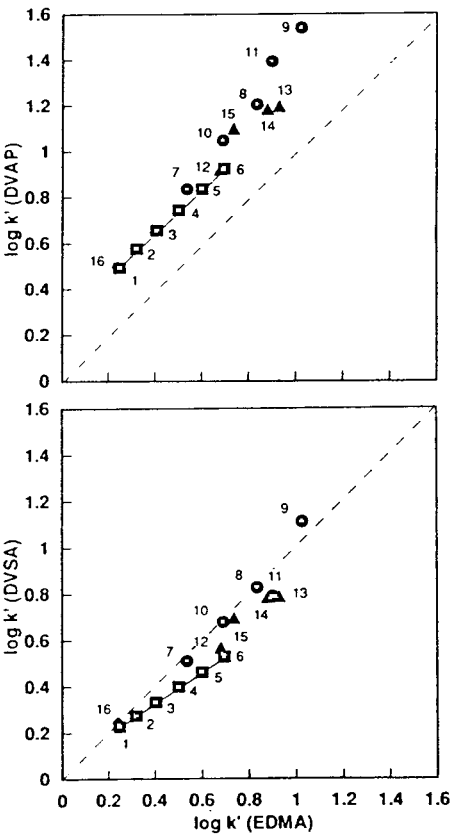

Fig. 6. Comparison of separation selectivities on polymer-based separation media. Solutes: 1 = benzene; 2 = toluene; 3 = ethylbenzene; 4 = propylbenzene; 5 = butylbenzene; 6 = pentylbenzene; 7 = naphthalene; 8 = anthracene; 9 = triphenylene; 10 = fluorene; 11 = pyrene; 12 = diphenylmethane; 13 = triphenylmethane; 14 = *o*-terphenyl; 15 = triptycene; 16 = nitrobenzene. Chromatographic conditions: mobile phase, 60% aqueous acetonitrile; flow-rate, 0.8 ml/min; detection, UV at 254 nm.

VMA shows a better column efficiency than DVSA and DVAP for the separation of alkylbenzenes in 60% aqueous acetonitrile. The chromatogram with VMA is presented in Fig. 7 [7]. The separation selectivities of VMA were compared with other polymer-based packing materials as discussed above and depicted in Fig. 8. Although vinyl methacrylate monomer has the second smallest k' on the C_{18} stationary phase

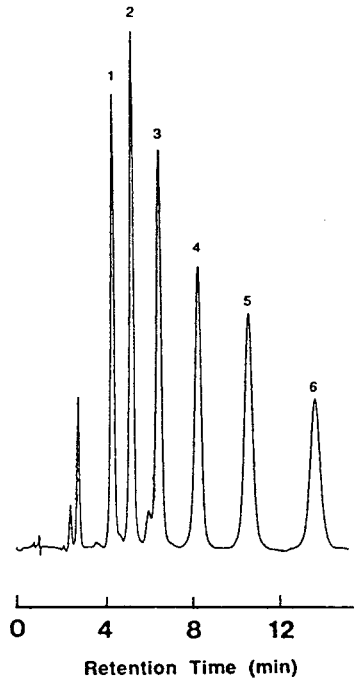

Fig. 7. Chromatogram for the separation of alkylbenzenes with VMA. Chromatographic conditions: column size, 100 mm × 4.6 mm I.D.; mobile phase, 60% aqueous acetonitrile; flow-rate, 0.8 ml/min; detection, UV at 254 nm.

(Table 2) in spite of having the highest carbon content, VMA unexpectedly affords much larger retention volumes even than DVAP, consisting of a more hydrophobic monomer. As also indicated in Table 2, the $\alpha(CH_2)$ value of VMA is the largest and the $\alpha(T/O)$ value is the smallest. This is useful because the predicted possible dimeric structure of vinyl methacrylate resembles those of divinyl succinate and divinyl adipate, but the separation selectivity observed is similar to that with EDMA.

Finally, if the capacity factors of the seven halogenated organic solvents with VMA are compared with those of common hydrophobic separation media, VMA affords a much larger retention than ST–DVB and C_{18} stationary phases, as shown in Fig. 9. This simply means that VMA will afford a much higher concentration ratio than the other stationary phases, which is one of the targets of this work. The separation selectivity of VMA is very similar to

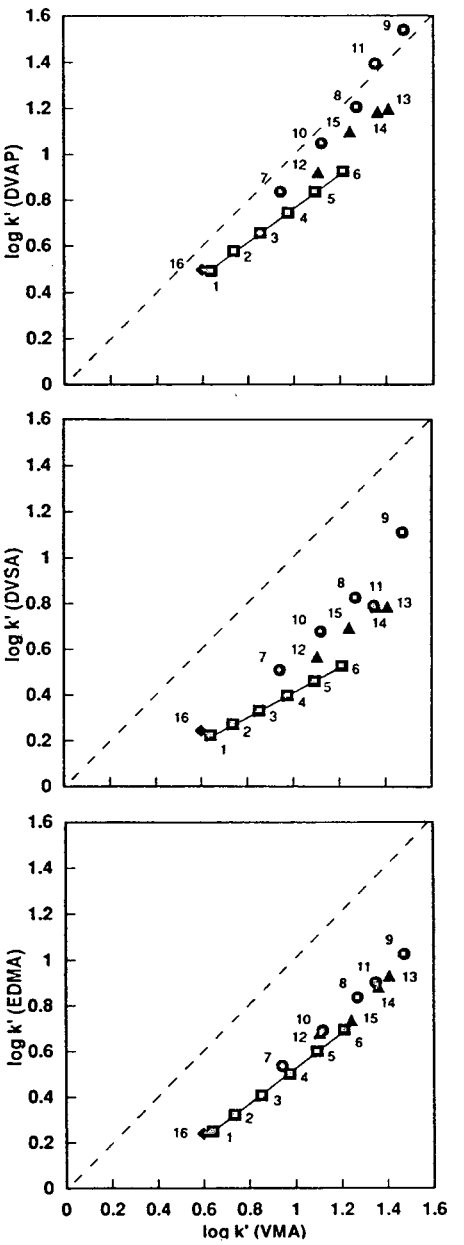

Fig. 8. Comparison of separation selectivities on polymer-based separation media. Solutes: 1 = benzene; 2 = toluene; 3 = ethylbenzene; 4 = propylbenzene; 5 = butylbenzene; 6 = pentylbenzene; 7 = naphthalene; 8 = anthracene; 9 = triphenylene; 10 = fluorene; 11 = pyrene; 12 = diphenylmethane; 13 = triphenylmethane; 14 = *o*-terphenyl; 15 = triptycene; 16 = nitrobenzene. Chromatographic conditions: mobile phase, 60% aqueous acetonitrile; flow rate, 0.8 ml/min; detection, UV at 254 nm.

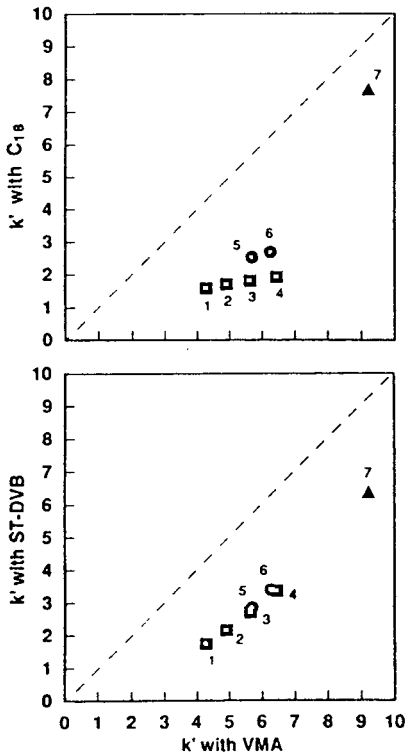

Fig. 9. Comparison of separation selectivities toward halogenated organic solvent with polymer- and silica-based packing materials. Chromatographic conditions: mobile phase, 60% aqueous acetonitrile; flow-rate, 0.8 ml/min; detection, UV at 205 nm. Solutes: 1 = chloroform; 2 = bromodichloromethane; 3 = dibromochloromethane; 4 = bromoform: 5 = 1,1,1-trichloroethane; 6 = trichlorethylene; 7 = tetrachloroethylene.

those of ST–DVB, which means that the separation selectivity of polymer-based separation media is retained. As mentioned before, EDMA rather than DVSA or DVAP shows a similar separation selectivity to VMA, and therefore the retention volume, which is one of the most important parameters of adsorbents for solid-phase extraction, can be enhanced using vinyl methacrylate.

4. Conclusion

Vinyl methacrylate afforded stable macroporous separation media with good size monodispersity. Although the monomer utilized has a simple and hydrophilic structure, the polymer beads prepared unexpectedly show a much larger retention volume than common hydrophobic separation media which have been utilized as commercial adsorbents for solid-phase extractions. So far, detailed investigations have not been completed, but the chromatographic properties obtained with VMA are of interest and useful for the preparation of a new variety of stationary phases and adsorbents.

References

[1] C. Molina, M. Honing and D. Barcelo, Anal. Chem., 66 (1994) 4444.
[2] Y. Sato, M. Sugawara, R. Watabe, M. Kikuchi, Y. Mishima, T. Kato and M. Oba, Shokuhin Eiseigaku Zasshi, 35 (1994) 390.
[3] K. Kimata, K. Hosoya, T. Araki, N. Tanaka, E.R. Barnhart, L.R. Alexander, S. Sirimanne, P.C. McClure, J. Grainger and D.G. Patterson, Jr., Anal. Chem., 65 (1993) 2502.
[4] A.J.H. Louter, F.D. Rinkema, R.T. Ghijsen and U.A.T. Brinkman, Int. J. Environ. Anal. Chem., 56 (1994) 49.
[5] J. Krupcik, I. Skacani and I. Surina, Chem. Listy 88 (1994) 528.
[6] K. Hosoya, E. Sawada, K. Kimata, T. Araki and N. Tanaka, J. Chromatogr. A, 662 (1994) 37.
[7] K. Hosoya and J.M.J. Fréchet, J. Liq. Chromatogr., 16 (1993) 353.
[8] G. Odian, Principles of Polymerization, Wiley, New York, 1991.
[9] A. Ichimura, personal communication, 1992.
[10] K. Hosoya, Y. Kageyama, K. Kimata, T. Araki, N. Tanaka and J.M.J. Fréchet, J. Polym. Sci., submitted for publication.
[11] V. Smigol, F. Svec, K. Hosoya, Q. Wang and J.M.J. Fréchet, Angew. Makromol. Chem. 195 (1992) 151.
[12] J. Ugelstad, K.H. Kaggerud, F.K. Hansen and A. Berge, Makromol. Chem., 180 (1979) 737.
[13] A. Guyot, in D.C. Sherrington and P. Hodge (Editor), Syntheses and Separations Using Functional Polymers, Wiley, New York, 1988, p. 11.
[14] K. Kikukawa, S. Nozakura and S. Murahashi, J. Polym. Sci., Part A-1, 10 (1972) 139.
[15] K. Hosoya and J.M.J. Fréchet, J. Polym. Sci., Part A, Polym. Chem., 31 (1993) 2129.
[16] K. Kimata, K. Iwaguchi, S. Onishi, K. Jinno, R. Eksteen, K. Hosoya, M. Araki and N. Tanaka, J. Chromatogr. Sci., 27 (1989) 721.

ELSEVIER

Journal of Chromatography A, 711 (1995) 257–267

JOURNAL OF CHROMATOGRAPHY A

Comparison of sorbents for the solid-phase extraction of the highly polar degradation products of atrazine (including ammeline, ammelide and cyanuric acid)

V. Pichon, L. Chen, S. Guenu, M.-C. Hennion*

Ecole Supérieure de Physique et de Chimie Industrielles, Laboratoire de Chimie Analytique (URA CNRS 437), 10 rue Vauquelin, 75231 Paris cedex 05, France

First received 20 December 1994; revised manuscript received 19 April 1995; accepted 1 May 1995

Abstract

Three different types of non-polar sorbents, i.e., C_{18} silica, apolar styrene–divinylbenzene copolymer (PRP-1) and porous graphitic carbon (PGC), were compared for the solid-phase extraction of atrazine, simazine and nine degradation products obtained by dealkylation, dehalogenation, hydroxylation or deamination mechanisms. The C_{18} silica was shown to be effective only for the first degradation products (deethyl-, deisopropyl- and hydroxyatrazine), the others being too polar. Despite a higher retention provided by PRP-1, the retention of the hydroxy-dealkylated derivatives is too low to allow the handling of a sufficiently large volume for determinations below the μg/l level. The more polar derivatives, i.e., ammeline, ammelide and cyanuric acid, are not retained by either C_{18} silica or PRP-1, whereas the capacity factor measured on a PGC column eluted with water was above 100. The conditions of extraction and elution using a cartridge packed with 500 mg of PGC are described for all the series of compounds and recoveries above 90% were obtained from 500-ml samples. The analytical separation was carried out using a C_{18} silica column and confirmation was obtained using a PGC column. Determinations of the degradation products in real samples are presented with detection limits below the 0.1 μg/l level.

1. Introduction

Chlorotriazine herbicides have been extensively used as pre- and post-emergence weed control agents on crops. The potential for contamination of waters and sediments by the widely used herbicides simazine and atrazine is high owing to their relatively high solubility, their weak adsorptivity, as measured by the partition coefficient between soil organic carbon and water, and their relatively long hydrolysis half-life in some soils. Residue levels between 0.01 and 300 μg/l in ground waters have been reported [1]. The degradation of these herbicides after their spreading depends on several factors such as hydrolysis, photolysis and microbial activity.

The main degradation products so far in ground and surface waters and in soils are dealkylated metabolites [1–7] and therefore deethyl- and deisopropylatrazine have been included in the National Pollutants Survey (NPS) list in the USA [8]. According to European Directives for drinking water, the concentration

* Corresponding author.

0021-9673/95/$09.50
SSDI 0021-9673(95)00527-7

of each pesticide and related components should be lower than 0.1 μg/l. Although it is not clear whether degradation products are included in this regulation, some European countries are now routinely monitoring these two dealkylated metabolites in drinking and ground waters. Another important pathway for atrazine degradation is its conversion to the hydroxy analogue and methods have been reported for the extraction and determination of hydroxyatrazine in soils and waters [2,9–14]. Data on the pollution of ground water with hydroxyatrazine are less numerous because many environmental laboratories employ mostly gas chromatographic (GC) techniques and hydroxyatrazine cannot be determined by GC, but by liquid chromatography (LC). Other degradation products formed by mechanisms involving further dealkylation and hydrolysis have been mentioned in the literature, but their trace-level determination in environmental waters or soils has not been reported [15–20]. One reason is that these further degradation products are more polar so that their extraction from the aqueous media is difficult and/or impossible using conventional extraction techniques.

It is of environmental interest to establish the degradation pathway directly in environmental media, which requires the corresponding analytical techniques. Atrazine is now detected in many surface waters which are used for drinking supply after further purification in treatment plants. Atrazine is oxidazable with difficulty by some classical treatments. It is therefore important that trace-level analytical methods are available for studying the transformation of atrazine during the process under real field conditions and not in laboratory conditions with concentrated pure spiked water samples.

The objectives of the investigation reported in this paper were to provide extraction procedures for the polar degradation products, i.e., for hydroxydeethylatrazine, hydroxydeisopropyl atrazine, deethyldeisopropylatrazine (2,4-diamino-6-chloro-1,3,5-triazine) ammeline (2,4-diamino-6-hydroxy-1,3,5-triazine), ammelide (2-amino-4,6-dihydroxy-1,3,5-triazine) and cyanuric acid (2,4,6-trihydroxy-1,3,5-triazine), allowing their determination in environmental waters at the 0.1 μg/l level. No methods are available for extracting these polar metabolites from water. Previous work has shown that the retention of some polar and water-soluble organic compounds in water can be very high using porous graphitic carbon (PGC), available recently as a stationary phase for LC [21,22]. The potential of extraction using C_{18} silica, the apolar styrene–divinylbenzene copolymer PRP-1 and the carbon PGC was investigated with respect to the polarity of the main transformation products, on the basis of LC data, by measuring directly or calculating the capacity factors of each solute. An application to the trace-level determination of the whole series of compounds is presented with detection limits as low as 0.1 μg/l in drinking waters.

2. Experimental

2.1. Apparatus

A Model 5060 liquid chromatograph equipped with a UV 200 variable-wavelength or a Model 9065 Polychrom diode-array detector (Varian, Palo Alto, CA, USA) was used for direct injection of standard solutions and extracts obtained with off-line preconcentration procedures. On-line preconcentration was performed using a Varian 2010 Model pump for percolation of samples. Precolumn and analytical columns were connected with two Rheodyne (Berkeley, CA, USA) valves. Quantitative measurements were provided by a CR3A integrator computer from Shimadzu or by using the software of the Polychrom detector.

2.2. Stationary phases, columns and precolumns

A commercial column packed with Hypercarb porous graphitic carbon (100 mm × 4.6 mm I.D., 7 μm particle size) from Shandon HPLC (Runcorn, UK), a column laboratory packed with PRP-1 copolymer (150 mm × 4.6 mm-I.D., 10 μm particle size) from Hamilton (Reno, NV, USA) and a commercial column packed with

Sepralyte C_{18} silica (250 mm × 4.6 mm I.D., 5 μm particle size) from Analytichem International (Harbor City, CA, USA) were used for retention measurements. The void volumes of the columns were measured by injecting a 2 *M* solution of sodium nitrate for each buffered mobile phase. The analytical separations were performed on a commercial column packed with Spherisorb ODS-2 C_{18} silica (250 mm × 4.6 mm I.D., 5 μm particle size) from Whatman (Macherey–Nagel, Düren, Germany). A Hypercarb analytical column (100 mm × 4.6 mm I.D., 7 μm) was also used for confirmation.

On-line preconcentrations were made through stainless-steel precolumns (10 mm × 4.6 mm) prepacked with 10–15-μm Hypercarb PGC, provided by Shandon HPLC. These precolumns were coupled on-line to the Hypercarb analytical column. Off-line preconcentrations were performed by packing disposable cartridges with 300–1000 mg of 40–60-μm Hypercarb PGC also provided by Shandon HPLC.

2.3. HPLC conditions

The separation of the three more polar products, ammeline, ammelide and cyanuric acid, was performed using the Spherisorb ODS-2 column, eluted with water, adjusted to pH 3 with perchloric acid, at a flow-rate of 1 ml min^{-1} and with UV detection at 205 nm. The separation of the six other degradation products plus simazine and atrazine was performed on the same analytical column at the same flow-rate with a $5 \cdot 10^{-3}$ *M* aqueous phosphate buffer (pH 7)–acetonitrile gradient. The gradient was 5% of acetonitrile from 0 to 2 min, 30% at 6 min and 80% at 25 min. Detection was carried out at 210 nm.

2.4. Chemicals

HPLC-grade acetonitrile was kindly provided by Baker France (Noisy-le-Grand, France) and methanol was purchased from Prolabo (Paris, France). LC-grade water was obtained from Baker or was prepared by purifying demineralized water in a Milli-Q filtration system (Millipore, Bedford, MA, USA). Pesticides and degradation products were supplied by Riedel-de Haën (Seelze, Germany) or by Cluzeau (Sainte-Foy-la-Grande, France), except ammelide and ammeline, which were prepared by synthesis. Their purities were higher than 98% and traces of ammeline were identified in ammelide and vice versa. Other chemicals were purchased from Prolabo, Merck (Darmstadt, Germany) or Fluka (Buchs, Switzerland).

Stock standard solutions of degradation products were prepared by weighing and dissolving them in methanol, except ammeline, ammelide and cyanuric acid, which were prepared in water owing to their higher solubility in water than in methanol. The standard solutions were stored at 4°C and used for the preparation of working standard solutions and for spiking the water samples. Their stability was controlled by LC. The final spiked water samples did not contain more than 0.5% of methanol.

2.5. Sorption and desorption procedures

Because of their differences in terms of polarity and water solubility, the degradation products were divided into two groups, one containing ammeline, ammelide and cyanuric acid and the second, all the other compounds. Before any use, the PGC cartridge was washed with 10 ml of methanol and conditioned with 10 ml of LC-grade water. For the first group, the water samples were adjusted to pH 3 and 250–500 ml were percolated through the cartridge containing 500 mg of PGC at a flow-rate of 5–10 ml/min using vacuum aspiration. The residual water was removed by air aspiration and elution was performed with 20 ml of methanol, the eluate subsequently being évaporated to dryness at 50°C under nitrogen. The residue was dissolved in 500 μl of the mobile phase used for the separation (water adjusted to pH 3 with perchloric acid) and a 100-μl aliquot was injected.

For the second group, sample volumes of 500 ml of water were percolated through a cartridge containing 300 mg of PGC. After removal of residual water, elution was achieved with a mixture of 15 ml of methanol and 15 ml of tetrahydrofuran. After evaporation of the eluate

to dryness under the same conditions as used for the first group, the residue was dissolved in 500 μl of methanol and 20 μl were injected on to the analytical column.

Previous work indicated that the breakthrough volume of cyanuric acid was ca. 50 ml using a 10 mm × 4.6 mm I.D. precolumn and that the detection limit from 50-ml samples was 3 μg/l. An on-line set-up could not be used here for direct determination at low-μg/l levels. However, on-line preconcentration was used for confirmation of cyanuric acid, in order to inject the whole extract. The precolumn was placed at the loop position of a six-port switching valve. In the load position, the PGC precolumn was washed with 10 ml of methanol and conditioned with 10 ml of LC-grade water. The raw water sample was percolated, then the precolumn was placed in front of the Hypercarb analytical column by switching the valve in the inject position and elution was effected with an aqueous mobile phase containing 30% of methanol. In order to analyse the whole extracts obtained by off-line concentration from the cartridge, the dry extracts were dissolved in 30 ml of LC-grade water and 25 ml were percolated through the precolumn and analysed on-line.

3. Results and discussion

3.1. Degradation products of atrazine

The degradation products studied in this work are listed in Table 1. The water–octanol partition coefficients, P_{oct}, which have been shown to be useful for the prediction of the extraction parameters [23], decrease with the number of dealkylation and hydroxylation, showing that the degradation products can be much more polar than the parent molecule. The last five have negative values, indicating that these compounds are more soluble in water than in octanol and cannot be extracted from water using liquid–liquid extraction techniques. In the literature, there is a great variation in log P_{oct} values depending on the authors and on the methods [24]. An average value of 2.7 was obtained for atrazine using the shake-flask method whereas values measured by HPLC were between 2.2 and 2.8. For simazine, only values calculated or obtained via HPLC have been reported and are between 1.5 and 2.3. The values in Table 1 were calculated according to the method described by Rekker [25] and from the mean value of 2.7 for atrazine. In Ref. [24], values of 1.53 and 1.51

Table 1
Substituents on the 1,3,5-triazine ring, water–octanol partition coefficients and ionization constants of atrazine, simazine and degradation products

Compound	Abbreviation	Substituents in position			Log P_{oct}	pK_a
		2-	4-	6-		
Atrazine	A	$NHCH(CH_3)_2$	NHC_2H_5	Cl	2.7[a]	1.7
Simazine	S	NHC_2H_5	NHC_2H_5	Cl	2.3	1.65
Deethylatrazine	DEA	$NHCH(CH_3)_2$	NH_2	Cl	1.6	1.3
Hydroxyatrazine	OHA	$NHCH(CH_3)_2$	NHC_2H_5	OH	1.4	4.9
Deisopropylatrazine	DIA	NH_2	NHC_2H_5	Cl	1.2	1.3
Hydroxydeethylatrazine	OHDEA	$NHCH(CH_3)_2$	NH_2	OH	0.2	4.5
Deethyldeisopropylatrazine	DAA	NH_2	NH_2	Cl	0	1.5
Hydroxydeisopropylatrazine	OHDIA	NH_2	NHC_2H_5	OH	−0.1	4.6
Cyanuric acid	ACY	OH	OH	OH	−0.2	6.9
Ammelide	ADE	NH_2	OH	OH	−0.7	1.8; 6.9; 13.5
Ammeline	ANE	NH_2	NH_2	OH	−1.2	4.5; 9.4

[a] Value from Ref. [24]; ionization constants from Ref. [16] or measured according to Ref. [13].

were calculated and measured by HPLC, respectively for deethylatrazine (1.12 and 1.15, respectively, for deisopropylatrazine), so that the agreement with the values in Table 1 is good. Another important parameter for the environmental analytical chemist is the ionization constant, because when using a non-polar sorbent for extraction, it is of prime importance to adjust the pH so that the compounds should be in their neutral form.

These compounds were selected because they represent the most probable transformation products. Studies of drinking water treatment with ozone and addition of hydrogen peroxide under laboratory conditions indicated that the ultimate identified transformation products are ammeline and cyanuric acid; most of the compounds in Table 1 have been identified as intermediate compounds [26–28].

3.2. Comparison of retention factors in water

To a first approximation, solid-phase extraction is a simple chromatographic process, the sorbent being the stationary phase and the water of the sample the mobile phase, so that data generated by LC measurements can be used for predicting the SPE parameters [23,29]. Solutes are trapped provided that they are not eluted by water. In practice, the most important parameter is the volume that can be percolated with 100% recovery, known as the breakthrough volume, V_b, which can be estimated from the retention volume V_r measured with water as mobile phase. As V_r can be easily calculated from the capacity factor of solutes in water, k'_w, by the equation $V_r = V_0\ (1 + k'_w)$, V_0 being the void volume, one can rapidly obtain the order of magnitude of the breakthrough volume. For example, a log k'_w value higher than 2.2 is required for a V_r value higher than 100 ml using a cartridge packed with 500 mg of sorbent.

The values of k'_w can be measured in water or can be extrapolated from more rapid measurements in water–methanol. For the three reversed-phase sorbents, the capacity factors were measured for each solute in Table 1 with various methanol–water mobile phases and the results are reported in Fig. 1. As expected, only DEA, OHA and DIA can be preconcentrated using C_{18} silica. The others are not retained enough and ADE, ANE and ACY were not reported as they have log k' values below -0.5 even in pure water. These results could have been predicted, without any calculation, from the relationship between log k'_w and log P_{oct}, which has been intensively studied in reversed-phase chromatography with C_{18} silicas [30].

The retention of compounds on the apolar copolymer PRP-1 was shown to be between 20 and 40 times higher than that measured on C_{18} silicas [22]. Fig. 1b effectively shows that atrazine, simazine, DEA, OHA and DIA are more retained. However, the log k'_w values of the more polar OHDEA, DAA, OHDIA, ADE, ANE and ACY are very similar to those obtained on C_{18} silica. The limitation of the extraction potential of both C_{18} and the apolar copolymer is clearly shown for highly polar compounds.

The retention mechanism was shown to be different on PGC, so that log k'_w cannot be predicted from the hydrophobicity (Fig. 1c). First, simazine and atrazine are more retained than they are on PRP-1 and the retention order is different. The same inversion is found for DEA and DIA and for OHDEA and OHDIA. In comparison with simazine, atrazine contains a more hydrophobic substituent, isopropyl instead of ethyl, on the nitrogen atom in position 2, and the retention order on C_{18} silica and on PRP-1 is easily explained by this difference in hydrophobicity. On PGC, the retention mechanism depends on both the hydrophobicity and the local dipoles in the molecule, so that the inversion between simazine and atrazine can be explained. However, the most important point is that the very polar ACY, ANE and ADE are very well retained by the PGC in water with log k'_w values higher than 2.5. All other compounds have log k'_w values above 3. These results are in agreement with previous work where we have shown that the log k'_w values of 1,3,5-trihydroxybenzene

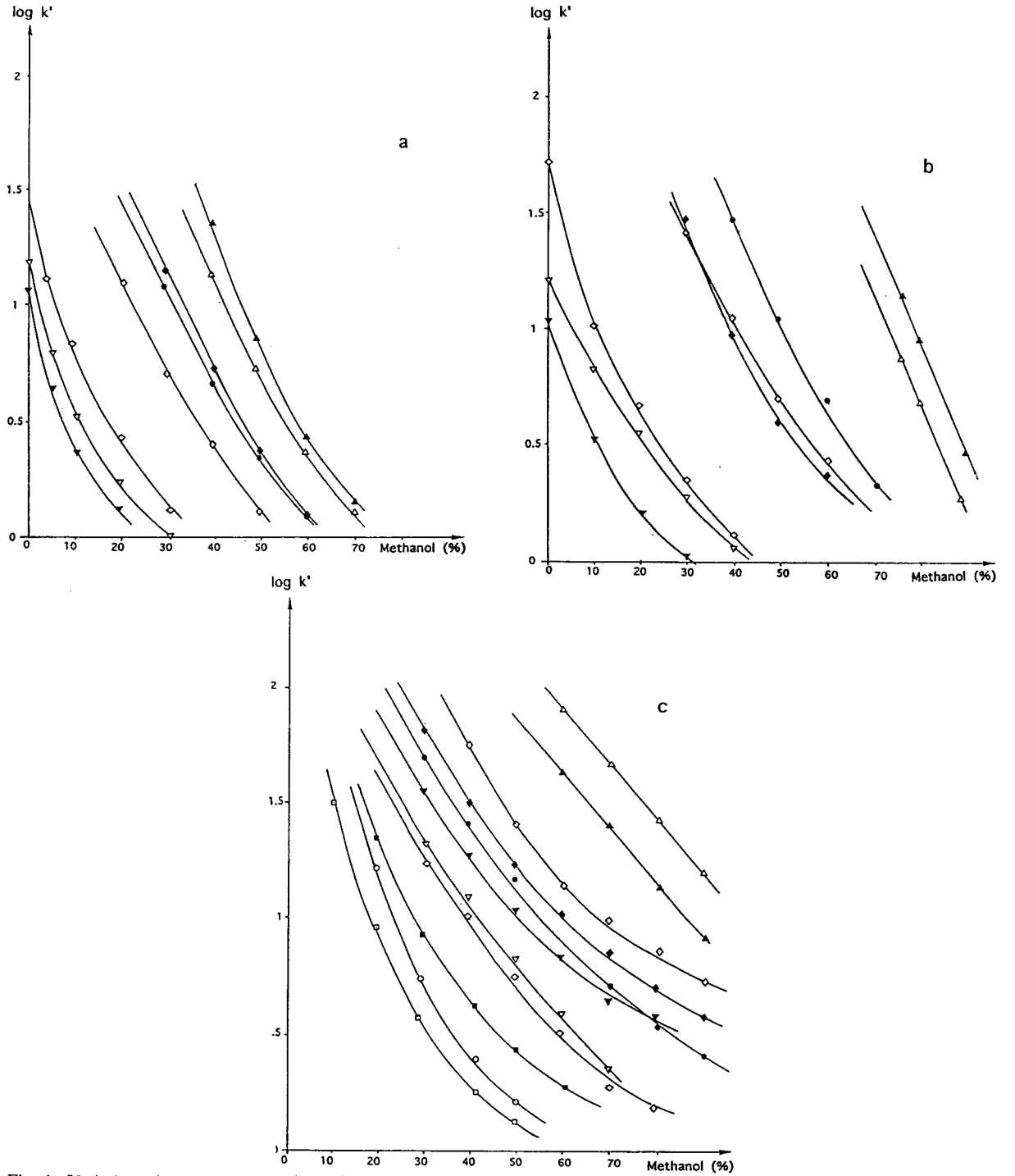

Fig. 1. Variation of capacity factors ($\log k'$) with the mobile phase composition obtained on (a) C_{18} silica, (b) PRP-1 copolymer and (c) porous graphitic carbon. Solutes: ▲ = atrazine; △ = simazine; ◆ = OHA; ● = DEA; ◊ = DIA; ◇ = OHDEA; ▽ = DAA; ▼ = OHDIA; ■ = ACY; ○ = ADE; □ = ANE. Mobile phase, methanol–0.05 *M* sodium phosphate adjusted to pH 7, except for ADE and ACY on PGC (pH 3); flow-rate, 1 ml/min; unretained compound, 2 *M* sodium nitrate.

were around 3 whereas this compound was not retained at all on C_{18} silica [21].

3.3. Analytical separation

The analytes were divided into two groups because of their different solubility properties and also because of the different pH values that should be used. The separation of ADE, ANE and ACY was performed on a C_{18} column eluted with pure water adjusted to pH 3, showing that these compounds are just slightly retained with C_{18} silica (Fig. 2). Bad peak shapes were obtained on dissolving the injection mixture in aqueous solutions containing methanol or acetonitrile. The solubility in other solvents was very poor and this practical problem prevented us from separating these compounds in the normal-phase mode. The other compounds were separated with an acetonitrile gradient at pH 7. A similar separation was not possible using the only available 10-cm long analytical column of PGC because of the lack of efficiency in comparison with a 25-cm C_{18} column [31]. Nevertheless, the PGC column was used as a confirmation column, the retention volume of ACY being the same as that with C_{18} silica, but using an aqueous mobile phase containing 30% of methanol.

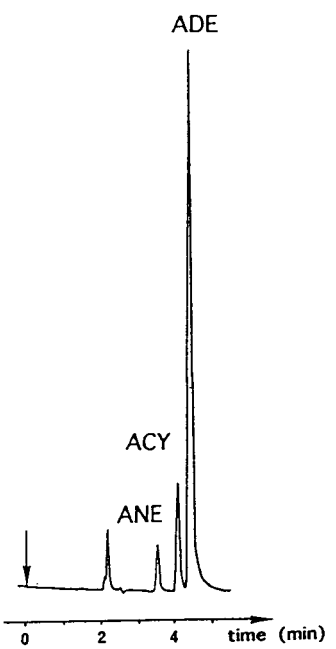

Fig. 2. Analytical separation of simazine, atrazine and the degradation products on a C_{18} column. Mobile phase, 10^{-3} *M* perchloric acid; detection UV, at 205 nm.

3.4. Solid-phase extraction conditions

The extraction also has to be carried out separately for the two groups, owing to the different solvents used for dissolving the corresponding extracts. Only water was effective for dissolving the extract when the three more polar analytes were studied. For the three more polar analytes, a cartridge packed with 500 mg of PGC was selected in order to increase the V_b values. Recoveries were first measured by preconcentrating 250 ml of LC-grade water samples spiked with 5 μg/l of ADE, ANE and ACY. Average recoveries above 95% were obtained on eluting the cartridge with 15 ml of methanol or 15 ml of acetone. The organic solvent was evaporated to dryness at ambient temperature under a stream of nitrogen and the residue was dissolved in 0.5 ml of water adjusted to pH 3. An aliquot of 100 μl was injected and recoveries were calculated by comparison with standard solutions. The sample volume can be increased to 500 ml with an amount of 1 g of PGC sorbent and a desorption volume of 20 ml of methanol. The recovery obtained with 500 ml of water samples spiked with 5 μg/l of ACY was 96 ± 5% (three replicate extractions). ANE was shown to be fairly unstable. This was verified by regularly monitoring the stock solution containing ADE, ANE and ACY and it was observed that the concentration of ADE increased while the concentration of ANE decreased, indicating a slow transformation of ANE into ADE.

For the other group, as the log k'_w values were above 3, a 300-mg PGC cartridge was selected. However, the elution was more difficult owing to the strong retention of the less polar analytes. The curves Fig. 1c indicate that simazine and atrazine are still retained in pure methanol. The recoveries were first measured with an elution volume of 15 ml of pure organic solvent. Metha-

nol, acetonitrile, THF and methylene chloride could not elute each analyte completely. The highest recoveries were obtained with THF, except for the hydroxy analogues, which were better eluted with methanol. The recoveries obtained with an eluent consisting of 15 ml of methanol and 10 ml of THF were above 90% for each analyte with a sample volume of 500 ml and using a cartridge containing 300 mg of PGC.

3.5. Application to drinking waters

Cyanuric acid was first studied. The off-line procedure described previously using a 500-mg PGC cartridge was applied to 250 ml of LC-grade water spiked with 5 μg/l of cyanuric acid, to 250 ml of non-spiked drinking water and to a 250-ml sample of the same drinking water spiked with 5 μg/l of cyanuric acid. The chromatograms of the extracts are presented in Fig. 3. The drinking water shows numerous interfering compounds and peaks identified with asterisks have the same retention times as ammeline, cyanuric acid and ammelide, indicating that PGC is not a selective extraction sorbent and that C_{18} silica is not able to separate the interferents from the analytes in the extract. As the mobile phase is pure water, it is impossible to modify it to delay the analytes. When spiking the drinking water with cyanuric acid alone, it was verified that both the retention time and the shape of the peak were identical (Fig. 3c). The analytical PGC column was therefore used as a confirmation column. As it was impossible to dissolve the whole dry extract in less than 500 μl of water and to inject more than 100 μl on to the 10-cm long Hypercarb column, this procedure could not provide determinations below 3 μg/l. Owing

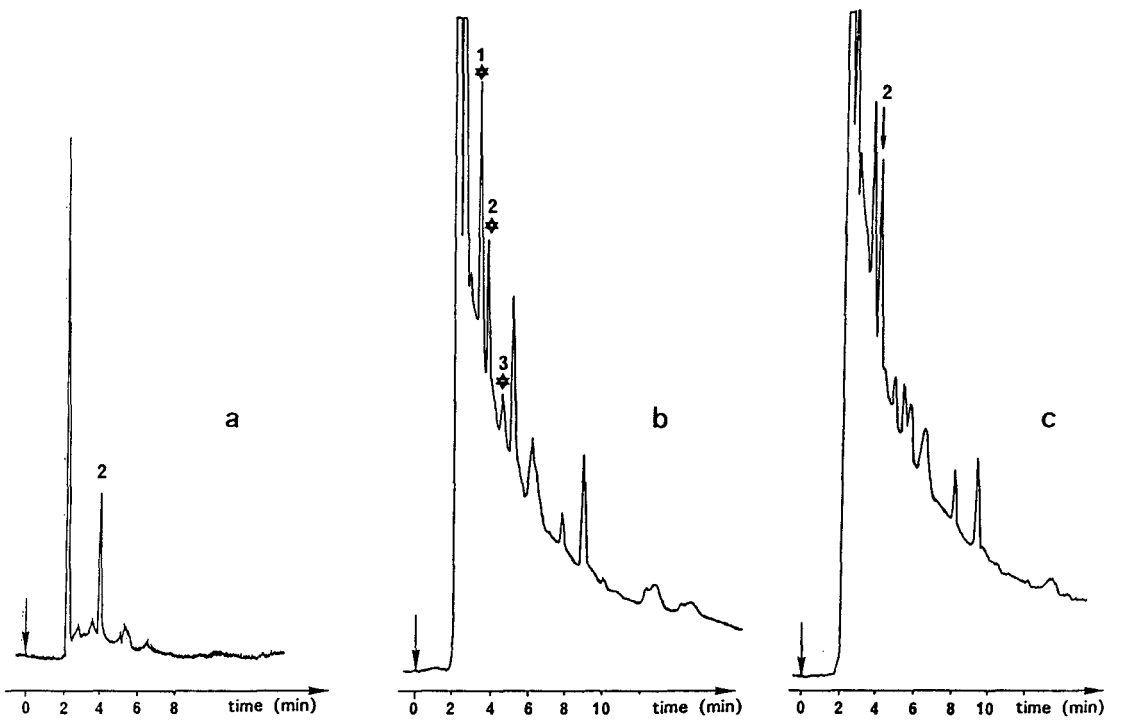

Fig. 3. Analysis of the off-line water extracts on the C_{18} analytical column. (a) 250 ml of LC-grade water spiked with 5 μg/l of cyanuric acid; (b) 250 ml of drinking water, non-spiked, taken in Paris, May 1993; 1 = ANE, 2 = ACY and 3 = ADE; (c) 250 ml of the same drinking water spiked with 5 μg/l of cyanuric acid (peak 2). Experimental conditions as in Fig. 2a. Dissolution of the extract in 0.5 ml of mobile phase and injection of a 100-μl aliquot; UV detection at 205 nm, (a) 0.01 AUFS, (b) and (c) 0.02 AUFS.

to the poor UV property of cyanuric acid, there was interest in injecting nearly all of the dry extract, which was possible by diluting it in a larger volume of water and using an on-line set-up, as described in the Experimental section. The three extracts analysed in Fig. 3 were then analysed on the PGC analytical column and the corresponding chromatograms are presented in Fig. 4. There are considerable differences between the chromatograms in Figs. 3 and 4 and it can be seen that the analytical PGC column is able to separate the interferents from the analytes using an aqueous mobile phase containing 30% of methanol. Therefore, it was possible to confirm that the chromatograms in Fig. 3b were false-positive. The detection limit obtained using this procedure was 0.2 μg/l in drinking water samples.

The other less polar metabolites were also determined using a 300-mg PGC cartridge, according to the experimental conditions described above. Fig. 5 represents the analysis of an extract obtained from the preconcentration of 500 ml of drinking water spiked with 0.5 μg/l of each analyte. Detection limits below the 0.1 μg/l level are easily obtained even for OHDIA, OHDEA and DAA.

4. Conclusion

Many transformation products of pesticides are more polar than the parent molecules and their extraction from aqueous media requires specific sorbents. Although the limitations of C_{18} silica and apolar copolymers can be predicted according to the well known retention behaviour of solutes with the sorbents in LC, little is known about the retention mechanism of polar compounds on PGC and more studies are necessary. The potential of PGC for the extraction of some water-soluble analytes has been demonstrated in this study, since previously no conventional sorbent was able to extract the water-soluble degradation products of atrazine in drinking waters. Moreover, it was also pointed out in this particular example that C_{18} silica columns were not able to analyse the extracts, but that PGC used as an HPLC stationary phase was able to separate interferents from the analytes, thus

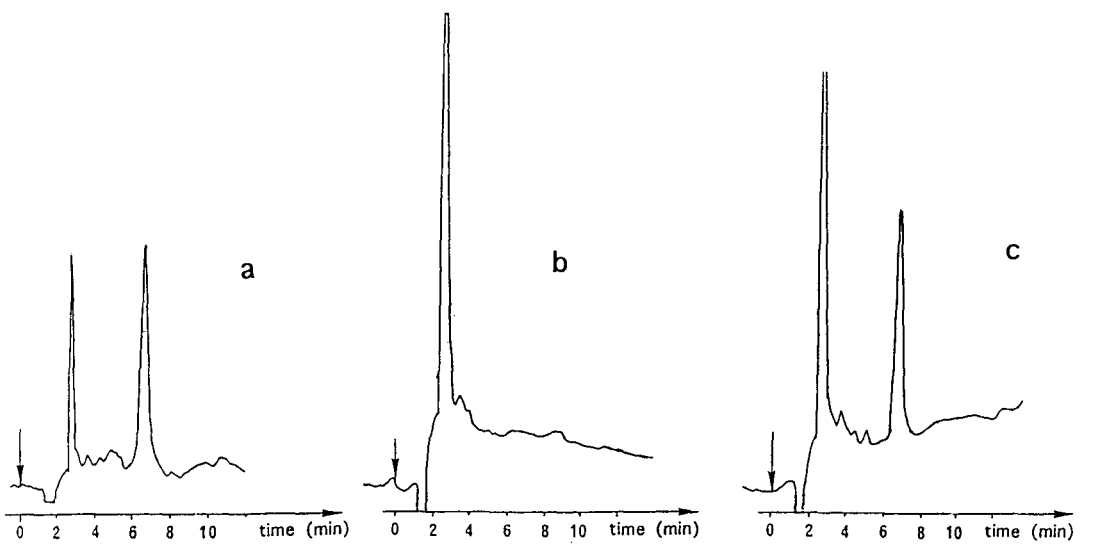

Fig. 4. On-line analysis of water extracts using a PGC precolumn and a PGC analytical column. (a) LC-grade water extract spiked with 5 μg/l of cyanuric acid; (b) non-spiked drinking water extract; (c) spiked drinking water extract with 5 μg/l of cyanuric acid. Dry extracts (obtained by off-line preconcentration) were dissolved in 30 ml of LC-grade water and 25 ml were analysed on-line (see text). Mobile phase, methanol–0.05 *M* sodium phosphate buffer (pH 7) (30:70) detection UV, at 220 nm, 0.05 AUFS.

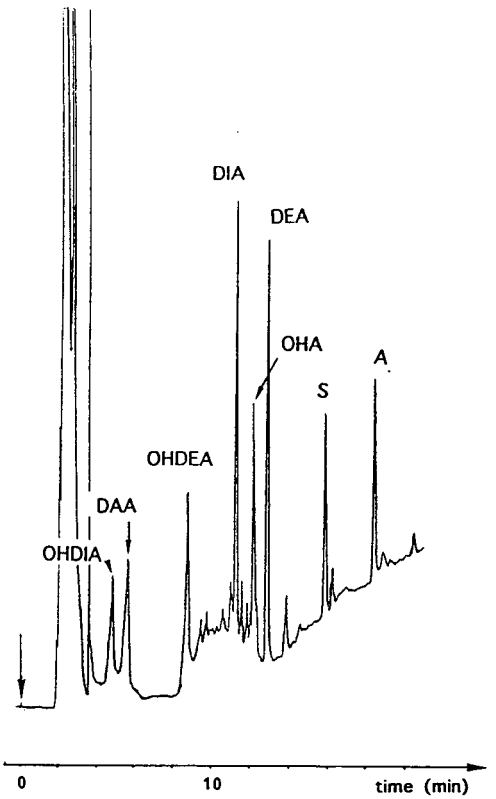

Fig. 5. Off-line analysis of the extract corresponding to 250 ml of drinking water spiked with 0.5 μg/l of each analyte. Experimental conditions: water–acetonitrile gradient at pH 7 (see Experimental section for the gradient shape); dissolution of the extract in 0.5 ml of methanol and injection of a 100-μl aliquot; detection, UV at 210 nm, 0.02 AUFS.

providing a useful confirmation method. Therefore, PGC will contribute to the increase in the number of polar analytes that can be monitored at trace levels in water. The solid-phase extraction of very polar compounds is certainly an area which needs to be developed with the introduction of new sorbents.

Acknowledgements

This work was supported by the National Agronomic Research Institute of France (AIP programme) and by the Environmental R&D programme 1991–94 of the European Communities (contract No. EV5V-CT92-0114). Shandon HPLC (France and UK) are thanked for the supply of carbon materials.

References

[1] M. Fielding, D. Barcelo, A. Helweg, S. Galassi, L. Tortensson, P. van Zoonen, R. Wolter and G. Angeletti, Pesticides in Ground and Drinking Waters, Water Pollution Research Report No. 27, Commission of the European Community, Brussels, 1992, pp. 1–136.
[2] W.E. Pereira and C.E. Rostad, Environ. Sci. Technol., 24 (1991) 1400–1406.
[3] E.M. Thurman, D.A. Goolsby, M.T. Meyer and D.W. Kolpin, Environ. Sci. Technol., 25 (1991) 1794–1796.
[4] A. Pachinger, E. Eisner, C. Tertsch, H. Begutter and H. Klus, J. High Resolut. Chromatogr., 15 (1992) 302–304.
[5] G. Durand, R. Forteza and D. Barcelo, Chromatographia, 28 (1989) 597–604.
[6] G. Karlaganis, R. Von Arx, H.K. Ammon and R. Camenzind, J. Chromatogr., 549 (1991) 229–236.
[7] E.M. Thurman, D.A. Goolsby, M.T. Meyer, M.S. Mills, M.L. Pomes and D.W. Kolpin, Environ. Sci. Technol., 26 (1992) 2440.
[8] D. Barcelo, J. Chromatogr., 643 (1993) 117–143.
[9] J.M. Schaeppli, W. Fory and K. Ramsteiner, J. Agric. Food Chem., 37 (1989) 1532–1538.
[10] G. Durand, N. De Bertrand and D. Barcelo, J. Chromatogr., 554 (1991) 233–250.
[11] G. Durand and D. Barcelo, Toxicol. Environ. Chem., 25 (1989) 1–11.
[12] Q. Wenheg, N.A. Schultz, J.D. Stuart, J.C. Hogan and A.S. Mason, J. Liq. Chromatogr., 14 (1991) 1367–1392.
[13] V. Coquart, P. Garcia Camacho and M.-C. Hennion, Int. J. Environ. Anal. Chem., 52 (1992) 99–112.
[14] D.S. Gamble and S.U. Khan, J. Agric. Food Chem., 38 (1990) 297.
[15] D.J. Subach, Chromatographia, 14 (1981) 371–373.
[16] V. Pacakova, K. Stulik and M. Prihoda, J. Chromatogr., 442 (1988) 147–155.
[17] E.M. Thurman, M.T. Meyer, M.L. Pomes and C.A. Perry, Anal. Chem., 62 (1990) 2043–2048.
[18] A.M. Cooks and R. Hutter, J. Agric. Food Chem., 29 (1981) 1132–1135.
[19] G. Durand and D. Barcelo, J. Chromatogr., 502 (1990) 275–286.
[20] E. Pelizzeti, C. Minero and V. Carlin, New J. Chem., 17 (1993) 315–319.
[21] V. Coquart and M.-C. Hennion, J. Chromatogr., 600 (1992) 195–201.
[22] M.-C. Hennion and V. Coquart, J. Chromatogr., 642 (1993) 211–224.
[23] M.-C. Hennion and P. Scribe, in D. Barcelo (Editor) Environmental Analysis, Techniques, Applications and Quality Assurance, Elsevier, Amsterdam, 1993, Ch. 2, p. 24.

[24] A. Noble, J. Chromatogr., 642 (1993) 3–14.
[25] R.F. Rekker, in The Hydrophobic Fragmental Constant (Pharmaco-Chemistry Library, Vol. 1), Elsevier, Amsterdam, 1977.
[26] B. Legube, S. Guyon and M. Doré, Ozone Sci. Eng. 9 (1987) 233–246.
[27] P.C. Kearney, M.T. Muldoon and C.J. Somich, Chemosphere, 16 (1987) 2321–2330.
[28] P.C. Kearney, M.T. Muldoon, C.J. Somich, J.M. Ruth and D.J. Voaden, J. Agric. Food Chem., 36 (1988) 1301–1306.
[29] M.-C. Hennion and V. Pichon, Environ. Sci. Technol., 28 (1994) 576A–583A.
[30] T. Braumann, J. Chromatogr., 373 (1986) 191–225.
[31] S. Guenu and M.-C. Hennion, J. Chromatogr. A, 665 (1994) 243–251.

ELSEVIER

Journal of Chromatography A, 711 (1995) 269–276

JOURNAL OF CHROMATOGRAPHY A

Ion-pair–supercritical fluid extraction of clenbuterol from food samples

M.M. Jimenez-Carmona, M.T. Tena, M.D. Luque de Castro*

Department of Analytical Chemistry, Faculty of Sciences, University of Córdoba, E-14004 Córdoba, Spain

First received 21 January 1995; revised manuscript received 20 April 1995; accepted 1 May 1995

Abstract

Simultaneous ion-pair/supercritical fluid extraction (SFE) was investigated as an alternative to liquid solvent extraction for clenbuterol determination. Clenbuterol was extracted from diatomaceous earth and food matrices (feedstuff, lyophilized milk and liver) as its 10-camphorsulfonate ion-pair using supercritical (SC) CO_2 for 30 min of dynamic extraction at 383 bar and 40°C. The ion-pair forming reagent was added to the extraction cell prior to SFE. Recoveries ranged from 12 to 87% with mean R.S.D. of 15% for triplicate extractions. The use of the ion-pair reagent as a CO_2 modifier was also studied in depth.

1. Introduction

Supercritical fluid extraction (SFE) has proved to be an expeditious technique to leach quantitatively non-polar organic compounds from a great variety of matrices [1–4]. Nevertheless, addition of a polar modifier to the extractant fluid is required for the quantitative extraction of polar or ionic analytes when the fluid is non-polar (e.g. CO_2). In situ derivatization [5–8], complexation [9–17] and ion-pairing [18,19] under supercritical conditions are recently used approaches to improve efficiency of polar- and ionic-species extraction.

Quaternary ammonium salts have been used for ion-pair–supercritical fluid extraction. Aliphatic and aromatic surfactants have been quantitatively (>90%) extracted from sewage sludges as their tetrabutylammonium ion-pairs using supercritical CO_2 [18], while trimethylphenylammonium hydroxide has been used to improve the extraction of sulphonamides [19]. Metals ions [9,11–15,17] and organometallic compounds [8,10,16] have been extracted with CO_2 after conversion to non-charged species.

The use of clenbuterol, a β-adrenergic agonist drug, as feed additive is not permitted in the European Union (EU) but it is illegally used as a growth promoter in meat-producing animals. Clenbuterol persist in liver at levels much higher than in other edible tissues. For this reason rapid methods for the determination of clenbuterol in liver samples are required. Enzyme immunoassay has been used for β-agonist screening of bovine urine [20,21], liver [21,22] and eye [21] samples, whereas liquid [23–26] and gas [27–30] chromatography have been used after laborious and time-consuming preliminary steps (liquid–

* Corresponding author.

0021-9673/95/$09.50
SSDI 0021-9673(95)00526-9

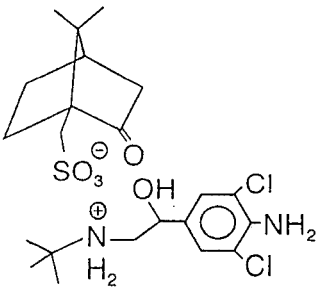

Fig. 1. Proposed interaction between camphorsulfonate ion and protonated clenbuterol.

liquid and solid-phase extractions) for the determination of clenbuterol in biological matrices. The aim of this work was to study the supercritical fluid extraction of clenbuterol from different matrices to overcome those preliminary steps.

Aminoalcohols form stable ion-pairs with camphorsulfonic acid in a non-polar medium. In addition to electrostatic attraction, hydrogen bonding between the aminoalcohol and camphorsulfonic acid takes place in a non-polar medium such as supercritical CO_2. In this paper camphorsulfonate is proposed as counterion for ion-pair–SFE of clenbuterol. The proposed interaction between camphorsulfonate ion and protonated clenbuterol is shown in Fig. 1.

2. Experimental

2.1. Instrumentation

A Hewlett-Packard HP 7680A supercritical fluid extractor equipped with a 7-ml thimble as extraction cell and a packing of small stainless-steel balls as analyte trap was used. An HP 1050 liquid chromatograph and an HP 1040A diode-array detector were used for the determination of clenbuterol in the extracts. A Fisons supercritical fluid extractor consisting of an SFC 300 double-syringe pump, an SFE 30 collector unit, an SFE 300 control system and a Haake K20 cooling circulator (ethanol-filled) and a VR 100 variable restrictor (CCS Instrument Systems, PA, USA) were used for continuous addition of the ion-pair reagent during the SFE process. An Ultraterm 6000383 P-Selecta recirculating thermostat was used to control the collector temperature.

2.2. Materials

Stock standard solution of clenbuterol hydrochloride (>95%, Sigma) of 0.4 g/l in HPLC-grade methanol (Romil Chemicals) was prepared. Diatomaceous earth (Sigma) was used as solid support.

SFE/SFC-grade CO_2 (Air Products) and methanol-modified CO_2 (nominally 10% methanol in CO_2, SEO, Spain), HPLC-grade methanol and acetonitrile (Romil Chemicals), glacial acetic acid and ammonia (Panreac, Spain) were also used.

Ion-pair reagents were prepared as 0.1 *M* methanolic solutions except where noted. The reagents tested included (1*S*)-(+)-10-camphorsulfonic acid (*S*-CamH), (1*R*)-(−)-10-camphorsulfonic acid (*R*-CamH, Sigma) and (1*R*)-(−)-10-camphorsulfonic acid ammonium salt (*R*-$CamNH_4$, Aldrich). The 0.1 *M* (1*S*)-(+)-10-camphorsulfonic acid ammonium salt (*S*-$CamNH_4$) solution was prepared from *S*-CamH and ammonia.

2.3. Coupling of the ion-pair reagent and supercritical fluid extraction modes

The ion-pair reagent was incorporated into the system in three different ways. (a) A small volume (500 μl) of reagent methanolic solution was added to the sample in the extraction cell before the extraction with supercritical CO_2 was started. (b) The reagent was dissolved in the cosolvent used as polar modifier of CO_2 and so continuously added to the fluid in the dynamic procedure. (c) A static addition followed by a dynamic addition of the ion-pair reagent was also performed.

Static addition

Extractions were performed using the HP extractor (Fig. 2A). CO_2 and methanol-modified CO_2 were delivered from a cylinder supplied with a dip tube, and they were aspirated by a

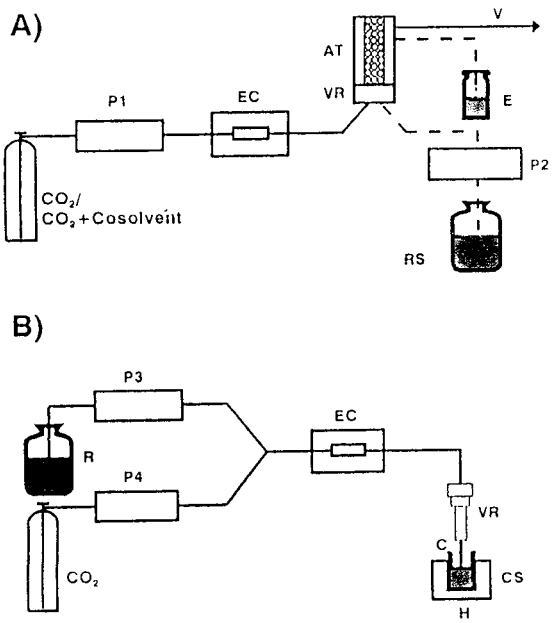

Fig. 2. Schematic diagram of the extraction systems used for ion-pair–SFE with (A) static addition and (B) dynamic addition of the ion-pair reagent. (P) pump, (EC) extraction chamber, (AT) analyte trap, (VR) variable restrictor, (E) extract, (RS) rinsing solvent, (V) vent, (R) ion-pair reagent solution, (C) collector, (CS) collection solvent and (H) collector heater with thermostat.

double-piston pump and passed through the 7-ml extraction cell which contained the sample. The extraction cell was ca. 25% filled and not-inert filler was added. The leached clenbuterol was driven to a 0.45-ml stainless-steel bead trap through an automated variable-diameter restrictor which virtually avoided plugging and provided a constant flow-rate during the extraction process. In a subsequent step (rinsing), an acetonitrile–acetic acid/ammonium acetate buffer (30:70) stream at 0.5 ml/min flow-rate was pumped through the trap by a syringe pump. In order to avoid methanol retention in the trap the temperature of this device was increased to 70°C during the extraction step when either methanol-modified CO_2 or methanolic solutions were used or added to the samples, respectively. Restrictor and trap temperatures were 60°C during the rinsing step. The extract was collected in vials which had been previously weighed in order to determine the weight of the extract as the difference. The recoveries were calculated from analyte concentrations determined by HPLC and the volume of the extract, the latter being obtained from weight/density data, which were more precise than those obtained from the values of the volume dispensed by the extractor.

Dynamic addition

Extractions were performed using the Fisons extractor (Fig. 2B). Pure CO_2 and cosolvent (pure methanol or methanolic solution of the reagent) were separately delivered by a dual-syringe pump and mixed prior to the extraction chamber. The fluid flow-rate through the 3-ml extraction cell was controlled by a manually actuated variable restrictor that was immersed in a solvent trap (4 ml of 30:70 acetonitrile–acetic acid/ammonium acetate buffer in the collector at 50°C). Larger cells were difficult to handle due to the dimensions of the extraction chamber. The collector was heated at 50°C to avoid freezing during the fluid expansion.

2.4. Chromatographic separation and detection

A liquid chromatograph with a diode-array detector equipped with an Ultrabase-C_{18} (250 × 4.6 mm, 5 μm) column was used to determine clenbuterol in the extracts. The injection volume was 20 μl. A 70:30 10 m*M* acetic acid–ammonium acetate buffer solution (pH 4.6)/acetonitrile mobile phase was used at a 1 ml/min flow-rate. The chromatogram was recorded at 244 nm, the maximum-absorbance wavelength of clenbuterol, and the peak area was used to quantify the analyte. The peak was identified by both the retention time (4.98 ± 0.08 min) and the spectrum. The calibration curve obtained by using the peak area was linear over the range 1–60 μg/ml. The equation for the linear segment obtained by the least-squares method was: $A = 1.77 + 25.65c$ (where A and c denote peak area and concentration of clenbuterol expressed in μg/ml, respectively), and the regression coefficient was 0.99989. The precision (expressed as the relative standard deviation, R.S.D.) of the HPLC method was 3.62% ($n = 11$, 10 μg/ml of clenbuterol).

2.5. Support and sample preparation

Diatomaceous earth (0.5 g) and samples (0.3–0.5 g) were directly weighed in the extraction cell following addition of 50–100 μl of clenbuterol stock solution and 0.5 ml of ion-pair reagent solution. No drying stage was performed. Support and samples were extracted 15 min after spiking.

3. Results and discussion

3.1. Static addition of the ion-pair reagent

Preliminary experiments were carried out to determine the extraction efficiency of clenbuterol with supercritical CO_2 and to search for alternatives to improve the extraction efficiency.

Ion-pair reagent survey

The two enantiomers of both camphorsulfonic acid and its ammonium salt were tested as ion-pair reagents. An amount of 0.5 ml of methanolic solution of the reagent (0.1 *M*) was added to 0.5 g of diatomaceous earth in the extraction cell that had previously been spiked with 20 μg of clenbuterol prior to SFE with pure CO_2. Recoveries were greatly improved by using the ammonium salt instead of the acid form, while there was no difference using the *R*- or *S*-enantiomers. Clenbuterol recoveries from diatomaceous earth with SC-CO_2 were 30% and 70% using camphorsulfonic acid and the ammonium salt, respectively. The (1*R*)-(−)-10-camphorsulfonic acid ammonium salt was chosen as ion-pair reagent for further experiments. This behaviour is in accordance with the features of clenbuterol, a polar compound with two–NH_2 groups which could be protonated under the extraction conditions used. A charged analyte can not be extracted with pure CO_2 unless it is converted into a neutral form, i.e. by ion-pair formation. Camphorsulfonic acid hardly would form the ion-pair, so a prior deprotonation would be mandatory, which in turn could give rise to protonation of the second amino group of clenbuterol. This latter effect, highly undesirable, does not appear when the ammonium salt is used.

Methanol and dichloromethane were studied as solvents to prepare the ion-pair reagent solution. Methanol gave higher recoveries than dichloromethane. In addition, the latter gave rise to extract turbidity, probably due to retention of dichloromethane somewhere between the trap and the vent, where the temperature was not controlled. The presence of dichloromethane caused drawbacks in the chromatographic determination, such as baseline noise.

The trap temperature was increased to 70°C during the extraction step to avoid solvent retention. The addition of volumes of reagent solution larger than 0.5 ml (1.5 ml) resulted in irreproducible results. Reproducibility was improved by decreasing the amount of liquid added to the extraction cell and increasing the trap temperature.

Solutions of ion-pair reagent with a concentration higher than 0.1 *M* were used to optimize the amount of reagent used. There was no improvement using 0.3 *M* (close to saturation) solution compared to 0.1 *M* solution.

Influence of the extraction fluid

Some experiments were performed with the aim of choosing the optimal extraction fluid. Extractions of clenbuterol from diatomaceous earth were carried out using SC-CO_2 (40°C, 281 bar, $d \simeq 0.9$ g/ml) and supercritical methanol-modified CO_2 premixed, (nominally 10%, 70°C, 314 bar, $d \simeq 0.8$ g/ml), the latter as the only procedure to use cosolvent in the HP extractor employed. Working conditions were as follows: 30 min at a flow-rate of 0.5 ml/min with and without addition of 0.5 ml of *R*-CamNH_4 methanolic solution or pure methanol.

Clenbuterol could not be extracted (0% recovery) into pure CO_2 without prior ion-pair formation. Recoveries increased (15–30%) when methanol was added to the extraction cell or when methanol-modified CO_2 was used. Regardless of the fact that the CO_2–MeOH premixed fluid was a better extractant than pure CO_2 in the absence of camphorsulfonate, the best result (80% recovery) was obtained with pure CO_2 and prior addition of *R*-CamNH_4 to the extraction

cell; this procedure was selected for further experiments. Only 60% of clenbuterol was recovered with methanol-modified CO_2 and *R*-CamNH_4 addition.

Influence of SFE variables

The experimental variables as density, temperature, equilibration, extraction time and CO_2 flow-rate were optimized in order to maximize extraction in a short time. The univariate method was used for this purpose. CO_2 density and extraction time had the largest influence on extraction efficiency.

CO_2 density. Increasing the density (or pressure) at 40°C resulted in increased recovery throughout the range studied (0.70–0.95 g/ml). A density of 0.95 g/ml was chosen for further experiments.

Temperature. The effect of this variable was studied at a constant CO_2 density of 0.8 g/ml, which allowed a wider range of temperatures than 0.9 g/ml (because of instrumental pressure limitations). The temperature range over which the effect was investigated was 40–80°C. Increasing the temperature resulted in increased recoveries, but the recovery at the highest temperature was lower than 80%, the value achieved at 0.95 g/ml and 40°C. Thus a temperature of 40°C was selected as optimum.

Dynamic variables. CO_2 flow-rate and equilibration time were studied in the range of 0.5–4.0 ml/min and 1–30 min, respectively; both variables had no influence on the recovery. Extraction times from 5 to 60 min were studied; increasing extraction time up to 30 min resulted in increased recovery, above this value recovery remained almost constant.

Reproducibility

The precision, expressed as relative standard deviation ($n = 7$), obtained for the overall process, i.e. ion-pair–SFE (static addition)–HPLC) under optimum conditions was 8.9%.

3.2. Dynamic addition of the reagent

In the dynamic addition mode, the ion-pair reagent is continuously introduced in the extractor by dissolving it in the cosolvent used as CO_2 modifier. The amount of reagent that can be used in the dynamic mode is limited by the solubility of the reagent in the supercritical CO_2–cosolvent mixture, which is lower than that in the cosolvent. The use of amounts of reagent larger than the saturation concentration could give rise to precipitation in the extraction system and restrictor plugging.

Extractions of clenbuterol (50 μl stock solution added to 0.5 g diatomaceous earth) were carried out using concentrations of 1 and 5% 10 m*M* *R*-CamNH_4 in the methanolic solution modified CO_2 with and without previous addition of this reagent to the extraction cell. Extraction time was 30 min and the flow-rate was kept between 0.8 and 1.2 ml/min. The recoveries obtained are listed in Table 1. Neither dynamic nor combined static and dynamic addition modes improved extraction compared to reagent addition to the extraction cell before SFE with CO_2. The low extraction recovery obtained in the dynamic addition mode should be expected due to the presence of methanol as cosolvent. The fact that a different extraction system was used must also be taken into account. The extraction system became plugged and CO_2 almost stopped flowing in the combined static and dynamic addition mode with 5% cosolvent, and it was unfeasible to reset the flow-rate at 1 ml/min by opening the variable restrictor. This

Table 1
Recovery of clenbuterol from diatomaceous earth

Addition procedure	Recovery ± R.S.D.[a] (%)
Static addition[b]	85 ± 8
Dynamic addition[c]	
1% cosolvent	14 ± 5
5% cosolvent	67 ± 7
Static + dynamic addition[c]	
1% cosolvent	38 ± 7
5% cosolvent	39 ± 6

[a] Here $n = 3$ except that for static addition ($n = 7$).
[b] Conditions: HP extractor, CO_2 at 40°C and 383 bar (≈0.95 g/ml).
[c] Conditions: Fisons extractor, CO_2 modified with 1% and 5% of methanolic solution of *R*-CamNH_4 (10 m*M*) at 40°C and 281 bar (≈0.90 g/ml) and 50°C and 314 bar (≈0.88 g/ml), respectively.

Table 2
Recovery of spiked clenbuterol by ion-pair–SFE

Sample	Recovery ± R.S.D.[a] (%)	
	20 μg	40 μg
Diatomaceous earth	73 ± 10	82 ± 6
Feedstuff	47 ± 12	63 ± 10
Lyofilized milk	59 ± 7	86 ± 11
Lyofilized liver	12 ± 2	37 ± 7

[a] $n = 3$.

could be the reason of the decreased recovery in this mode.

The stability of the ion pair increases in a non-polar medium such as pure CO_2, so increasing the fluid polarity by adding methanol is unfavourable. Moreover, competition of the methanol dissolved in CO_2 for the groups of clenbuterol and camphorsulfonate involved in the hydrogen bonding decreases the ion-pair stability.

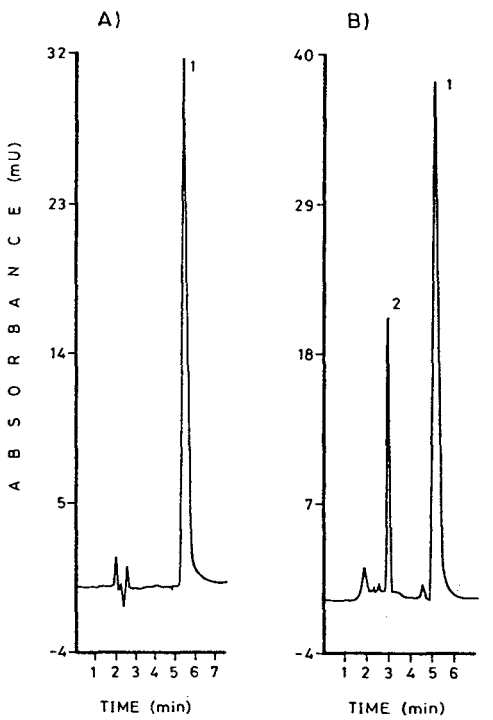

Fig. 3. HPLC chromatogram for the 20 μg/ml clenbuterol standard solution (A) and for the ion-pair–SFE extract of spiked diatomaceous earth (B). Peak identification: clenbuterol (1) and camphorsulfonate (2). For HPLC conditions see text. SFE conditions: 0.5 ml/min pure CO_2 at 40°C and 383 bar for 30 min and addition of 0.5 ml of 0.1 *M* *R*-$CamNH_4$ prior to extraction.

3.3. Application of ion-pair–SFE to spiked samples

The performance of the proposed ion-pair–SFE was tested by applying it to the recovery of clenbuterol at two different concentration levels from several food matrices (lyophilized milk, feedstuff and liver). Spiked samples were used because no real samples containing native clenbuterol were available. In addition, the HPLC–UV method used to determine clenbuterol in the extracts is not sensitive enough for the residue levels occurring in real samples. Extractions were performed in triplicate and provided good results. Table 2 shows the mean recovery and R.S.D. ($n = 3$) for each sample and spiked level (20 and 40 μg). The recoveries from food matrices were generally lower than those from diatomaceous earth. The sample amounts were 0.5 g for diatomaceous earth, feedstuff and lyophilized liver and 0.35 g for lyophilized milk.

The lowest recovery was obtained for lyophilized liver (12% for 20 μg). Recoveries from lyophilized milk ranged from 59 to 86% and were higher than that from milk mixed with diatomaceous earth as water sorbent.

Additional and successive rinsings of the analyte trap with acetone, hexane and acetone (this sequence was used in order to avoid miscibility problems with the aqueous rinsing solvent) were necessary after the extraction of milk samples to remove extracted matrix components that were not soluble in the rinsing solvent and remained in the trap after the rinsing step. In the case of feedstuff and lyophilized liver only one rinsing step with acetone was sufficient to clean the analyte trap. The extracts were very clear and did not need clean-up before HPLC analysis. Chromatograms of the extracts of diatomaceous earth and food samples are shown in Figs. 3 and 4, respectively.

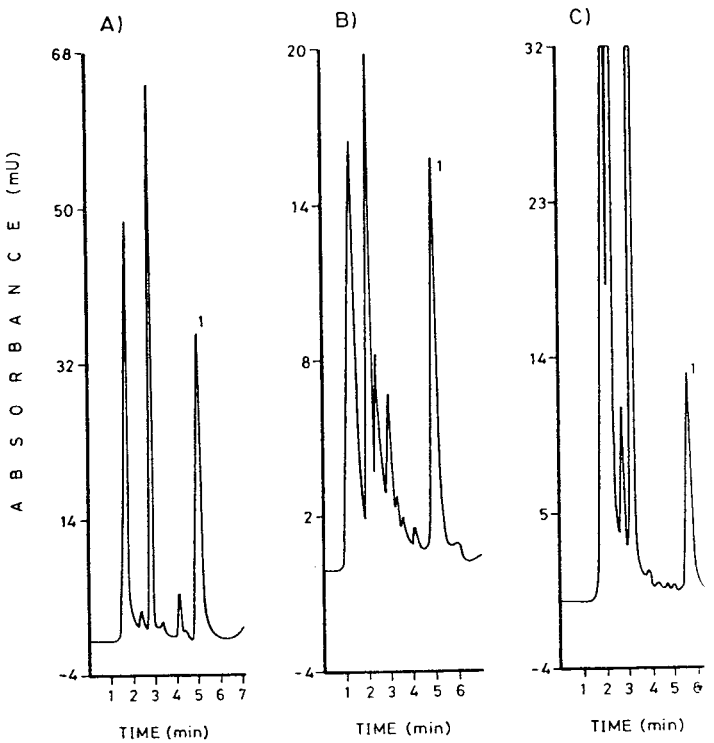

Fig. 4. HPLC chromatogram for the ion-pair–SFE extracts of lyophilized milk (A), feedstuff (B) and lyophilized liver (C). Peak identification and conditions as in Fig. 3.

4. Conclusions

The extraction of clenbuterol into supercritical CO_2 is enhanced by using camphorsulfonate as counterion to form an ion-pair. The clenbuterol–camphorsulfonate ion-pair formed is less polar than clenbuterol and so more soluble in SC-CO_2.

Extraction efficiency is not enhanced by a previous static extraction. Although the SFE efficiency of clenbuterol is improved by methanol modification of CO_2, the opposite occurs for ion-pair–SFE of the target analyte since the ion-pairing extraction is favoured in a non-polar medium.

The recovery study performed on food matrices (milk, liver and feedstuff) demonstrates that ion-pair–SFE with camphorsulfonate and CO_2 reduces preliminary steps in the determination of clenbuterol by a sensitive technique, although it did not provide good recoveries for some kinds of samples, such as liver.

Acknowledgement

Comisión Interministerial de Ciencia y Tecnología (CICyT) is thanked for financial support (Grant No. ALI93-0296).

References

[1] S.B. Hawthorne, Anal. Chem., 62 (1990) 633A.
[2] T.L. Chester, J.D. Pinkston and D.E. Raynie, Anal. Chem., 66 (1994) 106R.
[3] M.D. Luque de Castro, M. Valcárcel and M.T. Tena, Analytical Supercritical Fluid Extraction, Springer, Heidelberg, 1994.
[4] S.A. Westwood (Editor), Supercritical Fluid Extraction and its Use in Chromatographic Sample Preparation, Chapman and Hall, Glasgow, 1993.
[5] S.B. Hawthorne, D.J. Miller, D.E. Nivens and D.C. White, Anal. Chem., 64 (1992) 405.
[6] J.W. Hills, H.H. Hill and T. Maeda, Anal. Chem., 63 (1991) 2152.

[7] J.W. Hills and H.H. Hill, J. Chromatogr. Sci., 31 (1993) 6.
[8] Y. Cai, R. Alzaga and J.M. Bayona, Anal. Chem., 66 (1994) 1161.
[9] Y. Lin, R.D. Brauer, K.E. Laintz and C.M. Wai, Anal. Chem., 65 (1993) 2549.
[10] Y. Liu, V. Lopez-Avila, M. Alcaraz and W. F. Beckert, Anal. Chem., 66 (1994) 3788.
[11] Y. Lin and C.M. Wai, Anal. Chem., 66 (1994) 1971.
[12] J. Wang and W.D. Marshall, Anal. Chem., 66 (1994) 1658.
[13] K.E. Laintz and E. Tachikawa, Anal. Chem., 66 (1994) 2190.
[14] Y. Lin, C.M. Wai, F.M. Jean and R.D. Brauer, Environ. Sci. Technol., 28 (1994) 1190.
[15] Y. Liu, V. Lopez-Avila, M. Alcaraz, W.F. Beckert and E.M. Heithmar, J. Chromatogr. Sci., 31 (1993) 310.
[16] C.M. Wai, Y. Lin, R. Brauer, S. Wang and W.F. Beckert, Talanta, 40 (1993) 1325.
[17] J. Wang and W.D. Marshall, Anal. Chem., 66 (1994) 3900.
[18] J.A. Field, D.J. Miller, T.M. Field, S.B. Hawthorne and W. Giger, Anal. Chem., 64 (1992) 3161.
[19] M.T. Tena, M.D. Luque de Castro and M. Valcárcel, Chromatographia, 40 (1995) 197.
[20] R. Angeletti, M. Paleologo Oriundi, R. Piro and R. Bagnati, Anal. Chim. Acta, 275 (1993) 215.
[21] M.J. Sauer, R.J.H. Pickett and A.L. MacKenzie, Anal. Chim. Acta, 275 (1993) 195.
[22] S.D. Bucknall, A.L. MacKenzie, M.J. Sauer, D.J. Everest, R. Newman and R. Jackman, Anal. Chim. Acta, 275 (1993) 227.
[23] D. Courtheyn, C. Desaever and R. Verhe, J. Chromatogr., 102 (1991) 537.
[24] H. Hooijerink, R. Schilt, W. Haasnoot and D. Courtheijn, J. Pharm. Biomed. Anal., 9 (1991) 485.
[25] D.R. Doerge, S. Bajic and S. Lowes, Rapid Commum. Mass Spectrom., 7 (1993) 462.
[26] L. Debrauwer and G. Bories, Anal. Chim. Acta, 275 (1993) 231.
[27] A. Polettini, A. Groppi, M.C. Ricossa and M. Montagna, Biol. Mass Spectrom., 22 (1993) 457.
[28] M.-P. Montrade, B. Le Bizec, F. Monteau, B. Siliart and F. Andre, Anal. Chim. Acta, 275 (1993) 253.
[29] J. Girault and J.B. Fourtillan, J. Chromatogr., 518 (1990) 41.
[30] T. Visser, M.J. Vredenbregt, A.P.J.M. de Jong, L.A. van Ginkel, H.J. van Rossum and R.W. Stephany, Anal. Chim. Acta, 275 (1993) 205.

ELSEVIER

Journal of Chromatography A, 711 (1995) 277–288

JOURNAL OF CHROMATOGRAPHY A

Lipopolysaccharide determination by reversed-phase high-performance liquid chromatography after fluorescence labeling

Alexandr Parlesak*, Ch. Bode

Hohenheim University, Ernährungsphysiologie (140), Fruwirthstraße 12, D-70593 Stuttgart, Germany

First received 9 February 1995; revised manuscript received 13 April 1995; accepted 28 April 1995

Abstract

A sensitive method for the quantitative determination of lipid A, the covalently bound hydrophobic component of lipopolysaccharides (endotoxins), has been developed. The determination of lipid A was based on the quantitative measurement of β-hydroxymyristic acid and β-hydroxylauric acid by reversed-phase HPLC. β-Hydroxy acids were liberated from ester and amide linkages in endotoxins by acid catalyzed methanolysis. The resulting methyl esters were derivatized with 9-anthracene-carboxyl chloride, 9-fluorene-carboxyl chloride and 4-(1-pyrenyl)butyric acid chloride and quantified with a fluorescence detector. The effectiveness of the three derivatizing agents was compared.

As internal standards-β-hydroxytridecanoic acid [β-OH(13:0)] and β-hydroxypentadecanoic acid [β-OH(15:0)] ethyl esters were used. The limits of detection of β-hydroxymyristic acid were 0.5 pg for the 9-anthroyl and 2 pg for the fluorenoyl and 4-(1-pyrenyl)butyroyl ester per sample (signal-to-noise ratio of 3). The detection limits of lipopolysaccharide from a smooth strain (*Escherichia coli* 0111:B4) was 20 pg, while that from two rough strains (*E. coli* Nissle 1917 and *Salmonella typhimurium* SL 1181) was 5 pg per sample after methanolysis and derivatization with 9-anthroyl chloride.

1. Introduction

Endotoxins constitute a part of the outer membrane of the cell wall of Gram-negative bacteria [1]. The lipid A moiety of endotoxins is responsible for the toxic effects of lipopolysaccharides (LPS), like fever, tissue necrosis, endotoxic shock and activation of the complement system [2,3].

A common technique for the determination of endotoxins is the *Limulus* amebocyte lysate (LAL) test [3], in which endotoxins activate a clotting cascade in the amebocyte lysate derived from the crab *Limulus polyphemus*. Endotoxins are measured by determination of the induced gel formation. For quantitative measurements of endotoxins, a chromogenic reaction has been coupled to the clotting cascade [4,5]. However, the selectivity of the LAL test remains questionable considering that some non-endotoxic substances are known to activate the LAL clotting enzymes [6,7].

β-Hydroxy acids, especially β-hydroxymyristic acid [8–10] and β-hydroxylauric acid [11], constitute an essential part of lipid A and have been used therefore as chemical markers for the quantitation of lipid A. These acids have been

* Corresponding author.

0021-9673/95/$09.50
SSDI 0021-9673(95)00518-8

analyzed by gas chromatography–mass spectrometry [8–11].

This study aimed at developing a sensitive, specific and reproducible reversed-phase HPLC method for the determination of lipid A by detection of β-hydroxymyristic acid and β-hydroxylauric acid after derivatization with a fluorophore.

The reaction of acid chlorides with hydroxyl groups is known to be fast and to result in high yields. Hence, fluorescent polycyclic hydrocarbons with an adjacent carboxyl chloride group like 9-anthracene carboxylic chloride have been used on several occasions for sensitive detection of compounds containing hydroxyl groups [12–15].

In this work, three reagents [9-anthroyl chloride, 9-fluorenoyl chloride and 4-(1-pyrenyl)-butyroyl chloride] were tested to determine their suitability for fluorescent labeling and quantitation of β-hydroxymyristic and β-hydroxylauric acid esters as endotoxin markers (Fig. 1).

2. Experimental

2.1. Chemicals and glassware

α-Bromoethyl acetate, decanal, undecanal, dodecanal and tridecanal (technical grade, 90%–97%) were obtained from Aldrich (Steinheim, Germany) and distilled twice in vacuo before

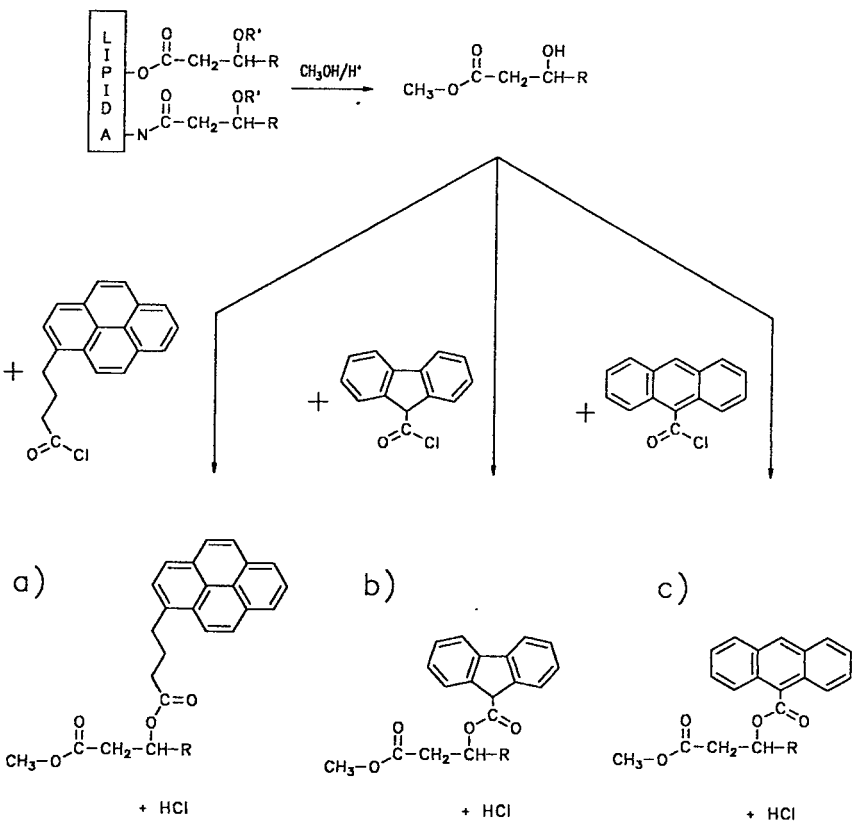

Fig. 1. Formation of β-hydroxy fatty acids from lipid A after methanolysis and derivatization with 4-(1-pyrenyl)butyroyl chloride, 9-fluorenoyl chloride and 9-anthroyl chloride. Resulting products are (a) 3-(4-(1-pyrenyl)butyroyl) fatty acid methyl ester, (b) 3-(9-fluorenoyl) fatty acid methyl ester and (c) 3-(9-anthroyl) fatty acid methyl ester. R:-$(CH_2)_{8/10}-CH_3$; R':-H or-fatty acid.

use. Zinc powder (99%) and boronic acid trimethylester (98%, distilled before use) were delivered by Fluka (Buchs, Switzerland). All solvents used for synthesis and purification were analytical grade (Merck, Darmstadt, Germany). 9-Anthracene carboxylic acid, 9-fluorene carboxylic acid and 4-(1-pyrene)butyric acid (Aldrich) were recrystallized three times in acetonitrile before derivatization with thionylchloride (Fluka, distilled twice). Solvents used for chromatography were of chromatography gradient grade (Merck) and used as delivered. Single use solid-phase extraction cartridges, type Lichrolut Si and Lichrolut RP 18 were obtained from Merck. Glassware for analysis was heated to 300°C for 14 h before use. Plasticware was extracted for 6 h in a Soxhlet apparatus with acetonitrile.

2.2. Apparatus and HPLC conditions

^{1}H NMR spectra were recorded with a Bruker WM 250 NMR spectrometer. Excitation and emission spectra were measured with a Shimadzu RF 551 fluorescence spectrophotometer, which was also used for detection during analysis.

The HPLC apparatus was a Merck-Hitachi system with a L-5000 LC low-pressure gradient controller and a C-655A-12 pump. Detector signals were integrated with a Shimadzu CR 3A Chromatopac integrator. Compounds were separated on a reversed-phase column (NuSil 5 μm 120 Å C_{18}, 250 × 3 mm I.D., Macherey-Nagel, Düren, Germany) with a guard column (20 × 3 mm I.D.), employing a 20 μl sample loop. Flow-rate was 1 ml/min.

2.3. Synthesis of β-hydroxy acid ethyl esters

β-Hydroxymyristic acid ethyl ester and β-hydroxylauric acid ethyl ester were synthesized for use as reference substances, while β-hydroxytridecanoic acid ethyl ester and β-hydroxypentadecanoic acid ethyl ester were synthesized as internal standards. Synthesis was performed by Reformatzky reaction from α-bromoethyl acetate and a 10 g mass of the corresponding aldehyde in tetrahydrofuran in the presence of boronic acid trimethylester and zinc powder [16]. The products were extracted with diethyl ether and the diethyl ether solution was washed three times with water. After removal of the organic solvent, the crude product was distilled twice in vacuo. Table 1 shows the yield, the boiling point at 20 mbar, and the molecular mass obtained from mass spectrometry of the product for each aldehyde reacted. Chemical structures of products were verified by ^{1}H NMR.

^{1}H NMR specifications in $CDCl_3$ δ (ppm) were: 0.88 (6H, t,–C*H*$_3$), 4.17 (2H, q, CH_3–C*H*$_2$–CO_2–), 4.00 (1H, m,–C*H*OH–), 2.34 and 2.55 (2H, m, RCO_2–C*H*$_2$–CHOH–), 1.26–1.38 (16H/18H/20H/22H – $(CH_2)_8$– / –$(CH_2)_9$– / –$(CH_2)_{10}$–/–$(CH_2)_{11}$–).

2.4. Synthesis of carboxylic acid chlorides

For fluorescence labeling, carboxylic acid chlorides were synthesized by derivatization of 9-anthracene carboxylic acid, 9-fluorene carboxylic acid and 4-(1-pyrene)butyric acid with thionylchloride in dried toluene [11]. After removal of the solvent, the product was recrystallized three

Table 1
Yields, boiling points and molecular masses determined by mass spectrometry (m/z M^+) of β-hydroxy acids (first row) formed by the Reformatzky reaction of an aldehyde (second row) with α-bromoacetic acid ethyl ester

Product (~ ethyl ester)	Aldehyde	Yield (%)	b.p. at 20 mbar (°C)	M_r
β-OH(12:0)	Decanal	69	123	244
β-OH(13:0)	Undecanal	74	133	258
β-OH(14:0)	Dodecanal	78	143	272
β-OH(15:0)	Tridecanal	77	152	286

times in dried hexane. During the recrystallization, the humidity of ambient air reacted with acyl chlorides and caused precipitation of insoluble carboxylic acid. These precipitates were removed by filtration of the hot solution through a dried ceramic filter. For color, yield and melting point (uncorrected) see Table 2.

2.5. Synthesis of fluorescence-derivatized β-hydroxy ethyl esters

For determination of fluorescence sensitivity, 1.00 g of β-hydroxymyristic acid ethyl ester, dissolved in 20 ml of dried acetonitrile, was allowed to react with 1.06 g 9-anthroyl chloride, 1.01 g 9-fluorenoyl chloride and 1.35 g 4-(1-pyrenyl)butyroyl chloride, each dissolved in 30 ml of dried acetonitrile (30 min, 22°C). The resulting products were recrystallized three times from ethanol–water. Melting points were determined for 3-(9-anthroyl)myristic acid ethyl ester (white powder, m.p. 37–38°C) and 3-(9-fluorenoyl)myristic acid ethyl ester (white powder, m.p. 36°C). The 3-(4-(1-pyrenyl)butyroyl)myristic acid ethyl ester was a honey-consistent, bright green fluorescent product.

^{1}H NMR specifications in $CDCl_3$ δ (ppm) were:

(1) 3-(9-anthroyl)myristic acid ethyl ester: 0.88 (6H, t,–CH_3), 1.22–1.38 (18H–(CH_2)$_9$–), 1.89 (2H, m,–$CHCO_2Ar$–CH_2–CH_2–), 2.73 and 2.90 (2H, m, RCO_2–CH_2–$CHCO_2Ar$–), 4.20 (2H, q, CH_3–CH_2–CO_2–), 5.86 (1H, m,–$CHCO_2Ar$–), 7.50 (4H, m, Ar–*H*), 8.03 (4H, m, Ar–*H*), 8.50 (1H, s, Ar–*H*).

(2) 3-(9-fluorenoyl)myristic acid ethyl ester: 0.88 (6H, t, CH_3), 1.22–1.38 (18H–(CH_2)$_9$–), 1.61 (2H, m,–$CHCO_2Ar$–CH_2–CH_2–), 2.51 and 2.63 (2H, m, RCO_2–CH_2–$CHCO_2Ar$–), 4.07 (2H, q, CH_3–CH_2–CO_2–), 4.85 (1H, s, Ar–*CH*–Ar), 5.34 (1H, m,–$CHCO_2Ar$–), 7.38 (4H, m, Ar–*H*), 7.65 (2H, m, Ar–*H*), 7.77 (2H, m, Ar–*H*).

(3) 3-(4-(1-pyrenyl)butyroyl)myristic acid ethyl ester: 0.88 (6H, t, CH_3–), 1.22–1.38 (20H–(CH_2)$_9$–), 1.61 (2H, m,–$CHCO_2Ar$–CH_2–CH_2–), 2.17 (2H, m,–$CHCO_2$–CH_2–CH_2–CH_2–CH_2–Ar), 2.43 (2H, t,–$CHCO_2$–CH_2–CH_2–CH_2–CH_2–Ar), 2.57 (2H, m, RCO_2–CH_2–$CHCO_2Ar$–), 3.37 (2H, t, $CHCO_2$–CH_2–CH_2–CH_2–CH_2–Ar), 4.10 (2H, q, CH_3–CH_2–CO_2–), 5.29 (1H, m,–$CHCO_2Ar$–), 7.85 (1H, d, Ar–*H*), 7.94–8.17 (7H, m, Ar–*H*), 8.29 (1H, d, Ar–*H*).

Table 2
Color, yield and melting points of polycyclic hydrocarbon acyl chlorides used for derivatization of β-hydroxy acids

Acid chloride	Color	Yield (%)	m.p. (°C)
9-Anthroyl-	Bright yellow	82	95
9-Fluorenoyl-	Pale brown	85	72
4-(1-pyrenyl)-butyroyl-	Brown	79	82

The maximum excitation and emission wavelengths, fluorescence intensities and detection limits at individual wavelengths of each compound have been determined after HPLC separation.

2.6. Endotoxin standards

Pure endotoxins were obtained by extracting dried bacteria mass (*E. coli* Nissle 1917; Ardeypharm, Herdecke, Germany), using the phenol–water extraction procedure [17]. Further endotoxin standards from *E. coli* serotype 0111:B4 and *Salmonella typhimurium* serotype SL 1181 (Re mutant) were obtained from Sigma (Deisenhofen, Germany).

2.7. Methanolysis of endotoxins and isolation of β-hydroxy acid methyl esters

Endotoxin from *E. coli* Nissle 1917 and *E. coli* 0111:B4 was dissolved in aqueous 0.05% triethylamine solution. The stock solution (1 mg/ml endotoxin) was diluted to give 1 μg/ml endotoxin. The kinetics of methanolysis was investigated using hydrochloric acid (1 mol/l and 4 mol/l in methanol) and sulfuric acid (0.5 mol/l and 2 mol/l in methanol). The acid–methanol mixture was added to 100 μl of the endotoxin

solution to give a final volume of 5 ml. Temperature during methanolysis was kept at 110°C [9,18–20]. The liberation of β-hydroxymyristic acid as methyl ester from endotoxin was determined as a function of acid concentration and duration of heating (procedure described later).

After cooling, 2 ml of water and 1.5 ml of *n*-hexane were added to the clear reaction mixture. This was shaken vigorously (2 min) and the resulting emulsion was centrifuged (10 min, 1500 *g*). The upper hexanoic layer was transferred to a Lichrolut Si cartridge. Washing (4 ml) and elution (double portion of 700 μl) of β-hydroxy acid esters were optimized with various concentrations of *tert.*-butyl methyl ether in *n*-hexane. The eluted solution was collected in screw-cap vials (vial volume 1.5 ml) and the solvent was removed with a dry nitrogen stream at room temperature.

2.8. Derivatisation of β-hydroxy acid methyl esters

A 100-μl volume of 9-anthroyl chloride, 9-fluorenoyl chloride, or 4-(1-pyrenyl)-butyroyl chloride in acetonitrile (5 mg/ml) was added separately to residues obtained from the above described procedure. The vials were closed with Teflon-sealed screw-caps and allowed to react after vigorous shaking. According to the reported kinetics of acylation of hydroxyl groups with 9-anthroyl chloride [12,15], β-hydroxy acid methyl esters were allowed to react with 9-anthroyl chloride for 20 min at room temperature or kept for 10 min at 60°C.

The reaction mixture could not be employed directly for analysis in HPLC because of the high ratio of reagent to product. At a β-hydroxymyristic acid [β-OH(14:0)] amount of 10 pg, the mass ratio of 9-anthroyl chloride to β-OH(14:0) was 50 millions to one. The initial peak (9-anthracene carboxylic acid) intensity descended too slowly to enable quantitation of the β-OH(14:0) derivative. Therefore, the reaction mixture was adsorbed on a Lichrolut RP 18 cartridge, and excess reagent was removed by an acetonitrile–water mixture.

Before adsorption, C_{18} cartridges were conditioned with 1 ml acetonitrile–water (60:40, v/v) avoiding dry-running of the cartridge filling prior to the addition of the sample. Water (40 μl) was added to the reaction mixture. After 5 min, the solution was applied to a RP 18 cartridge and allowed to adsorb (5 min). The cartridge was washed with 5 ml acetonitrile–water (60:40) and dried by the vacuum-induced air flow (10 min). The fluorescence-derivatized compounds were extracted with acetonitrile. The solvent was removed from eluent with dry nitrogen at room temperature, and the residue was redissolved in 150 μl acetonitrile. This solution was employed directly for HPLC quantitation.

According to the described procedure, β-hydroxylauric acid methyl ester, β-hydroxytridecanoic acid methyl ester, β-hydroxymyristic acid methyl ester, β-hydroxypentadecanoic acid methyl ester and the ethyl esters of the mentioned β-hydroxy acids were esterified with 9-anthroyl chloride, 9-fluorenoyl chloride, and 4-(1-pyrenyl)butyroyl chloride. Fluorescence spectra of the synthesized 24 reaction products were compared with regard to their excitation and emission wavelengths, their signal intensities and their detection limits.

3. Results

3.1. Fluorescence spectra, linearity of standard curve, HPLC separation and detection limits of fluorescence-labeled β-hydroxy acid esters

The synthesized fluorescent products were dissolved in acetonitrile–water (95:5, v/v, 10 ng/ml). From this solution, fluorescence spectra of the anthroyl-, the fluorenoyl- and the 4-(1-pyrenyl)butyroyl)derivatized β-hydroxy acid ethyl esters were recorded (Fig. 2) and the excitation and emission maxima were determined (Table 3). The highest signal intensities were obtained using the following excitation/emission wavelengths: anthroyl derivative: 250 nm/462 nm, fluorenoyl derivative 262 nm/310 nm and 4-(1-pyrenyl)butyroyl derivative: 238

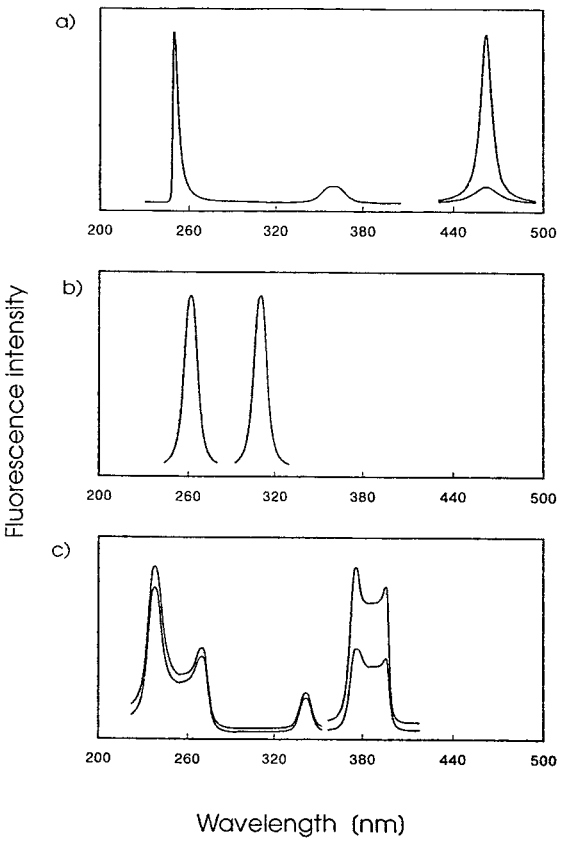

Fig. 2. (a) Fluorescence spectrum of 3-(9-anthroyl)myristic acid methyl ester dissolved in acetonitrile–water (95:5, v/v, 10 ng/ml); excitation wavelength maxima were at 250 nm and 360 nm, emission maxima were at 462 nm for both excitation wavelengths; fluorescence intensity ratio of 462 nm emission at 250 nm excitation to that at 360 nm was 12:1. (b) Fluorescence spectrum of 3-(9-fluorenoyl)myristic acid methyl ester dissolved in acetonitrile–water (95:5, v/v, 10 ng/ml); excitation wavelength maximum was at 262 nm; emission maximum was at 310 nm. (c) Fluorescence spectrum of 3-(4-(1-pyrenyl)butyroyl)myristic acid methyl ester dissolved in acetonitrile–water (95:5, v/v, 10 ng/ml); excitation wavelength maxima were at 238 nm, 270 nm and 336 nm; emission maxima were at 376 nm and 395 nm; fluorescence intensity ratio of emissions (376 nm and 395 nm) at 238 nm excitation to emission at 270 nm excitation was 2.4:1, fluorescence intensity ratio of emission at 376 nm to emission at 395 nm at maximum intensity excitation wavelengths (238 nm and 270 nm) was 1.15:1.

nm/376 nm. These wavelength pairings were used for comparison of sensitivity of the single compounds.

Table 3
Excitation and emission wavelengths of β-hydroxymyristic acid ethyl ester after derivatization with three different polycyclic acyl chlorides

β-Hydroxy acid ethyl ester derivative	Excitation (nm)	Emission (nm)
9-Anthroyl-	**250**, 360	462
9-Fluorenoyl-	262	310
4-(1-pyrenyl)-butyroyl-	**238**, 270, 342	**376**, 396

In case of more than one excitation/emission maxima, the values of the most intensive wavelength combination are in bold.

No influence of the chain length of the β-hydroxy acid esters or the kind of ester (methyl or ethyl ester, spectra recorded prior and after methanolysis) on the fluorescence spectra was observed. Using a 250 mm 5 μm RP 18 column and acetonitrile–water (95:5, v/v) as mobile phase resulted in baseline separation of each of the investigated β-hydroxy acid methyl ester derivatives (Fig. 3).

The lowest detection limit (signal-to-noise ratio 3:1) was obtained for the anthroyl derivative (0.4 fmol). Amounts between 2 fmol [0.5 pg β-OH(14:0)] and 1 pmol [240 pg β-OH(14:0)] showed a linear correlation to the measured fluorescence signal. The comparison of the signal intensities was based on the detector response (area under the curve, unit: mVs).

Two fmol, 4 fmol, 8 fmol, 14 fmol, and 20 fmol of 3-(9-anthroyl)myristic acid ethyl ester, 3-(9-fluorenoyl)myristic acid ethyl ester, and 3-[4-(1-pyrenyl)butyroyl]myristic acid ethyl ester were separately dissolved in 150 μl acetonitrile. Signal intensities of this solutions were measured after HPLC separation at specific excitation and emission wavelengths for each fluorophore (Fig. 4). The fluorescence signal intensity of the anthroyl derivative was 7.4 times higher, the intensity of the 9-fluorenoyl derivative 2.5 times higher than that of the 4-(1-pyrenyl)butyroyl derivative. Therefore, all further studies were carried out using 9-anthroyl chloride as derivatizing agent.

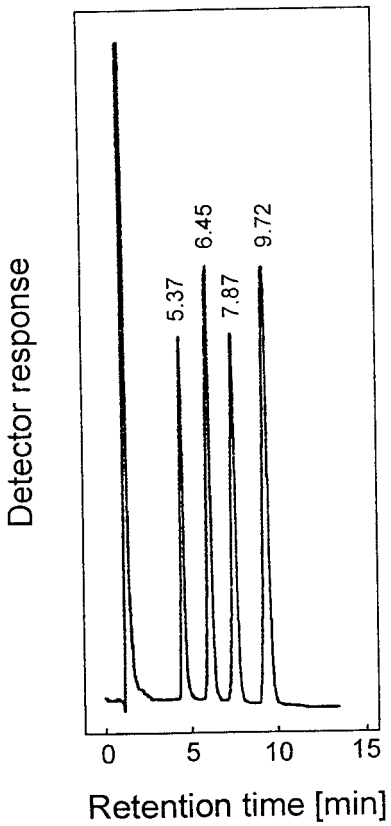

Fig. 3. Chromatogram showing peaks of 3-(9-anthroyl)lauric acid methyl ester (5.37 min), 3-(9-anthroyl)tridecanoic acid methyl ester (6.45 min), 3-(9-anthroyl)myristic acid methyl ester (7.87 min) and 3-(9-anthroyl)pentadecanoic acid methyl ester (9.72 min). Derivatization was carried out on a sample containing 10 ng each of β-hydroxy acid ethyl esters. HPLC: column, 5 μm RP 18, 250 × 3 mm I.D.; mobile phase, acetonitrile–water (95:5, v/v), 1 ml/min; sample loop, 10 μl; fluorescence detection at excitation (Ex) = 250 nm and emission (Em) = 462 nm.

3.2. Formation of β-hydroxy acid methyl esters from endotoxin

The literature-cited concentration of acid catalyst used for the liberation of β-hydroxymyristic acid from endotoxins for methanolysis prior to GC–MS analysis varies between 1 mol/l [21] and 4 mol/l [10], the duration of the heating between 1 h [19] and 18 h [10]. For optimization of both these reaction parameters, hydrochloric acid (1 mol/l and 4 mol/l) and sulfuric acid (0.5 mol/l and 2 mol/l) were used. The samples with 100 ng endotoxin from *E. coli* 0111:B4 were heated for 0.5, 1, 2, 4 and 8 h. Fig. 5 shows the kinetics of the liberation of β-hydroxymyristic acid from endotoxin. β-Hydroxypentadecanoic acid was used as an internal standard. Recoveries were calculated from the fluorescence intensity/concentration ratio of the isolated derivatives.

After 4 h, the reaction showed a steady state

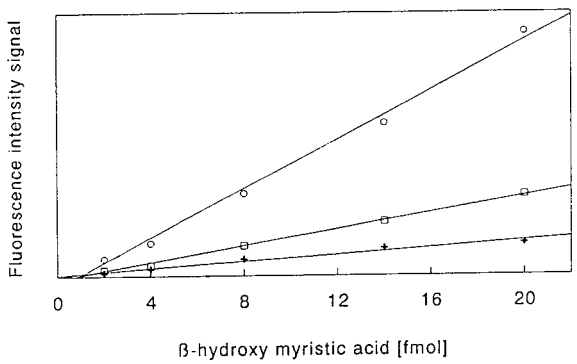

Fig. 4. Comparison of fluorescence signal intensities (average of three determinations) of 3-(9-anthroyl)myristic acid methyl ester (○: Ex = 250 nm, Em = 462 nm), 3-(9-fluorenoyl)myristic acid methyl ester (□: Ex = 262 nm, Em = 310 nm) and 3-(4-(1-pyrenyl)butyroyl)myristic acid methyl ester (+ : Ex = 238 nm, Em = 376 nm). HPLC conditions as in Fig. 3.

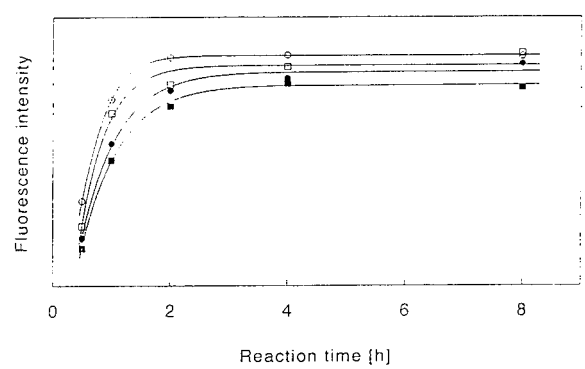

Fig. 5. Kinetics of formation of free β-hydroxymyristic acid methyl ester from endotoxin of *E. coli* 0111:B4 with varying concentrations of hydrochloric acid (○: 4 mol/l; ●: 2 mol/l) and sulfuric acid (□: 2 mol/l; ■: 1 mol/l). β-Hydroxymyristic acid methyl ester was analyzed according to described procedure. HPLC conditions as in Fig. 3.

with all employed acid concentrations and the best results were obtained with sulfuric acid. Therefore, heating at 110°C for 4 h with 2 mol/l sulfuric acid was selected for methanolysis.

3.3. Separation of β-hydroxy acid methyl esters

After methanolysis, extraction with *n*-hexane, and solid-phase adsorption on Lichrolut Si cartridges, β-hydroxy (myristic and pentadecanoic) acid methyl esters were washed (4 ml), and eluted (2 × 700 μl) with increasing concentrations of *tert.*-butyl methyl ether in *n*-hexane. β-Hydroxy fatty acids were not eluted from the adsorbent at a *tert.*-butyl methyl ether concentration of 8% (v/v), but were completely eluted with 1 ml of a solvent containing 25% *tert.*-butyl methyl ether in hexane (Fig. 6a).

3.4. Removal of excess reagent

Because of the high ratio of excess reagent to product, the reaction mixture could not be employed directly for analysis in HPLC. For removal of excess reagent, the reaction mixture was allowed to adsorb on RP 18 cartridges. For optimization of cartridge washing, increasing acetonitrile concentrations were tested (Fig. 6b). Best results were obtained using 5 ml of a acetonitrile–water mixture (60:40, v/v) for washing. The product was eluted completely from the cartridge with 1 ml acetonitrile. The whole analysis method is summarized in Table 4.

3.5. Detection limits of endotoxins

Standard solutions with concentrations between 10 pg/ml and 10 ng/ml of each of the three investigated endotoxins were analyzed according to the optimized procedure. β-Hydroxypentadecanoic acid ethyl ester was used as an internal standard for quantitation of endotoxins with β-hydroxymyristic acid. Endotoxins may have a changing number of oligosaccharide units in their polysaccharide chain and do not posses a defined molecular mass [4]. The content of β-hydroxy acid varies, depending on the length of the polysaccharide chain. So, the different con-

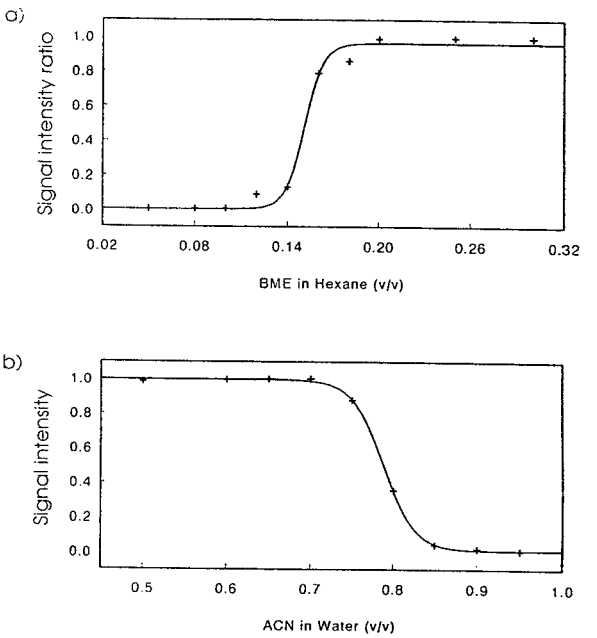

Fig. 6. (a) Elution profile of β-hydroxymyristic acid methyl ester from Lichrolut Si cartridges with increasing concentration of *tert.*-butyl methyl ether (BME) in hexane; elution volume: 2 × 700 μl. Signal intensity ratio was calculated from the signal intensities of eluted β-hydroxymyristic acid methyl ester before and after adsorption on cartridges. The ester concentration was 100 pg/ml, 387 fmol/ml) in hexane, the applied volume 1.5 ml. The ester was derivatized with 9-anthroylchloride (5 mg/ml in acetonitrile, 100 μl, 20 min at room temperature) after removal of hexane. HPLC conditions as in Fig. 3. (b) Elution of 3-(9-anthroyl)myristic acid methyl ester from RP 18 cartridges with increasing concentration of acetonitrile in water during the preelution procedure; 3-(9-anthroyl)myristic acid methyl ester (277 pg dissolved in 50 μl acetonitrile–water, 50:50) was applied to a cartridge and washed with 5 ml of varying acetonitrile concentrations in water. After preelution, remaining derivatives were eluted with 1 ml acetonitrile. HPLC conditions as in Fig. 3.

tents of β-hydroxymyristic acid were determined in the investigated lipopolysaccharides (LPS). β-Hydroxy acid content of the endotoxins from the smooth strain (*E. coli* 0111:B4) was only 32 μg β-OH(14:0)/mg LPS. Endotoxin from the rough strains (*Salmonella typhimurium* SL 1181 and *E. coli* Nissle 1917) contained more β-hydroxymyristic acid [154 μg β-OH(14:0)/mg LPS and 108 μg β-OH(14:0)/mg LPS], according to a reduced or missing polysaccharide chain. De-

Table 4
Summary of steps used in lipopolysaccharide determination

Step	Reagent/volume	Reaction time/ reaction temperature
Methanolysis	4 *M* H_2SO_4 in methanol, 5 ml total volume	4 h/110°C
Extraction	with 1.5 ml hexane, after addition of 2 ml water	
Solid-phase extraction I	Si cartridges	
Washing I	*tert.*-butyl methyl ether–hexane 8:92, 4 ml	
Extraction I	*tert.*-butyl methyl ether–hexane 25:75, 2 × 700 μl	
Derivatization	9-anthroylchloride in acetonitrile (5 mg/ml), 100 μl	20 min, room temperature or 10 min 60°C
Hydrolysis of excess reagent	40 μl water	5 min, room temperature
Solid-phase extraction II	RP 18 cartridges, preconditioned with acetonitrile–water 60:40	adsorption time: 5 min
Washing II	acetonitrile–water 60:40, 5 ml	
Extraction II	acetonitrile, 1 ml	
HPLC analysis	(HPLC conditions see caption for Fig. 3)	

tection limits of endotoxins were 20 pg for smooth strain and 5 pg of rough strain endotoxin per sample (Fig. 7). These endotoxin amounts were detected successfully dissolved in 10 ml pyrogen-free water, if a vacuum centrifuge was used prior to analysis. No disturbing peaks at related retention times were found in pyrogen-free water and buffer solutions, investigated with the described method. Pyrogen-free bovine serum albumin (up to 1 mg/ml) did not affect the accuracy of the test.

3.6. Recovery

Endotoxin from *E. coli* 0111:B4 was dissolved in 0.05% aqueous solution of triethylamine and diluted to give concentrations of 10 ng/ml and 1 ng/ml. Recoveries and reproducibility were determined from six-fold analysis of each solution (100 μl) with β-hydroxypentadecanoic acid ethyl ester as internal standard (100 pg/sample and 10 pg/sample). The measured recovery was 92.5 ± 6.4% (mean ± S.D.) for the 1 ng amount and 78.5 ± 8.8% for the 100 pg amount. The 100% value was determined from the purified 3-(9-anthroyl)pentadecanoic acid ethyl ester.

4. Discussion

The described results indicate a highly sensitive method for analysis of β-hydroxy acids used

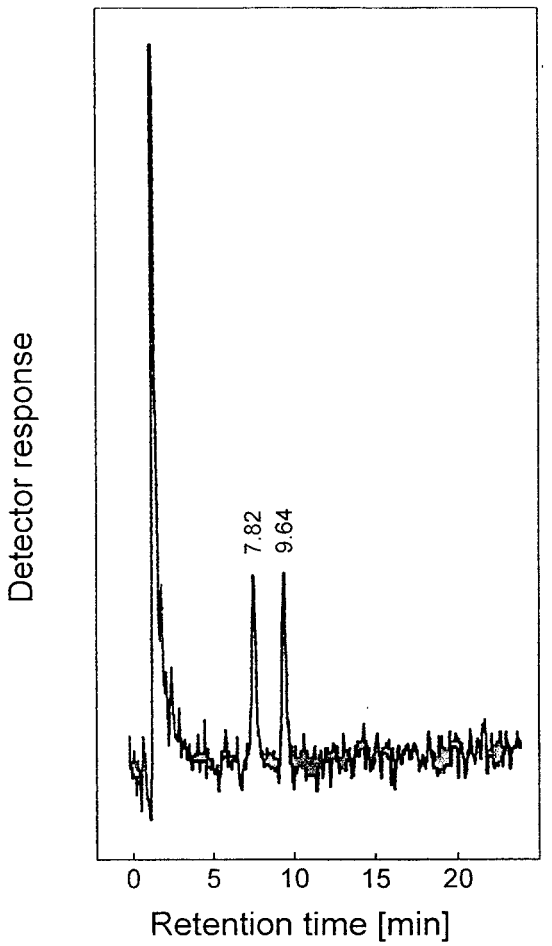

Fig. 7. Chromatogram of 20 pg endotoxin from *E. coli* Nissle 1917 (7.82 min) and 2 pg β-hydroxypentadecanoic acid ethyl ester (9.64 min) after methanolysis and derivatization with 9-anthroyl chloride followed by twofold solid-phase extraction. HPLC conditions as in Fig. 3.

as markers for the determination of lipid A, the toxic component of lipopolysaccharides.

Analysis of specific microbial pyrogenic components is of special importance for investigation of compounds having contact with the systemic blood stream or tissue of mammals. The most common technique of measuring endotoxin content in aqueous solutions is the LAL test, an assay where lipid A activates the clotting cascade in a lysate from amebocytes from *Limulus polyphemus* [22]. Values for endotoxin contents in outer bacteria membranes determined by radioimmuno assays were about 10 times higher than the amounts measured with the LAL assay [23]. Further, false-negative results have been reported for the LAL assay as a result of inactivation of the enzymes of the clotting cascade [24]. Comparison of endotoxin contents in airborne dusts from poultry-processing industries by the LAL test and GC–MS analysis showed that the values determined by GC–MS were 10^2 to 10^5 above those obtained by LAL [9], calculated from the content of β-hydroxymyristic acid.

The discrepancy in these results is caused by the different approaches to the measurement of endotoxins. The LAL test is very sensitive (<5 pg/ml) [5], but rather measures a biological effect of endotoxins, which can be affected by physical, biological and chemical properties of the sample matrix [25,26]. Electrolytes, proteins and hormones for example may inactivate the clotting cascade of the LAL assay [24].

β-Hydroxy acids are essential for pyrogenity of endotoxins [22,27]. Hence, the absence of these acids is a sufficient evidence for the absence of pyrogens from Gram-negative bacteria. A further established technique for measuring the content of endotoxins is the determination via GC–MS [8–11,18], but the expensive equipment and the great demand on personnel qualification limits the application of this method.

The described method may be used to determine endotoxins in aqueous solutions, using β-hydroxy acids as markers, detecting lipopolysaccharides in both the free and the hidden state. Since proteins are destroyed by acid-catalyzed methanolysis, no "hiding" of endotoxins by protein adsorption can occur. Endotoxins can be quantitated by the described method even in the presence of proteins. In the presence of albumin (1 mg/ml), endotoxins could be still detected with the same precision. The applicability of this assay still has to be proved for other matrices.

With acetonitrile as a solvent there were no noticeable problems of adsorption on the used plastic- and glassware, even at sub-ng/ml con-

centrations. This fact can also be seen from the determined recovery at sub-ng/ml levels.

Contamination and memory effects were circumvented by using only single-use adsorption cartridges and heating glassware for 14 h at 300°C. After keeping glassware at this temperature, no contamination or memory effects occurred.

Although a normal-phase HPLC separation of β-hydroxy acids with adjacent aromatic polycyclic hydrocarbons has been described [15], we decided to develop a reversed-phase HPLC assay. During acylation with acyl chlorides, it is unavoidable that a part of the acyl chloride reacts with ubiquitous traces of water forming the free acid. This acid is adsorbed on the column during normal-phase HPLC, changing the surface properties of the stationary phase and making it difficult to obtain reproducible results. In reversed-phase chromatography, the polar carboxylic acid is eluted prior to the acylated products, so that no disturbance can occur during the following analysis.

Obtaining really dry acetonitrile and keeping it dry for and in routine applications is of essential interest carrying out derivatisations with carboxylic chlorides. Even commercially obtainable "ultra-dried" solvents contain about 50 ppm water. This amount, together with surface-adsorbed water on glass vials and air humidity reacts with the derivatizing agent. The reactivity of the hydrolyzed product, the free carboxylic acid, is too poor for formation of β-hydroxy acid methyl esters. Hence, acyl chloride concentrations of 1 μg/ml [15] proved to be too low for complete derivatization during routine analysis.

Apart from water, other reactive compounds such as alcohols and amines if present in the sample, can react with the acyl chloride making the derivatization incomplete. This makes it necessary to use excess derivatizing agent. In practice, a concentration of 5 mg/ml of anthroyl chloride showed the best results, making a visual control during analysis possible. The yellow color of the 9-anthroyl solution in acetonitrile faded to nearly colorless if the acid chloride was destroyed by the presence of reactive compounds. In this case, practically no acylation of β-hydroxy acids could be observed. A further control of complete acylation is given by the use of an internal standard.

β-Hydroxylauric acid could also be detected by this assay (Fig. 2) with comparable detection limits, indicating the presence of *Neisseria meningitidis* [11]. Because of the high pathogenity of this microorganism and the lack of commercially available *Neisseria* endotoxin the applicability of this HPLC assay was not tested.

The catalysis of acylation with 9-anthroyl chloride by organoamine bases like pyridine or 4-dimethylaminopyridine has been reported to be unsuccessful [28], therefore no efforts were made to prove reaction enhancement by these compounds.

Acknowledgements

We are indebted to Drs. B. Vogler and C.O. Meese for assistance in the recording and interpretation of NMR spectra. This work was supported by the Robert-Bosch-Stiftung (grant F2).

References

[1] E. Rietschel, T. Kirikae, U. Schade, A. Ulmer, O. Holst, H. Brade, G. Schmidt, U. Mamat, H.-D. Grimmecke, S. Kusumoto and U. Zähringer, Immunobiol., 187 (1993) 169.
[2] C. Galanos, O. Lüderitz, E. Rietschel and O. Westphal, Int. Rev. Biochem. Biochemistry of Lipids II, (T. Goodwin, Editor), 14 (1977) 239.
[3] J. Hewett and R. Roth, Pharmacol. Rev., 45 (1993) 381.
[4] P. Friberger, in J. ten Cate, H. Büller, A. Sturk and J. Levin (Editors), Bacterial Endotoxins: Structure, Biomedical Significance and Detection with the Limulus Amebocyte Lysate Test, Alan R. Liss, New York, 1985, p. 139.
[5] H. Fukui, B. Brauner, J. Ch. Bode and Ch. Bode, J. Hepat., 12 (1991) 162.
[6] R. Elin and A. Utter, J. Clin. Microbiol., 12 (1980) 502.
[7] T. Mikami, T. Nagase, T. Matsumoto, S. Suzuki and M. Suzuki, Microbiol. Immunol., 26 (1982) 403.
[8] S.K. Maitra, R. Nachum and F.C. Pearson, Appl. Environ. Microbiol., 52 (1986) 510.
[9] A. Sonesson, L. Larsson, A. Schutz, L. Hagmar and T. Hallberg, Appl. Environ. Microbiol., 56 (1990) 1271.

[10] A. Sonesson, L. Larsson, R. Andersson, N. Adner and K.G. Tranberg, J. Clin. Microbiol., 28 (1990) 1163.
[11] P. Brandtzaeg, K. Bryn, P. Kierulf, R. Ovstebo, E. Namork, B. Aase and E. Jantzen, J. Clin. Invest., 89 (1992) 816.
[12] M. Bayliss and R. Homer, J. Chromatogr., 445 (1988) 393.
[13] H. Takamura and M. Kito, J. Biochem., 109 (1991) 436.
[14] J. Browning and D. Nelson, J. Membrane Biol., 49 (1979) 75.
[15] K. Tanamoto, Adv. Exp. Med. Biol., 256 (1990) 203.
[16] K. Nützel, Organo-Zink Verbindungen, Bd. XIII/2 Springer, Stuttgart, 1976, p. 809.
[17] O. Westphal and K. Jann, Meth. Carbohydr. Res., 63 (1965) 83.
[18] S.K. Maitra, M.C. Schotz, T.T. Yoshikawa and L.B. Guze, Proc. Natl. Acad. Sci. USA, 75 (1978) 3993.
[19] J. Parker, G. Smith, H. Fredrickson, J. Vestal and D. White, Appl. Environ. Microbiol., 44 (1982) 1170.
[20] A. Sonesson, L. Larsson and J. Jimenez, J. Chromatogr., 490 (1989) 71.
[21] A. Sonesson, L. Larsson, G. Westerdahl and G. Odham, J. Chromatogr., 417 (1987) 11.
[22] H. Takada, S. Kotani, S. Tanaka, T. Ogawa, I. Takahashi, M. Tsujimoto, T. Komuro, T. Shiba, S. Kusumoto, N. Kusunose, A. Hasegawa and M. Kiso, Eur. J. Biochem., 175 (1988) 573.
[23] R. Munford and C. Hall, in S. Watson, J. Levin and T. Novitsky (Editors), Detection of Bacterial Endotoxins with the Limulus Amebocyte Lysate Test, Alan R. Riss, New York, 1987, p. 93.
[24] A. Weiss, in S. Watson, J. Levin and T. Novitsky (Editors), Detection of Bacterial Endotoxins with the Limulus Amebocyte Lysate Test, Alan R. Riss, New York, 1987, p. 235.
[25] D. Morrison, S. Vukajlovich, J. Ryan and J. Levin, in S. Watson, J. Levin and T. Novitsky (Editros), Detection of Bacterial Endotoxins with the Limulus Amebocyte Lysate Test, Alan R. Riss, New York, 1987, p. 55.
[26] F. Pearson, R. Caruana, J. Burkart, D. Katz, D. Chenoweth, J. Dubczak, J. Bohon and M. Weary, in S. Watson, J. Levin and T. Novitsky (Editors), Detection of Bacterial Endotoxins with the Limulus Amebocyte Lysate Test, Alan R. Riss, New York, 1987, p. 211.
[27] J. Homma, M. Matasura, S. Kanegasaki, Y. Kawakubo, Y. Kojima, N. Shibukawa, Y. Kumazawa, A. Yamamoto, K. Tanamoto, T. Yasuda, M. Imoto, H. Yoshimura, S. Kusumoto and T. Shiba, J. Biochem., 98 (1985) 395.
[28] M. Bayliss, R. Homêr and M. Shepherd, J. Chem. Soc., Chem. Commun., (1990) 305.

ELSEVIER

Journal of Chromatography A, 711 (1995) 289–295

JOURNAL OF CHROMATOGRAPHY A

Quantitation of digitoxin, digoxin, and their metabolites by high-performance liquid chromatography using pulsed amperometric detection

Kevin L. Kelly*, Bruce A. Kimball, John J. Johnston

U.S. Department of Agriculture, Animal and Health Inspection Service, Denver Wildlife Research Center, Building 16, Denver Federal Center, Denver, CO 80225, USA

First received 24 January 1995; revised manuscript received 25 April 1995; accepted 1 May 1995

Abstract

A novel detection method for the cardiac glycosides digitoxin, digoxin, and their metabolites is described. Both isocratic and gradient water–acetonitrile elutions were employed with an octadecylsilane column. The effluent was monitored by integrated pulsed amperometry in an alkaline medium (pH > 12) by adding sodium hydroxide post-column. Using isocratic elution, peak responses were linear from 10 to 70 ng, with lower limits of detection between 4 and 15 ng. This method allows easy modification of well-established high-performance liquid chromatographic systems, as well as comparable sensitivity and greater selectivity than UV detection.

1. Introduction

Digitoxin and digoxin are secondary cardiac glycosides which occur naturally in the foxglove plant (i.e. *Digitalis lanata* and *Digitalis purpurea*) through enzymatic conversion of their respective primary cardiac glycosides, lanatoside A and C. These compounds are widely used in the therapeutic treatment of heart disease. It is well known that cardioactive metabolites can be produced from these glycosides by stepwise cleavage of the three digitoxose sugars attached to the aglycone steroid at the C-3 atom [1,2]. The major metabolic products are digitoxose, mono- and bisdigitoxosides, and the remaining aglycone steroid, either digitoxigenin or digoxigenin (Table 1). In some cases, the metabolites are more toxic than the parent compounds [3].

A wide variety of chromatographic methods have been used for the separation of cardiac glycosides, including gas (GC) [4–6], thin-layer (TLC) [7–9], and high-performance liquid chromatography (HPLC) [10–16]. The GC procedures require hydrolysis to yield the corresponding aglycone, which is subsequently derivatized for greater volatility. Although these procedures employ sensitive GC detectors, the determination of individual cardiac glycosides within the same cardenolide series is not possible because they all contain the same aglycone. The TLC methods generally suffer from a lack of sensitivity, long development times, poor resolution, or require long post-separation conditioning times for more sensitive fluorescence detection [7]. High-performance liquid chro-

* Corresponding author.

SSDI 0021-9673(95)00525-0

Table 1
Structures of the cardiac glycosides and aglycones

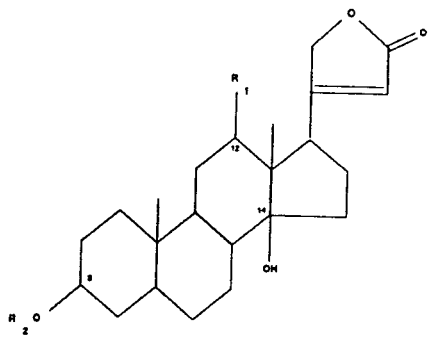

Compound	R_1	R_2^a
Digitoxin	H	-D-D-D
Digitoxigenin bisdigitoxoside	H	-D-D
Digitoxigenin monodigitoxoside	H	-D
Digitoxigenin	H	H
Digoxin	OH	-D-D-D
Digoxigenin bisdigitoxoside	OH	-D-D
Digoxigenin monodigitoxoside	OH	-D
Digoxigenin	OH	H

[a] D = D-digitoxose (2,6-dideoxy-ribo-hexose).

matographic separations of cardiac glycosides involve less labor, and yield fast, reproducible results. However, the cardiac glycosides contain a relatively weak UV chromophore with λ_{max} at about 220 nm. Many organic compounds absorb at this wavelength and will interfere if they are not adequately separated from the cardiac glycosides. In addition, mobile phase solvents with high transparency at 220 nm must be used in order to achieve low detection limits. Pre- or post-column derivatization is necessary to achieve more selective and sensitive UV or fluorescence detection [17,18].

This work focuses on the use of pulsed amperometric detection (PAD) for the quantitation of the cardiac glycosides and their corresponding aglycones. This method was investigated for the detection of the sugar moieties of the cardiac glycosides because of the success of previous works using PAD for the detection of carbohydrates [19–23]. Furthermore, pulsed amperometric detection allows specific electrochemical detection without derivatization. Carbohydrates are detected by direct oxidation on a gold working electrode under alkaline conditions. Standard high-performance liquid chromatographic systems can be easily modified to permit PAD detection of the cardiac glycosides and their aglycones.

2. Experimental

2.1. Instrumentation

A Hewlett-Packard 1090M liquid chromatograph equipped with a computer workstation (Hewlett-Packard, Palo Alto, CA, USA) was used for the separation of digitoxin, digoxin, and their metabolites. The octadecylsilane analytical column measured 250 × 4.6 mm I.D. (Deltabond, Keystone Scientific, Bellefonte, PA, USA).

The chromatograph was equipped with a pulsed electrochemical detector (Dionex Corp., Sunnyvale, CA, USA) operated in the integrated amperometry mode.

A gradient pump (Dionex, series 4500i) was used to deliver 1.0 *M* sodium hydroxide postcolumn. The electrochemical cell consisted of an organic solvent compatible gold working electrode (1.4 mm), a stainless steel counter electrode, and a Ag/AgCl reference electrode. The gasket, which permits flow across the working electrode, was 0.005 inch thick. The detector analog signal was inputted to the workstation via a multichannel interface (HP 35900, Hewlett-Packard).

2.2. Reagents

Digitoxin, digitoxigenin, digoxin, and digoxigenin were obtained from Sigma (St. Louis, MO, USA). Digoxigenin monodigitoxoside was provided by Burroughs Wellcome Co. (Research Triangle, NC, USA). All other mono- and bisdigitoxosides were obtained from Indofine Chemical Co. (Belle Mead, NJ, USA). All analytes were of analytical grade and used with-

out further purification. The molecular structures of these compounds are given in Table 1. Stock solutions of each cardiac glycoside and aglycone were prepared separately in HPLC grade methanol (Fisher Scientific, Fair Lawn, NJ, USA). The stock solutions were kept in the dark and refrigerated at 4°C. No degradation of the analytes was observed over 30 days when the stock solutions were in use. These stock solutions were then used to prepare separate and mixed diluted working standards of the cardiac glycosides on the day of the chromatographic experiments.

HPLC grade acetonitrile (ACN, Fisher Scientific) was filtered once through a 0.45-μm nylon filter before use. Water was purified using the Milli-Q + purification system (0.22 μm, Millipore, Molsheim, France). Concentrated 50% w/w sodium hydroxide (NaOH) was obtained from J.T. Baker (Phillipsburg, NJ, USA) and diluted with water to a concentration of 1.0 *M*. All solvents were degassed with industrial grade helium (Airco Gases, Denver, CO, USA). A helium headspace was maintained in the NaOH reservoir to prevent absorption of carbon dioxide.

2.3. Procedure

Separation of each cardenolide series was done under isocratic conditions. The mobile phase composition was water–ACN (67:33, v/v) for the digitoxin cardenolide series, and water–ACN (77:23, v/v) for the digoxin cardenolide series. For the separation of a combined mixture of both the digitoxin and digoxin cardenolide series, a linear gradient elution from water–ACN (90:10) to water–ACN (55:45) over 8 min was performed. The HPLC flow-rate was 1.0 ml/min for isocratic elution and 1.3 ml/min for gradient elution. The post-column addition of 1.0 *M* NaOH was done at an optimum flow-rate of 0.5 ml/min. A 500-μl reaction coil (Dionex) was used after the tee to ensure uniform mixing prior to the detector.

For PAD detection, the applied potentials and their durations were as followed: $E_1 = +0.07$ V, $t_1 = 400$ ms; $E_2 = +0.70$ V, $t_2 = 120$ ms; $E_3 = -1.00$ V, $t_3 = 300$ ms. The duration of the sampling period was 300 ms. The analog full-scale range was 100 nanocoulomb (nC) for isocratic elution and 300 nC for gradient elution.

The gold working electrode was lightly polished approximately every 200 h to remove oxidized materials. No degradation in the reproducibility or the stability of the gold working electrode was observed over a period of 9 months.

Calibration curves were constructed using the mean peak areas from triplicate chromatograms under the same isocratic conditions as discussed previously. A minimum of 4 standard solutions within the range of 10–70 ng/ml were used for each calibration curve.

To measure the effect of the concentration of ACN in the mobile phase on peak area, the column was replaced with a zero dead volume union connector and injections of digoxigenin monodigitoxoside were made. Small aliquots (100 μl) of the stock solution of the compound were evaporated under nitrogen and reconstituted in the same water–ACN solution as used for the HPLC mobile phase. The reconstituted solutions were further diluted to 1.0 ml each to achieve a final concentration of 48.9 μg/ml. Triplicate injections were made in the order of increasing % ACN composition at 10% increment intervals from 10% to 90%. The flow-rates for the HPLC and IC pumps were 0.6 ml/min and 0.3 ml/min, keeping the same flow-rate ratio as in the isocratic elutions. All other parameters remained the same.

3. Results and discussion

3.1. Chromatography

A representative chromatogram is shown in Fig. 1 for the digoxin cardenolides series using an isocratic mobile phase composition. In addition, separation of all 8 cardenolides compounds from both the digitoxin and digoxin series during gradient elution is shown in Fig. 2. The decreasing drift in the baseline in Fig. 2 is due to adsorption of ACN on the surface of the gold working electrode, hindering detection of the

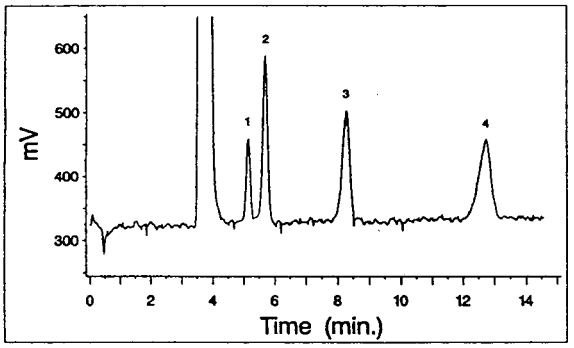

Fig. 1. Isocratic separation of a mixed standard of digoxigenin (1), digoxigenin monodigitoxoside (2), digoxigenin bisdigitoxoside (3), and digoxin (4) obtained by reversed-phase HPLC; 50 pmole of each compound injected in 10 μl of methanol. The mobile phase was water–ACN (77:23) at a flow-rate of 1.0 ml/min. The large unlabeled peak at ± 4 min is methanol.

analytes [22,24]. The chromatograms presented here demonstrate that the cardiac glycosides and aglycones can be quantitated in various mobile phase compositions of water and acetonitrile using pulsed amperometric detection.

3.2. Pulsed amperometric detection

The oxidation of the glycosides is believed to take place on the terminal digitoxose and lactone rings (Table 1). Both cyclic and acyclic conformations may be involved. Primary alcohols, polyhydroxyl compounds, glycols, and carbohydrates have been detected with PAD in alkaline media [19–23,25–28]. All of these are organic compounds with hydroxyl functional groups. Adsorption of the analyte onto the surface of the working electrode via hydrogen bonding with catalytic AuOH groups is important to several proposed detection mechanisms [22,29,30]. Hydroxyl groups on the terminal digitoxose and lactone rings are less sterically hindered than other functional groups elsewhere on the molecule. Thus for equal molar concentrations of terminal digitoxose and lactone units, the glycosides would be expected to have similar response factors. For the aglycones, the response factors would be expected to be different due to the absence of any digitoxose moieties. In addition to the lactone ring, oxidation may also take place on the hydroxyl group at the C-3 position. For example, the detection of cyclohexanol has been reported [22]. Other hydroxyl groups at positions C-12 and C-14 are more sterically hindered and would not be expected to be electroactive. For these reasons, both digitoxigenin and digoxigenin would be expected to have similar response factors.

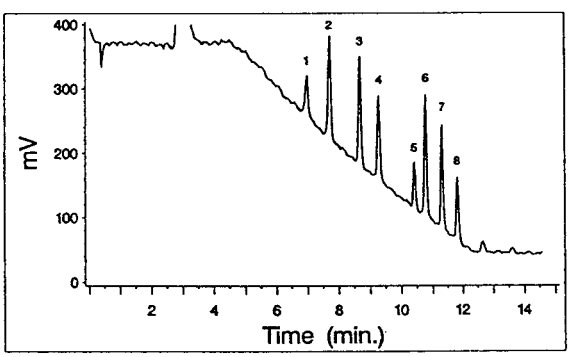

Fig. 2. Gradient separation of a mixed standard of digoxigenin (1), digoxigenin monodigitoxoside (2), digoxigenin bisdigitoxoside (3), digoxin (4), digitoxigenin (5), digitoxigenin monodigitoxoside (6), digitoxigenin bisdigitoxoside (7), and digitoxin (8). Conditions were indentical to those in Fig. 1 except that the mobile phase consisted of a linear gradient from water–ACN (90:10) to water–ACN (55:45) over 8 min at a flow-rate of 1.3 ml/min.

The peak area vs. analyte mass data are presented graphically in Fig. 3. Each pair of aglycone, bisdigitoxoside, monodigitoxoside, and secondary glycoside from both cardenolide series behaved similarly. This was expected since the only structural difference between the digitoxin and digoxin cardenolide series is at the sterically hindered C-12 position of the aglycone (Table 1). The hydroxyl group present at the C-12 position on the digoxigenin aglycone is not electroactive, as evidenced by the similar behavior of digitoxigenin and digoxigenin. For the glycosides, the slopes of the curves are related to the molecular mass of the compound. Since, at a given mass, molar concentrations of the terminal digitoxose and lactone moieties are inversely proportional to the molecular mass (i.e. monodigitoxosides > bisdigitoxisides > secondary glycosides), the electrochemical response is greater for the lower-molecular-mass com-

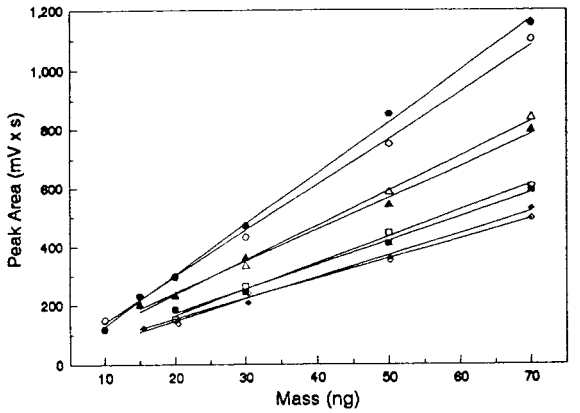

Fig. 3. Mean peak area vs. analyte mass for digitoxin, digoxin, and their metabolites. (■) digitoxin; (▲) digitoxigenin bisdigitoxoside; (●) digitoxigenin monodigitoxoside; (◆) digitoxigenin; (□) digoxin; (△) digoxigenin bisdigitoxoside; (○) digoxigenin monodigitoxoside; (◇) digoxigenin.

pounds. For the aglycones, the lack of any digitoxose moieties result in a lower oxidation current.

When the data in Fig. 3 was plotted as peak area vs. molar concentration of analyte, the resulting curves were found to be grouped into two distinct groups, the glycosides and the aglycones. At a given molarity, each glycoside has equal molar concentration of the terminal digitoxose and lactone units. As a result, they all have similar response factors. The lack of a digitoxose unit resulted in lower anodic oxidation rates for the aglycones. Upon closer inspection of the curves within the glycoside group, a pattern exists where the response factor is inversely related to the size of the compound: monodigitoxosides > bisdigitoxisides > secondary glycosides. Differences in response factors within the glycoside group may be attributed to small differences in molecular diffusion rates and oxidation reaction kinetics. Diffusion rates are inversely proportional to molecular mass according to Stokes' Law [31]. Larger molecules diffuse more slowly and would be less efficient at migrating to the surface of the gold working electrode. The kinetics of adsorption, dehydrogenation, electron and oxygen transfers, and displacement during the oxidation of the analyte may be also be influenced by the size of the molecule.

Table 2
Limits of detection for digitoxin, digoxin, and their metabolites

Compound	Limit of detection (injection volume, 10 μl)	
	Isocratic (ng/μl)	Gradient (ng/μl)
Digitoxin	1.43	0.40
Digitoxigenin bisdigitoxoside	1.22	0.28
Digitoxigenin monodigitoxoside	0.77	0.20
Digitoxigenin	1.34	0.35
Digoxin	1.06	0.23
Digoxigenin bisdigitoxoside	0.72	0.19
Digoxigenin monodigitoxoside	0.44	0.16
Digoxigenin	0.67	0.26

3.3. Limits of detection

The limits of detection for the various compounds are provided in Table 2 for both isocratic and gradient elutions. The conditions used are the same as those for Figs. 1 and 2. The limit of detection was calculated as the amount of compound which will produce a peak-height response equal to three times the detector baseline peak-to-peak noise. The limits of detection presented in Table 2 for PAD detection of the steroids are comparable to the limits of detection reported for UV detection at 220 nm [10,11,13,14]. However, PAD detection is more sensitive than the reported limits of detection for UV detection at 220 nm for the analysis of the digitoxose containing glycosides.

3.4. Response linearity

The curves in Fig. 3 are linear ($r^2 > 0.973$) in the range of 10–70 ng for the monodigitoxisides, 15–70 ng for the bisdigitoxosides and aglycones, and 20–70 ng for the secondary glycosides. The ranges were chosen to include concentrations typically used for chromatographic assays using UV detection [10–16]. The ranges are also applicable to pharmaceutical preparations of digitalis glycosides and extracts of *Digitalis*. The

method described here can be used for pharmaceutical quality control of digitoxin and digoxin tablets and injections, or for screening of *Digitalis* plant materials for maximum yield of the cardenolides. The mean coefficient of variation for the detector response in the range of 20–70 ng was 4.1% for the digitoxin cardenolide series and 7.6% for the digoxin cardenolide series.

3.5. Effect of ACN on detector response

The choice of organic modifier must be made with care. Some common oxygenated modifiers, such as methanol, acetone, dioxane, and tetrahydrofuran, produce prohibitively high background current. Acetonitrile is the most commonly used organic modifier for the reversed-phase separation of the cardiac glycosides. However, mobile phase compositions with high percentage of ACN greatly attenuated the peak areas of all of the cardiac glycosides and aglycones used in this study. Acetonitrile hinders detection by adsorbing to the surface of the gold working electrode [22,24]. The effect of % ACN composition on the peak area of a model compound, digoxigenin monodigitoxoside, is shown in Fig. 4. Digoxigenin monodigitoxoside was used because it is soluble in the mobile phase compositions chosen for this study. At ACN compositions of less than approximately 30%, detector response was not affected. At ACN compositions between 30% to 70%, the analyte peak area displays an inverse relationship with % ACN composition. At approximately 70% ACN, the baseline noise increased dramatically. At ACN compositions greater than 80%, the peak is no longer quantifiable due to decreased analyte response and increased background noise.

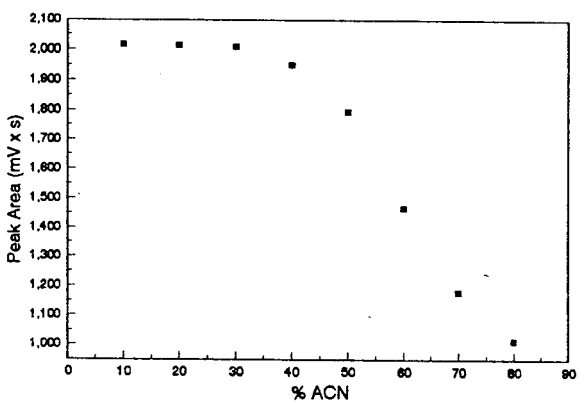

Fig. 4. Mean peak area vs. % mobile phase composition of ACN. Column was replaced with a zero dead volume connector. Solvent composition of the injected standard was the same as that of the mobile phase.

The isocratic separations of the digitoxin and digoxin cardenolide series were performed at the upper plateau region of the % ACN curve shown in Fig. 4. However, during the gradient separation shown in Fig. 2, peak areas of the compounds eluting at higher % ACN were probably attenuated. This explains why detection limits are higher for the digitoxin cardenolide series than for the digoxin cardenolide series during gradient elution.

3.6. Selectivity

Another major advantage of pulsed amperometric detection is direct and selective detection. No pre- or post-column derivatization is necessary. Selectivity is dependent on the oxidation potentials of the target and interfering compounds present in the sample. Adjustment of the applied potential (E_1) is made to reduce or eliminate interferences from other compounds. This helps reduce losses of the target analytes during clean-up of the sample extract or during derivatization reactions. In some cases, the adjustments of the % ACN composition in the mobile phase or the addition of ACN post-column can be made to reduce detector responses from potential interferences such as alcohols and simple sugars [22,24].

In conclusion, a HPLC method has been developed for the determination of the *Digitalis* cardiac glycosides with greater sensitivity and selectivity than UV detection at 220 nm. The analytes are separated on a conventional octadecylsilane column. Well-established HPLC methods can be easily modified to allow detection by PAD.

4. Safety

Safety precautions such as laboratory coats, gloves, safety goggles, and fume hoods should be used when handling solvents and cardioactive compounds.

Acknowledgements

The authors would like to thank Dionex Corporation for loaning the pulsed electrochemical detector. We are also grateful for the donation of digoxigenin monodigitoxoside from Burroughs Wellcome Company. The assistance of Paige Groninger for the preparation of the graphics is also greatly appreciated. Mention of commercial products is for identification only and does not constitute endorsement by the United States Department of Agriculture.

References

[1] K. Repke, in W. Wilbrandt (Editor), Proc. First Int. Pharmacol. Meeting, Vol. 3, Pergamon Press, New York, 1963, p. 47.
[2] G.T. Okita, in C. Fisch and B. Surawicz (Editors), Digitalis, Grune and Stratton, New York, 1969, p. 13.
[3] G.L. Lage and J.L. Spratt, J. Pharmacol. Exp. Ther., 152 (1966) 501.
[4] R.W. Jelliffe and D.H. Blakenhorn, J. Chromatogr., 12 (1963) 268.
[5] E. Watson, P. Tramell and S.M. Kalman, J. Chromatogr., 69 (1972) 157.
[6] L. Tan, J. Chromatogr., 45 (1969) 68.
[7] G.W. Ponder and J.T. Stewart, J. Chromatogr. A, 659 (1994) 177.
[8] S.M. Khafagy and A.N. Girgis, Planta Med., 25 (1974) 267.
[9] C.J. Clarke and P.H. Cobb, J. Chromatogr., 168 (1979) 541.
[10] W. Lindner and R.W. Frei, J. Chromatogr., 117 (1976) 81.
[11] M.C. Castle, J. Chromatogr., 115 (1975) 437.
[12] L. Sternson and R.D. Shaffer, J. Pharm. Sci., 67 (1978) 327.
[13] Y. Fujii, H. Fukuda, Y. Saito and M. Yamazaki, J. Chromatogr., 202 (1980) 139.
[14] F. Erni and R.W. Frei, J. Chromatogr., 130 (1977) 169.
[15] B. Pekic, S.M. Petrovic and B. Slavica, J. Chromatogr., 268 (1983) 237.
[16] B. Desta, E. Kwong and K.M. McErlane, J. Chromatogr., 240 (1982) 137.
[17] F. Nachtmann, H. Spitzy and R.W. Frei, J. Chromatogr., 122 (1976) 293.
[18] J.C. Gfeller, G. Frey and R.W. Frei, J. Chromatogr., 142 (1977) 271.
[19] S. Hughes and D.C. Johnson, Anal. Chim. Acta, 132 (1981) 11.
[20] R.D. Rocklin and C.A. Pohl, J. Liq. Chromatogr., 6 (1983) 1577.
[21] P. Edwards, Food Technol., 37 (1983) 53.
[22] D.C. Johnson and W.R. LaCourse, Anal. Chem., 62 (1990) 589A.
[23] B. Herbreteau, Analusis, 20 (1992) 355.
[24] W.R. LaCourse, W.A. Jackson and D.C. Johnson, Anal. Chem., 61 (1989) 2466.
[25] R.D. Rocklin and C.A. Pohl, J. Liq. Chromatogr., 30 (1983) 1577.
[26] P. Edwards and K.K. Haak, Amer. Lab., April (1983) 78.
[27] W.T. Edwards, C.A. Pohl and R. Rubin, Tappi J., 70 (1987) 138.
[28] J. Olechno, S.R. Carter, W.T. Edwards and D.G. Gillen, Am. Biotech. Lab., 5 (1987) 38.
[29] L.A. Larew and D.C. Johnson, J. Electroanal. Chem., 262 (1989) 167.
[30] Y.B. Vassilyev, O.A. Khazova and N.N. Nikolaeva, J. Electroanal. Chem., 196 (1985) 127.
[31] G.G. Stokes, Trans. Cambridge Phil. Soc., Ser. 9 (1851) No. 8.

ELSEVIER

Journal of Chromatography A, 711 (1995) 297–304

JOURNAL OF CHROMATOGRAPHY A

Combined polymerized chiral micelle and γ-cyclodextrin for chiral separation in capillary electrophoresis

Jian Wang, Isiah M. Warner*

Department of Chemistry, Louisiana State University, Baton Rouge, LA 70803, USA

First received 13 September 1994; revised manuscript received 27 April 1995; accepted 28 April 1995

Abstract

A combination of a polymerized chiral micelle, poly(sodium N-undecylenyl-D-valinate) [poly(D-SUV)] and γ-cyclodextrin (γ-CD) is used for the first time for chiral separation in capillary electrophoresis. A simple theory is presented to rationalize the synergistic effect of the enantioselectivity obtained by use of poly(D-SUV) and γ-CD in combination. A mixture of four enantiomeric pairs is successfully resolved by use of this combination. The resolutions of the enantiomers using this approach are far superior to those obtained by use of either poly(D-SUV) or γ-CD alone. In addition, the effects of the antipode (L-SUV), γ-CD concentration, buffer concentration, organic solvents, and urea concentration on the resolution are also examined.

1. Introduction

Chiral separation by use of capillary electrophoresis (CE) has become a research area of major focus in recent years [1–3]. This is largely due to the impact of CE on the pharmaceutical industry. Since a large fraction of therapeutic drugs are racemic compounds and many of them are either cationic or anionic, CE is an obvious tool to investigate the optical purity and separation of such drugs. Separation by use of CE offers greater separation efficiency within a shorter analysis time as compared to conventional chromatographic techniques. Direct chiral separation in CE is achieved either through the use of immobilized chiral phases or through the addition of chiral selectors as mobile phase additives. In the latter case, three types of chiral selectors are often employed: (1) host–guest chiral selectors [4–8], (2) chiral metal complexes [9,10], and (3) chiral surfactants [11–13]. The latter method has been termed micellar electrokinetic capillary chromatography (MECC).

Cyclodextrins (CDs) have been widely used as chiral selectors in chromatographic techniques and in CE [4–7,14] because of their ability to form highly selective molecular inclusion complexes with a variety of neutral or ionic organic species. The CDs are cyclic oligosaccharides consisting of α 1–4 linkage of D-(+)-glucopyranoside units. The unique torus shape of CDs and the fact that each glucose unit has five chiral centers are characteristics that have enabled these oligosaccharides to be effectively used in chiral separations. Since CDs are neutral compounds and migrate with the electroosmotic flow (EOF) in CE, their separation abilities are limited. Therefore, ionic derivatives of CDs and

* Corresponding author.

0021-9673/95/$09.50
SSDI 0021-9673(95)00515-3

CD–MECC have been used to achieve improved chiral separation [15–18]. The CD–MECC technique combines CDs and micellar systems into the same buffer. This approach was initially used to separate highly hydrophobic compounds [19], but is now widely used in chiral separations [16–18]. However, there is an inherent disadvantage with this approach. The available surfactant monomers in the buffer are partly associated in a complex with the CDs [20,21]. Thus, in many cases, complexation of surfactant monomers with CDs will interfere with interactions between the individual enantiomers and the CDs. This interference will directly affect the enantioselectivity of the system and may reduce the observed chiral resolution.

Chiral micelles have also been used for separation of enantiomers. Most polar organic solutes are able to interact with a micelle on the surface through polar–polar interactions as well as hydrophobic interactions with the core of the micelle. In addition, many chiral compounds will have chiral centers near a polar group. Thus, a surfactant having a chiral center near a polar head group should be suitable for enantiomeric separation by use of MECC. Different types of chiral surfactants have been used in CE chiral separation, including amino acid-derivatized synthetic surfactants, bile salts, and other natural surfactants. Furthermore, Okafo et al. [22] and Terabe et al. [23] have combined the use of bile salts and cyclodextrins for separation of enantiomers in a variety of compounds.

As discussed earlier, a normal micellar system combined with a CD will likely form an inclusion complex between the CD and the surfactant monomer. In many cases, this will reduce the enantioselectivity of CDs. In addition, the use of normal micelles in MECC separation has other limitations. For example, the concentration of the surfactant used in MECC has to be above the critical micellar concentration (CMC) in order to be effective. Thus, for a surfactant with a high CMC, the working concentration range may be very narrow, since at very high concentrations of a charged surfactant, excess heat will be generated in the capillary. This heat production will normally inhibit optimal separation.

We recently synthesized a novel polymerized chiral micelle, poly(sodium N-undecylenyl-L-valinate) and successfully used it for chiral separation in MECC [24]. The polymerized micelle not only possesses normal micellar properties but also has several advantages over normal micelles, including enhanced stability because of covalent linkage of the surfactant monomers. This property can be used in CD–MECC to diminish the normal inclusion phenomena associated with surfactant monomers and CDs. There is also no CMC for polymerized micelles. This property allows use of the polymerized micelle in MECC over a wider working concentration range [25]. Finally, polymerized micelles are typically more rigid than normal micelles. Since the solute cannot penetrate deep into the rigid, polymerized micelles, interactions between the solute and the polymerized micelle must occur near the surface of the micelles. Thus, the mass transfer rate of the solute, between a polymerized micelle and the bulk solution, should be faster than that of a normal micellar system, which allows penetration of the solute via dynamic equilibrium.

In this manuscript, we report the first chiral separation which employs a combination of a polymerized chiral micelle and γ-CD. The polymerized chiral micelles used in this study are poly(sodium N-undecylenyl-L-valinate) [poly(L-SUV)] and its antipode poly(sodium N-undecylenyl-D-valinate) [poly(D-SUV)]. The separation of a mixture of four enantiomeric pairs by use of poly(D-SUV) and γ-CD is superior to the separation obtained by using either poly(D-SUV) or γ-CD, separately. The separation mechanism of this synergistic effect is presented. In addition, the effects of the antipode [poly (L-SUV)], γ-CD concentration, the buffer concentration, and organic solvents on the chiral separation are also evaluated.

2. Experimental

2.1. Materials

The procedure for synthesis of poly(L-SUV) and the characterization of poly(L-SUV) have been recently reported [24]. The same procedure

is used for synthesis of poly(D-SUV) ($[a]_D^{25} = +8.0^0$ ($c = 1.00$ in water)). It is found that poly(D-SUV) has the same physico-chemical properties as poly(L-SUV) in achiral environments. (±)-1,1′-Bi-2-naphthol (99%), (*R*)-(+)-1,1′-bi-2-naphthol (99%), *S*-(−)-1,1′-bi-2-naphthol (99%), (±)-1,1′-binaphthyl-2,2′-diyl hydrogen phosphate ($BNPO_4$) (99%), and (±)-verapamil (95%) were purchased from Aldrich (Milwaukee, WI, USA). D,L-Laudanosine (95%), L-valine (>99%), D-valine (99%), and undecylenic acid (>99%) were obtained from Sigma (St. Louis, MO, USA). The γ-cyclodextrin used in this study was a gift from American Maize Products (Hammond, IN, USA). These items were used as received.

2.2. Capillary electrophoresis

Micellar electrokinetic capillary chromatography experiments were conducted by use of a CES I capillary electrophoresis system (Dionex, Sunnyvale, CA, USA). Data were collected by use of an AI-450 chromatography workstation. An untreated fused-silica capillary (effective length 60 cm, 75 μm I.D.) was purchased from Polymicro Technologies (Phoenix, AZ, USA) and used as a separation column. The solution was buffered at pH 9 using borate buffer. The polymerized micelles and γ-CD were added directly to the buffer system. The buffer solutions were filtered through a 0.45-μm membrane filter prior to use. Separations were performed at 12 kV with UV detection at 280 nm. Samples were prepared in a methanol–water mixture in a concentration range from 0.02 to 0.1 mg/ml.

3. Results and discussion

3.1. Theory

Since this CD-modified polymerized chiral micellar system is similar to a normal CD–MECC system, we can use normal CD–MECC theory [3] with minor modifications where appropriate. In our system, the polymerized chiral micelle behaves as a pseudo-stationary phase. It is assumed that the neutral γ-CD is part of the aqueous phase. In addition, it is assumed that the enantiomers interact independently with the polymerized micelle and the γ-CD. Thus, the capacity factor, k', can be defined as:

$$k' = \frac{n_{mp}}{n_{aq}} \tag{1}$$

where n_{mp} and n_{aq} are the moles of solute molecules associated with the polymerized micelle and the moles associated with the aqueous phase (including CD), respectively. In addition,

$$n_{aq} = n_f + n_{CD} \tag{2}$$

since the moles of solute in the aqueous phase include not only the moles of free solute, n_f, but also the solute molecules incorporated in CD, n_{CD}.

Based on a partitioning mechanism in this CD–chiral MECC system, there are two important partitions for an enantiomer A:

$$[A]_f \rightleftarrows [A]_{mp} \tag{3}$$

$$[A]_f \rightleftarrows [A]_{CD} \tag{4}$$

where $[A]_f$, $[A]_{mp}$, and $[A]_{CD}$ are the concentration of the enantiomer, A, in the aqueous phase, micelle polymer, and cyclodextrin, respectively. Thus, we can obtain

$$\frac{n_{mp,A}}{n_{f,A}} = K_{mp,A}\frac{V_{mp}}{V_f} \tag{5}$$

$$\frac{n_{CD,A}}{n_{f,A}} = K_{CD,A}\frac{V_{CD}}{V_f} \tag{6}$$

where K_{mp} and K_{CD} are partition coefficients between the polymerized micelle and the aqueous phase and between the CD and the aqueous phase, respectively, and V_f, V_{mp}, and V_{CD} are the volume of the aqueous phase, the micellar phase, and the cyclodextrin phase, respectively. We can combine Eqs. 1, 2, 5, and 6 to obtain

$$k' = \frac{K_{mp}V_{mp}}{V_f + V_{CD}K_{CD}} \tag{7}$$

Selectivity for an enantiomeric pair can be defined as

$$\alpha = \frac{k'_{app,B}}{k'_{app,A}} \quad (8)$$

where $k'_{app,A}$ and $k'_{app,B}$ are apparent capacity factors for the enantiomeric pair, A and B, respectively.

From Eqs. 7 and 8, we can derive:

$$\alpha = \frac{1 + \phi_{CD} K_{CD,A} K_{mp,B}}{1 + \phi_{CD} K_{CD,B} K_{mp,A}} \quad (9)$$

where ϕ_{CD} is the phase ratio of the volume of CD (V_{CD}) to that of the aqueous phase (V_f). Selectivity is directly related to resolution (R_s). For a given plate number N and apparent capacity factor k', the greater the value of α, the higher is the resolution (R_s). From Eq. 9, since α must be ≥ 1, it can be shown that there are only three combinations of these parameters: (1) if $K_{CD,A} > K_{CD,B}$ and $K_{mp,B} > K_{mp,A}$, chiral resolution will be superior to that obtained using either CD or the polymerized chiral micelle alone; (2) if $K_{CD,A} > K_{CD,B}$ and $K_{mp,A} > K_{mp,B}$, chiral resolution will be poorer than by use of γ-CD alone; (3) if $K_{CD,A} < K_{CD,B}$ and $K_{mp,B} > K_{mp,A}$, then resolution will be poorer than by use of the polymerized chiral micelle alone. Fig. 1 provides a demonstration of the enantiomeric separation obtained through a combination of γ-CD and poly(D-SUV) and also validates Eq. 9. When using only γ-CD as a chiral selector, *R*-1,1′-bi-2-naphthol has a high affinity for γ-CD and will migrate faster than the *S*-form (Fig. 1a). When using only poly(D-SUV) as a chiral selector, the *S*-1,1′-bi-2-naphthol interacts stronger with the polymer than the *R*-form and *R*-1,1′-bi-2-naphthol will migrate through the system faster than the *S*-form (Fig. 1b). If we combine these two chiral selectors, it is found that $K_{CD,R} > K_{CD,S}$ and $K_{mp,S} > K_{mp,R}$. Therefore, chiral resolution will be greater than by use of either chiral selector alone. This synergistic effect of γ-CD and poly(D-SUV) on the separation of *R*,*S*-1,1′-bi-2-naphthol is demonstrated in Fig. 1c. Furthermore, as shown in Fig. 1d, while combining γ-CD and poly(L-SUV), the chiral resolution is diminished, which corresponds to the condition where $K_{CD,R} > K_{CD,S}$ and $K_{mp,R} > K_{mp,S}$.

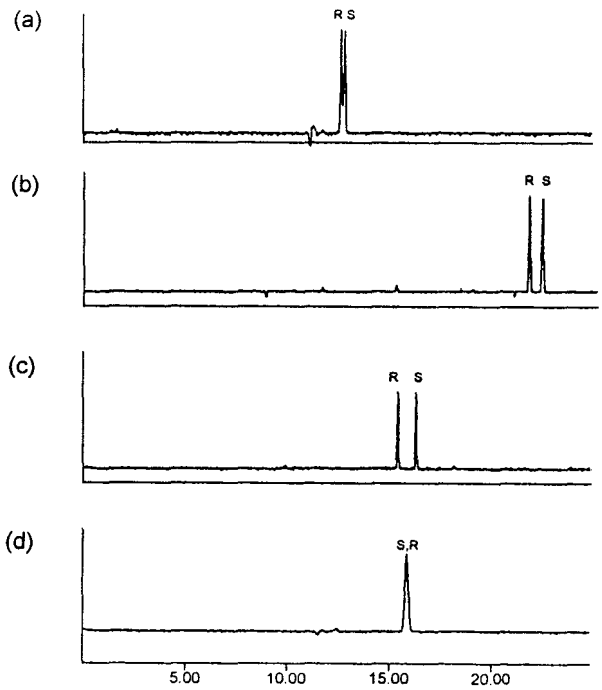

Fig. 1. Chiral separation of (±)-1,1′-binaphthol by use of poly(D-SUV) and γ-CD. CE conditions: 25 m*M* borate buffer (pH 9); applied voltage, 12 kV; UV detection, 280 nm. (a) 10 m*M* γ-CD, (b) 0.5% poly(D-SUV), (c) 10 m*M* γ-CD and 0.5% poly(D-SUV), (d) 10 m*M* γ-CD and 0.5% poly(L-SUV).

3.2. Separation of mixtures of chiral compounds by use of γ-CD and poly(D-SUV)

A combination of γ-CD and poly(D-SUV) not only enhances chiral selectivity but also extends the migration window of CD-modified CE since CDs are neutral compounds and migrate with the EOF. Fig. 2 shows the separation of a mixture of four enantiomeric compounds. Using either γ-CD or poly(D-SUV) alone at the concentrations examined, no satisfactory resolution is obtained (Fig. 2a,b). However, use of both γ-CD and poly(D-SUV) at the same concentrations resolves three enantiomeric pairs (Fig. 2c). With further optimization, all four compounds are resolved (Fig. 2d).

Since there are a number of parameters which affect chiral separations, the separation mechanism of polymerized chiral micelles is not always

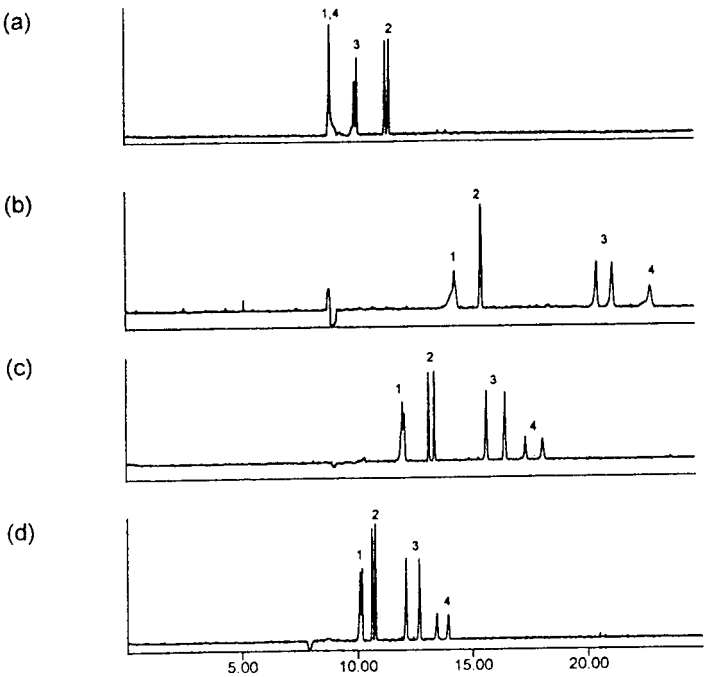

Fig. 2. Chiral separation of four enantiomeric pairs. Peaks: 1 = D,L-laudanosine, 2 = (±)-$BNPO_4$, 3 = (±)-1,1′-binaphthol, 4 = (±)-verapamil. CE conditions: (a) 10 m*M* γ-CD, (b) 0.5% poly(D-SUV), (c) 10 m*M* γ-CD and 0.5% poly(D-SUV), buffer for (a), (b) and (c) is 25 m*M* borate (pH 9), (d) 10 m*M* γ-CD and 0.5% poly(D-SUV), 5 m*M* borate (pH 9). Applied voltage, 12 kV; UV detection, 280 nm.

clear. In the present work, a series of experiments are conducted in order to optimize this CD–chiral MECC system.

3.3. Effect of γ-CD concentration on enantiomeric resolution

The effect of γ-CD concentration on the separation is investigated over the concentration range 5–20 m*M*. Fig. 3 shows the effect of CD concentration on the resolution of four enantiomeric compounds. Resolution generally increases with increasing cyclodextrin concentration up to a point where maximum separation is reached. Further increases in CD concentration result in a decrease in resolution. The optimum concentration of cyclodextrin is dependent on the enantiomeric pair being separated. These observations are consistent with data in the literature [7]. There are several models which can be used for quantitative optimization

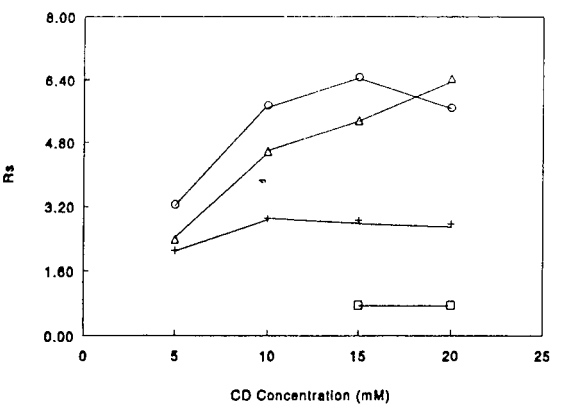

Fig. 3. Effect of γ-CD concentration on the resolution of the enantiomeric mixture. CE conditions: 0.5% poly(D-SUV), 25 m*M* borate (pH 9), 5–20 m*M* γ-CD; applied voltage, 12 kV; UV detection, 280 nm. (○) (±)-1,1′-binaphthol, (△) (±)-verapamil, (+) (±)-$BNPO_4$, (□) D,L-laudanosine.

[7,26,27]. However, we can qualitatively estimate the optimum CD concentration for (±)-$BNPO_4$ to be approximately 10 m*M*; for (±)-1,1′-bi-2-naphthol the optimum concentration is approximately 15 m*M*; for (±)-verapamil the optimum concentration is above 20 m*M*. In the case of D,L-laudanosine, an increase in γ-CD concentration initially improves the enantiomeric separation but further increase of the concentration does not significantly enhance the resolution. This observation suggests that the interactions between D,L-laudanosine enantiomers and γ-CD are weak and the resolution cannot be improved significantly by the addition of γ-CD alone.

3.4. Effect of buffer concentration on enantiomeric resolution

Generally, the buffer concentration controls the ionic strength of the electrolyte. Increasing the buffer concentration will reduce the EOF and also increase the viscosity of the electrolyte. This expands the migration time window for the CD–MECC system. However, this does not necessarily mean that resolution of the enantiomers will be increased. In our chiral separations, an increase in the borate buffer concentration from 5 to 45 m*M* lengthens the migration time for each compound. The resolutions of most enantiomeric pairs are enhanced, except for D,L-laudanosine where the resolution is decreased (Fig. 4). These observations are consistent with results obtained in our previous study [24]. The charged chiral polymer is more flexible at lower buffer concentration than at higher buffer concentration. This is because, at low buffer concentrations the polymerized micelle has fewer closely associated counterions than at high buffer concentrations. Thus, the micelle can extend more at low buffer concentrations than at high concentrations of buffer. This effect may induce a larger difference in affinities between the individual D- and L-enantiomeric forms at the lower buffer concentration and thus results in better resolution.

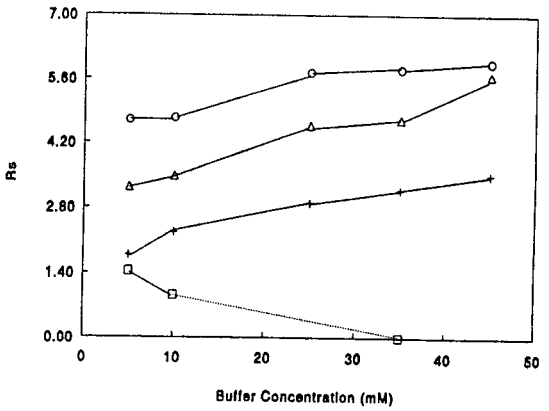

Fig. 4. Effect of buffer concentration on the resolution of the enantiomeric mixture. CE conditions: 0.5% poly(D-SUV), 5–45 m*M* borate (pH 9), 10 m*M* γ-CD; applied voltage, 12 kV; UV detection, 280 nm. (○) (±)-1,1′-binaphthol, (△) (±)-verapamil, (+) (±)-$BNPO_4$, (□) D,L-laudanosine.

3.5. Effect of organic solvents on enantiomeric resolution

The effects of organic modifiers on chiral resolution will not only depend on the type of chiral selectors used in the system but also on the properties of the enantiomers, e.g. their hydrophobic and hydrophilic properties. In general, the migration time of the samples increases with an increase in concentration of organic solvents. This is due to a decrease in the EOF. In normal MECC or CD–MECC, if the concentration of an organic solvent such as methanol is very high, the micelle will decompose into surfactant monomers and solute–micelle interaction is not possible. However, in our system, at very high concentrations of methanol (40%), the enantiomeric resolutions of the compounds examined are still very good (Fig. 5), except for D,L-laudanosine. Even in the presence of a small amount of methanol, separation of D,L-laudanosine is impaired. It is also very interesting in Fig. 5 that the remaining three enantiomeric pairs behave very differently. For example, the enantiomeric resolution of (±)-1,1′-bi-2-naphthol is improved by increasing methanol concentration. When only the poly(D-SUV) is used in the buffer, the resolution of (±)-1,1′-bi-

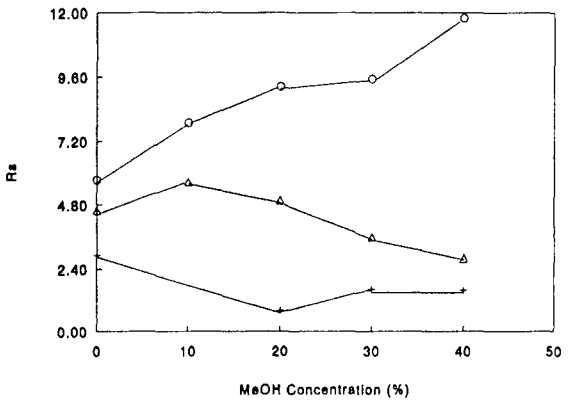

Fig. 5. Effect of methanol concentration on the resolution of the enantiomeric mixture. CE conditions: 0.5% poly(D-SUV), 25 m*M* borate (pH 9), 10 m*M* γ-CD, 0–40% MeOH; applied voltage, 12 kV; UV detection, 280 nm. (○) (±)-1,1′-binaphthol, (△) (±)-verapamil, (+) (±)-$BNPO_4$.

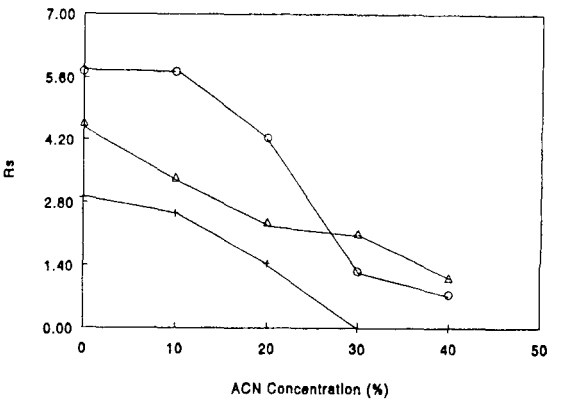

Fig. 6. Effect of ACN concentration on the resolution of the enantiomeric mixture. CE conditions: 0.5% poly(D-SUV), 25 m*M* borate (pH 9), 10 m*M* γ-CD, 0–40% ACN; applied voltage, 12 kV; UV detection, 280 nm. (○) (±)-1,1′-binaphthol, (△) (±)-verapamil, (+) (±)-$BNPO_4$.

2-naphthol is increased with an increase in methanol concentration. However, when only γ-CD is used, resolution is slightly decreased with an increase in methanol concentration. Thus, this combination shows a net increase of resolution upon addition of methanol. Enantiomeric resolution of (±)-verapamil increases with increasing concentration of methanol up to 10%. However, above 10% methanol, the resolution starts to decrease with increasing concentration of methanol. In contrast, the enantioselectivity of (±)-$BNPO_4$ is decreased with increasing methanol concentration up to 10%. Upon further addition of methanol, the resolution starts to increase, although the highest resolution is still obtained using the buffer without methanol. These observations show that the addition of methanol to the buffer produces different effects on the interactions between individual enantiomeric pairs with the chiral selectors [poly(D-SUV), γ-CD]. Since these effects are also solute-dependent, different resolution curves for different enantiomeric pairs are obtained.

Acetonitrile (ACN) is another frequently used organic solvent. As shown in Fig. 6, the addition of ACN decreases the resolution of the enantiomers. Since the pair of D,L-laudanosine has the weakest interaction with both the polymerized chiral micelle and the γ-CD, the presence of a small amount of ACN impairs the resolution of the enantiomers. It is known that ACN can displace solutes from cyclodextrin cavities, which would be expected to reduce the chiral recognition of the γ-CD.

4. Conclusions

As shown in these studies, chiral separation of the four enantiomeric pairs by use of poly(D-SUV) and γ-CD is superior to the use of either chiral selector alone. The modified theory we present here adequately explains the observed synergistic effect on the enantioselectivity by use of both chiral selectors. Since surfactant monomers do not exist in the covalently bonded polymerized micelle, the interference of surfactant monomers on the enantioselectivity of γ-CD is eliminated. Therefore, the use of a combination of poly(D-SUV) and γ-CD for chiral separation in CE proves to be a promising method for separation of mixtures of enantiomers. In addition, optimization of chiral separations in this binary system is more complicated than by use of only one chiral selector. This is because there are numerous factors which can affect the

enantioselectivity of this system. According to our experiments, some effects on the resolution of the enantiomers are very obvious, while others are ambiguous. It should be noted that each pair of enantiomers reaches an optimum resolution at a characteristic concentration of γ-CD. This is similar to what is observed in CD-modified CE. An increase in the buffer concentration causes the resolution of the enantiomers to increase, except for D,L-laudanosine. The addition of ACN to the buffer reduces the enantioselectivity of the chiral system. However, the effect of the addition of methanol is more complicated and more solute-dependent.

Acknowledgements

This work was supported in part by a grant from the National Science Foundation (CHE-9224177). The authors also thank G.A. Reed of American Maize Products for kindly donating the CDs used in this study.

References

[1] T.J. Ward, Anal. Chem., 66 (1994) 632A.
[2] M. Novotny, H. Soini and M. Stefansson, Anal. Chem., 66 (1994) 646A.
[3] S. Terabe, K. Otsuka and H. Nishi, J. Chromatogr. A, 666 (1994) 295.
[4] S. Fanali, J. Chromatogr., 474 (1989) 441.
[5] J. Snopek, H. Soini, M. Novotny and E. Smolkova-Keulemandova, J. Chromatogr., 559 (1991) 215.
[6] R. Kuhn, F. Stoecklin and F. Erni, Chromatographia, 33 (1992) 32.
[7] S.A.C. Wren and R.C. Roove, J. Chromatogr., 603 (1992) 235
[8] R. Kuhn, F. Stoecklin and F. Erni, Chromatographia, 33 (1992) 32.
[9] E. Gassmann, J.E. Kuo and R.N. Zare, Science, 230 (1985) 813.
[10] A.S. Cohen, A. Paulus and B.L. Karger, Chromatographia, 24 (1987) 15.
[11] A. Dobashi, T. Ono, S. Hara and J. Yamaguchi, Anal. Chem., 61 (1989) 1984.
[12] K. Otsuka and S. Terabe, J. Chromatogr., 515 (1990) 221.
[13] R.O. Cole, M.J. Sepaniak and W.L. Hinze, J. High. Resolut. Chromatogr., 13 (1990) 579.
[14] D.W. Armstrong, T.J. Ward, R.D. Armstrong and T.E. Beesley, Science, 232 (1986) 1132.
[15] S. Terabe, Trends Anal. Chem., 8 (1989) 129.
[16] H. Nishi, T. Fukuyama and S. Terabe, J. Chromatogr., 553 (1991) 503.
[17] T. Ueda, F. Kitamura, R. Mitchell, T. Metcalf, T. Kuwana and A. Nakamoto, Anal. Chem., 63 (1991) 2979.
[18] H. Nishi, Y. Kokusenya, T. Miyamoto and T. Sato, J. Chromatogr. A, 659 (1994) 449.
[19] S. Terabe, Y. Miyashita, O. Shibata, E.R. Barnhart, L.R. Alexander, D.J. Patterson, B.L. Karger, K. Hosoya and N. Tanaka, J. Chromatogr., 516 (1990) 23.
[20] T. Okubo, H. Kitana and N. Ise, J. Phys. Chem., 80 (1976) 2661.
[21] V.K. Smith, T.T. Ndou, A.M. La Pena and I.M. Warner, J. Incl. Phenom. Mol. Recog., 10 (1991) 471.
[22] G.N. Okafo, C. Bintz, S.E. Clarke and P. Camilleri, J. Chem. Soc. Chem. Commun., (1992) 1189.
[23] S. Terabe, Y. Miyashita, Y. Ishihama and O. Shibata, J. Chromatogr., 636 (1993) 47.
[24] J. Wang and I.M. Warner, Anal. Chem., 66 (1994) 3773.
[25] C.P. Palmer, M.Y. Khaled and H.M. McNair, J. High Resolut. Chromatogr., 15 (1992) 756.
[26] Y.Y. Rawjee, D.U. Staerk and G. Vigh, J. Chromatogr., 636 (1993) 291.
[27] S.G. Penn, D.M. Goodall and J.S. Loran, J. Chromatogr., 636 (1993) 149.

ELSEVIER

Journal of Chromatography A, 711 (1995) 305–311

JOURNAL OF CHROMATOGRAPHY A

Hydrogen-bonding interaction in capillary electrophoresis using polyether matrices

Yukihiro Esaka[a,*], Masashi Goto[a], Hiroki Haraguchi[b], Tokuji Ikeda[c], Kenji Kano[c,*]

[a]*Gifu Pharmaceutical University, 5-6-1 Mitahora-higashi, Gifu 502, Japan*
[b]*Department of Applied Chemistry, Faculty of Engineering, Nagoya University, Furo-cho, Chikusa-ku, Nagoya 464, Japan*
[c]*Department of Agricultural Chemistry, Faculty of Agriculture, Kyoto University, Sakyo-ku, Kyoto 606, Japan*

Received 22 March 1995; accepted 28 April 1995

Abstract

Polyethylene glycol (PEG) serves as a novel matrix in capillary electrophoresis. The purpose of this work was to explore some evidence for hydrogen-bonding complex formation between analytes and PEG in the separation system using benzoic acids as model analytes. An increase in the column temperature resulted in a significant decrease in the interaction between PEG and substituted benzoic acids with hydrogen-donating groups. Addition of urea suppressed the interaction. NMR spectra of phenol and salicylic acid in the presence of PEG in C^2HCl_3 showed an obvious electrostatic interaction, probably a hydrogen-bonding interaction, between the hydroxyl protons of the analytes and PEG. These results strongly support the contention that hydrogen-bonding interaction between the polyether segments of PEG and the hydrogen-donating groups of analytes occurs in the separation systems. Some other minor interactions controlling the separation are also described.

1. Introduction

Increasing attention has been paid to the use of capillary electrophoresis (CE) in the biological and pharmaceutical fields [1–3]. CE techniques for separation include capillary zone electrophoresis (CZE), electrokinetic chromatography and capillary gel electrophoresis. Each of these modes has achieved characteristic separations of a variety of samples. However, the development of a new separation mode is much in demand for further extension of the applicability of CE.

One of the possible interactions to be utilized for separation would be electrostatic interaction. With this in mind, we focused our attention on polyethers, which are known to serve as electrostatic electron donors via their ether oxygen atoms. Typical examples are inclusion phenomena of cations by crown ethers and non-cyclic polyethers [4–12]. It is noteworthy that hydrogen bonding is also observed between a polyether ionophore and amine complexes in hydrophobic media [13,14]. These studies stimulated us to utilize the hydrogen-bonding ability of polyethers to develop a new "hydrogen-bonding mode" or "electrostatic mode" in CE [15].

An earlier study revealed that the addition of polyethylene glycol (PEG) as a free matrix can greatly improve the CZE separation of benzoic

* Corresponding author.

0021-9673/95/$09.50
SSDI 0021-9673(95)00519-6

acid derivatives used as model analytes as a result of the interaction between PEG and the analytes [15]. The strength of the interaction is appropriate for controlling the mobility of the analytes and appears to depend on the hydrogen-donating activity of the substituents. Therefore, we described the phenomenon in terms of hydrogen-bonding interaction between PEG and the analytes.

In this study, we attempted to obtain further evidence for hydrogen bond formation between PEG and analytes during CZE separations. Our strategy was to investigate the effects of the temperature of capillary and of urea as an additive on the strength of the interaction between PEG and analytes, because hydrogen bonding is weakened at elevated temperatures and urea, a bifunctional hydrogen donor and acceptor, breaks hydrogen-bonding complexes as a result of hydrogen-bonding exchange. Furthermore, nuclear magnetic resonance (NMR) spectroscopy would provide direct evidence of hydrogen-bonding complex formation. We shall also discuss some other minor interactions controlling the separation.

2. Experimental

Three kinds of PEG with mean molecular masses of 400, 4000, and 20 000 (PEG 400, PEG 4000 and PEG 20 000) were obtained from Kishida Chemical (Osaka, Japan) and used as received. 4-Acetamidobenzoic acid ($4CH_3CONH$-BA), 4-acetoxybenzoic acid ($4CH_3COO$-BA), 4-aminobenzoic acid ($4NH_2$-BA), 4-hydroxybenzoic acid (4OH-BA), 4-methylbenzoic acid ($4CH_3$-BA), 4-carboxybenzaldehyde (4CHO-BA), 2-hydroxybenzoic acid (2OH-BA), 2-carboxybenzaldehyde (2CHO-BA), benzoic acid (BA) and [^{2}H]chloroform (C^2HCl_3, containing 1% TMS) were purchased from Nacalai Tesque (Kyoto, Japan). All other chemicals were of analytical-reagent grade.

Electrophoretic separation was performed in a fused-silica tube (GL Science, Tokyo, Japan) of 0.05 mm I.D. and a column length of 750 mm, with an effective length for separation of 500 mm. Samples were introduced at the end to be connected to the positive high voltage by siphoning at a height of 15 cm, usually for a 5–10-s period. When PEG was used at higher concentrations, a longer time was required for sample injection because of the increased viscosity. Thermal control of the column was performed as follows. About 60% of the effective length of the column was passed through silicone rubber tubing of 1.0 mm I.D. covered with a heat insulating material and then water maintained at a given temperature was pumped with a peristaltic pump (Gilson Minipuls 2, ca. 2 ml min^{-1}) through the tubing during separations in the direction opposite to the electroosmotic flow. UV spectrophotometric detection was effected at the negative potential side. The detection wavelength was set at 210 nm. Other details were described in previous papers [15,16].

A series of ^{1}H NMR measurements of benzoic acids at various concentrations of PEG 20 000 were carried out in C^2HCl_3 with a JEOL GX-270 instrument operating at 270 MHz.

3. Results and discussion

Nine benzoic acids, $4CH_3CONH$-BA, $4NH_2$-BA, 4OH-BA, 2OH-BA, $4CH_3COO$-BA, 4CHO-BA, $4CH_3$-BA, 2CHO-BA and BA, were used as model samples in CZE experiments. PEG 400 and PEG 4000 were used at concentrations ranging from 1 to 10% in an electrolyte solution of 10 m*M* phosphate buffer (pH 7.8). Under the present separation conditions, all the analytes are considered to be in the form of univalent anions because of complete dissociation of their carboxyl groups. As reported in a previous paper [15], the addition of PEG drastically influences the migration time of these benzoic acids. The influence can be described in terms of the following two factors. The first is non-specific and is ascribed to the increase in viscosity, resulting in an increase in the migration time. In the case of 2CHO-BA, the change in the migration time can be simply described by this effect, because it appears to

exhibit no specific interaction with PEG (see later also) [15]. The second, in which we are interested, is specific to the analytes. The addition of PEG accelerates the mobility of some benzoic acids, especially four with hydrogen-donating substituents ($4CH_3CONH$-BA, $4NH_2$-BA, 4OH-BA and 2OH-BA), compared with 2CHO-BA. The acceleration of the migration time resulted from some attractive interaction between the hydrogen-donating benzoic acids and PEG, as PEG migrates in the direction of the negative potential at the electroosmotic flow-rate (V_{eo}). In order to eliminate the first non-specific factor, we shall describe the electrophoretic behaviour using relative values of the migration time and electrophoretic velocity against those of 2CHO-BA as a reference compound (see Eq. 1 also).

3.1. Effect of temperature

Fig. 1 shows electropherograms of the nine benzoic acids under thermostated conditions at (A) 3°C and (B) 80°C in the presence of 7.5% (v/v) PEG 4000. Comparison of the two electropherograms reveals that the relative migration time of the four hydrogen-donating benzoic acids ($4CH_3CONH$-BA, $4NH_2$-BA, 4OH-BA and 2OH-BA) increases with increase in temperature. This means that the increase in the column temperature weakens the interaction between PEG and the four benzoic acids having a hydrogen-donor active substituent. It is well known that an increase in temperature weakens and breaks hydrogen bonds. Hence this behaviour is in accord with our previous description in terms of the hydrogen-bonding complex formation between the hydrogen-donating benzoic acids and PEG.

When we can assume a stoichiometric and equilibrated complex formation between an analyte and PEG, the observed electrophoretic velocity of the analyte ion (V_{ep}) is expressed as a function of the PEG concentration [PEG], as described in a previous paper [15]:

$$V_{ep}/V_{ep,0} = V_{ep,f}/V_{ep,0} + K[(V_{ep,c} - V_{ep,f})/V_{ep,0}][PEG] \quad (1)$$

where $V_{ep,f}$ and $V_{ep,c}$ are the electrophoretic velocity of the free analyte ion and the analyte–PEG complex, respectively, K is the complex formation constant of the analyte with PEG and $V_{ep,0}$ is the electrophoretic velocity of a reference compound with $K \approx 0$ (2CHO-BA in our case). In our experiments, $V_{ep}/V_{ep,0}$ exhibited linear relationships against [PEG] up to 7.5% (v/v) (data not shown; see Fig. 2 in Ref. [15] as an example). Values of K can be easily estimated from the slopes of the linear plots on the basis of a reasonable assumption that $V_{ep,c} - V_{ep,f} \approx -V_{ep,f}$. Fig. 2 shows the dependence of the K

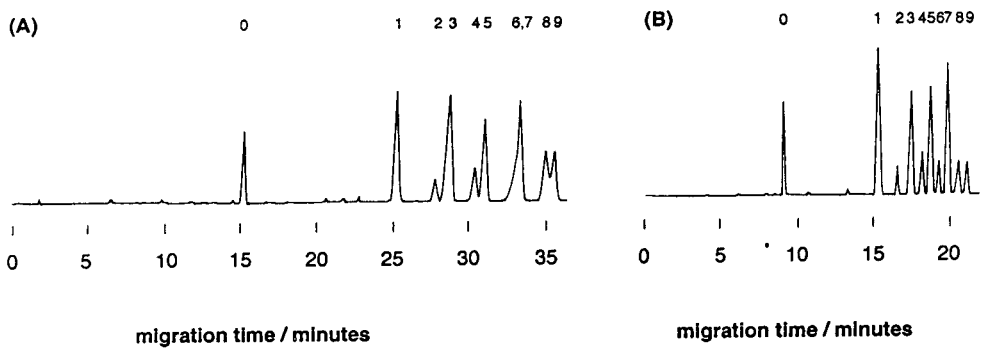

Fig. 1. Electropherograms of nine benzoic acids with 7.5% (v/v) PEG 4000 under thermostatic control at (A) 3°C and (B) 80°C. Electrolyte solution, 10 mM phosphate buffer (pH 7.8); capillary, 750 mm × 0.05 mm I.D. (500 nm effective length); applied voltage and current), (A) 14 kV and 4 μA and (B) 14 kV and 6 μA; detection wavelength, 210 nm. Peaks: 0 = mesityl oxide (electroosmotic flow marker); 1 = $4CH_3CONH$-BA; 2 = $4CH_3COO$-BA; 3 = 4OH-BA; 4 = $4CH_3$-BA; 5 = $4NH_2$-BA; 6 = 4CHO-BA; 7 = 2OH-BA; 8 = 2CHO-BA; 9 = BA.

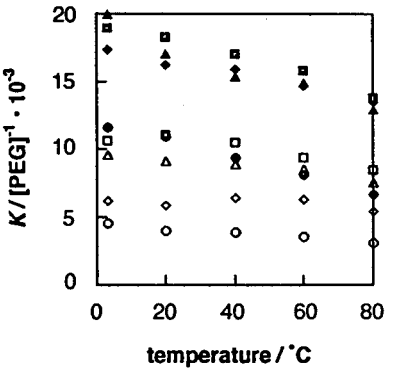

Fig. 2. Dependence of the complex formation constant (K) on the capillary temperature: ■ = $4CH_3CONH$-BA; ▲ = 4OH-BA; ◆ = 2OH-BA; ● = $4NH_2$-BA; □ = $4CH_3$-BA; △ = CH_3COO-BA; ◇ = 4CHO-BA; ○ = BA.

values of the analytes on the capillary temperature. In the cases of the four benzoic acids having a hydrogen-donating substituent ($4CH_3CONH$-BA, $4NH_2$-BA, 4OH-BA and 2OH-BA), the K values decrease significantly with increase in the capillary temperature. In contrast, in the case of 4CHO-BA, $4CH_3$-BA, $4CH_3COO$-BA and BA, which have no hydrogen-donating active substituent, the K values are almost independent of the capillary temperature or the dependence is very small. These results support the contention that the interaction between PEG and the four substituted benzoic acids with hydroxyl, amide or amino groups is predominantly governed by the hydrogen-bonding complex formation, in which the polyether oxygen atoms of PEG serve as hydrogen acceptors.

The above argument might mean that an increase in the capillary temperature is almost equivalent to a decrease in the PEG concentration. However, the two parameters controlling the experimental conditions are not exactly identical with each other. Therefore, from the point of view of practical application, both the capillary temperature and the PEG concentration can be useful parameters to improve separations in this method. In our experiment, the best separation was achieved at 80°C (Fig. 1B) for the samples used. Even when the use of a higher concentration of PEG is unavoidable to improve separation, an increase in the capillary temperature would be occasionally useful for rapid separation, because it results in a decrease in the viscosity and hence of the migration time.

3.2. Effect of urea

Urea works as a bifunctional hydrogen donor and acceptor and it is often employed to break intra- and/or intermolecular hydrogen bonds in biological molecules, such as proteins and DNA. Considering that the hydrogen-bonding interaction operates in the present separation mode for some analytes, addition of urea to the separation matrices would be expected to compete with PEG (hydrogen acceptor) to form hydrogen-bonding complexes with the analytes (hydrogen donors) and/or with analytes to form hydrogen-bonding complexes with PEG. Our assumption here is that the electrophoretic velocity of the urea–analyte hydrogen-bonding complex is not far from that of the free analyte, because the molecular mass of urea is sufficiently small compared with that of PEG. This assumption leads to an expectation that an apparent value of K evaluated by Eq. 1 will decrease at a sufficiently high concentration of urea.

The following experiments confirmed the expectation. Urea was added at 10 M to an electrolyte solution of 10 mM phosphate buffer (pH 7.8) containing several concentrations of PEG. In this work, PEG 400 was used, because urea is almost insoluble in an aqueous solution of PEG 4000 at 5% (v/v). The apparent K value was evaluated based on Eq. 1. Plots of $V_{ep}/V_{ep,0}$ vs. [PEG] gave straight lines in the range of [PEG] from 2.5 to 10% (v/v). Table 1 summarizes the K values of the samples in the absence and presence of 10 M urea. For all the analytes, the K values at 10 M urea decreased to 30–85% of those in the absence of urea. This decrease in K values is attributable to the suppression of the interactions, most significantly the hydrogen-bonding interaction, between PEG and the analytes. However, the urea effect was not restricted to the hydrogen-donating analytes. As will be mentioned later, we consider that several minor interactions exist in addition to the relatively

Table 1
Effects of addition of 10 *M* urea on *K* values

Analyte	$K \times 10^3/[\text{PEG}\ (\%, \text{v/v})]^{-1}$	
	No urea	10 *M* urea
4OH-BA	10.3	5.3
2OH-BA	9.8	5.6
$4CH_3CONH$-BA	9.5	3.9
$4NH_2$-BA	6.6	3.6
$4CH_3$-BA	7.0	3.6
$4CH_3COO$-BA	4.8	1.5
4CHO-BA	4.5	2.3
BA	2.7	2.3

strong hydrogen-bonding interaction between PEG and benzoic acids. Therefore, urea seems to suppress these minor interactions also by hydrogen-bonding complex formation with PEG molecules.

3.3. NMR spectral measurements

NMR spectroscopy is suitable for observing electrostatic interactions of molecules in solutions. When an electrostatic interaction of an analyte with PEG occurs, the distribution of the electron density of the analyte should change, resulting in a change in the chemical shifts. In this study, the interaction of the phenolic hydroxyl group with PEG 20 000 was followed in C^2HCl_3 using ^1H NMR spectroscopy. Phenol was used as a model compound, because 4OH-BA is insoluble in C^2HCl_3.

Fig. 3A shows the ^1H NMR spectra of 10 m*M* phenol in the absence and presence of PEG 20 000 at concentrations of 1–5% (v/v). The spectral change on addition of PEG was demonstrated by the signals of the hydroxyl proton. The ^1H signal of the hydroxyl group of phenol (4.8 ppm at 0% PEG) shifts significantly to lower field on addition of PEG. This provides direct evidence for hydrogen-bonding complex formation between the phenolic hydroxyl group and the polyether oxygen atoms of PEG. The electrostatic attractive interaction (hydrogen-bonding complex formation) between the phenolic hydroxyl group and PEG should increase the

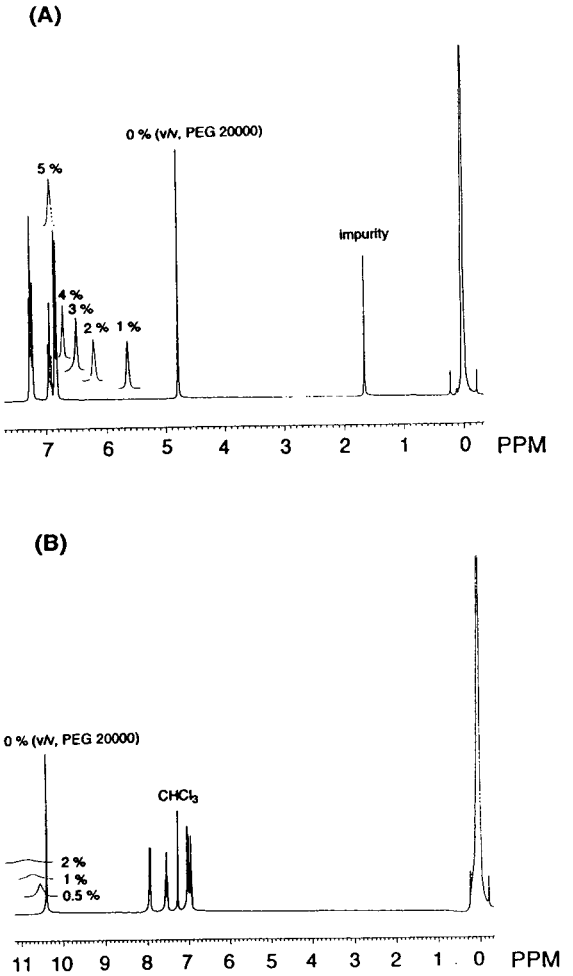

Fig. 3. ^1H NMR spectra of (A) phenol and (B) 2OH-BA in C^2HCl_3 with increasing concentration of PEG 20 000.

O–H bond length. Thus the interaction decreases the electron density around the proton, resulting in a lower-field shift owing to the deshielding. Similar lower field shifts of phenolic and alcoholic ^1H signals are observed with increasing concentration as a result of intermolecular hydrogen bonding with themselves [17].

The PEG molecule has two hydroxyl groups at the ends, and these end-groups are reasonably considered to serve as hydrogen donors. This consideration can be supported by NMR experiments. The NMR signal of the hydroxyl end-groups of PEG is broadened and shifted from 2.3

ppm to lower field with addition of BA (data not shown). This indicates the possibility of the occurrence of a hydrogen-bonding interaction between the carboxylate group of BA and the hydroxyl end-groups of PEG at least in C^2HCl_3. The numbers of hydroxyl groups in PEG molecules are generally far less than those of ether oxygen atoms. Hence the hydrogen-donating property of the end-groups of PEG would not be so significant compared with the hydrogen-accepting property of the polyether segments. In the following, we shall refer to the hydrogen-bonding interaction derived from the polyether segments and the hydroxyl end-groups as the major and minor hydrogen-bonding interactions, respectively.

3.4. Hydrophobic interaction

Judging from the K values in Table 1, $4CH_3$-BA seems to interact attractively with PEG at a strength comparable to that of $4NH_2$-BA. This could not be explained simply in terms of the hydrogen-bonding interaction, because the methyl group is inactive in hydrogen bonding. PEG can afford more or less hydrophobic surroundings. This property seems to work as an another sub-mode in addition to the hydrogen-bonding mode for separation in the CE system using PEG. Such a hydrophobic interaction with PEG could occur with the other analytes, but it was not as large as in the case of $4CH_3$-BA.

In addition to the direct effect of the hydrophobicity of PEG, a secondary effect might play a role in the hydrogen-bonding complex formation between the analytes and PEG, namely a solvation effect. Hydrogen-bonding interaction with PEG will occur more effectively in hydrophobic surroundings than in an aqueous phase. The benzoic acids used here are more or less hydrophobic in nature even in their monoanion state. Hence the analytes will be surrounded by the hydrophobic segments (or hydrophobic pockets) of PEG in part. The hydrophobic environments will enhance the hydrogen-bonding interaction in this separation system.

3.5. Comparison between ortho- and para-isomers

The K values of $4CH_3COO$-BA and 4CHO-BA were much larger than those of the *ortho*-isomers ($2CH_3COO$-BA and 2CHO-BA, respectively) (the K values of $2CH_3COO$-BA were $1.4 \cdot 10^{-3}$[PEG 400]$^{-1}$ and $3.8 \cdot 10^{-3}$[PEG 4000]$^{-1}$) [15]. This seems to suggest steric hindrance against the hydrophobic interaction of the analytes with the polyether segments of PEG and/or the minor hydrogen-bonding interaction in part (note that the major hydrogen-bonding interaction is not expected for these analytes). This steric effect seems to be a minor one, but it is occasionally useful for separation. A typical example is the separation between 2CHO-BA and 4CHO-BA. The two analytes could not be separated in the absence of PEG under our experimental conditions because of their hydrodynamic radius close to each other. However, the addition of PEG 4000 [more than 2.5% (v/v)] achieved the complete separation between them with the use of this steric effect. This would mean in turn that 2CHO-BA hardly interacts with PEG. Thus 2CHO-BA is the best reference substance for the determination of the complex formation constant of analytes with PEG (K) (see above).

A complicated situation is observed with 2OH-BA. Even though 2OH-BA is the *ortho*-isomer of 4OH-BA, the K value of 2OH-BA was comparable to that of 4OH-BA (Fig. 2, Table 1). This result can be interpreted as follows. The hydroxyl group in both 2OH-BA and 4OH-BA is strong hydrogen donor. Hence the major hydrogen-bonding interaction is reasonably considered to govern the overall interaction with PEG and is larger than the steric hindrance effect observed for other *ortho*-isomers. Another reason may be related to the hydrodynamic radius of 2OH-BA. In the absence of PEG, 2OH-BA migrates faster than 4OH-BA [15]. This is in contrast to the case with 2CHO-BA and 4CHO-BA, which migrate simultaneously in the absence of PEG (see above). This result means that the hydrodynamic radius of 2OH-BA is smaller than that of 4OH-

BA. Fig. 3B shows the ^1H NMR spectra of 10 m*M* 2OH-BA in the absence and presence of PEG 20 000 at concentrations of 0.5–2% (v/v). The chemical shift of the hydroxyl proton of 2OH-BA is observed at 10.4 ppm. This low-field resonance indicates intramolecular hydrogen-bond formation between the hydroxyl group and the dissociated carboxyl group. Therefore, the small hydrodynamic radius compared with 4OH-BA can be attributed to the intramolecular hydrogen-bond formation. With the addition of PEG, the ^1H signal of the hydroxyl group broadened and disappeared. This indicates the formation of an intermolecular hydrogen-bonding complex with PEG. Once the interaction with PEG has occurred, the hydroxyl group bonded to the carboxylate group of 2OH-BA will turn out to form a complex with PEG. This will result in a larger increase in its apparent hydrodynamic radius than that expected for 4OH-BA. Such an amplified effect may cancel the steric hindrance effect observed for other *ortho*-isomers.

4. Conclusion

The use of PEG as a matrix is very useful in CE separations. The present NMR experiments have demonstrated that PEG works as a hydrogen acceptor via its polyether segments and in part as a hydrogen donor via its hydroxyl end-groups. The effects of temperature and urea addition can be described fundamentally in terms of the hydrogen-bonding interaction between PEG and analytes. The hydrogen-bonding interaction in the aqueous phase will not be as strong as demonstrated by NMR in C^2HCl_3. However, the strength is fortunately appropriate for improving the separation in CZE. Hence the CE method using PEG as a matrix would open up routes to develop electrostatic capillary electrophoresis. From a physico-chemical point of view, this method might be applicable to the determination of the hydrogen-donating properties of analytes or hopefully of the hydrogen-accepting properties of analytes using a hydrogen-donating matrix.

This study suggested the occurrence of some other minor interactions in addition to the hydrogen-bonding interaction, such as hydrophobic and steric interactions. These interactions work in conjunction for hydrogen-donating analytes and sometimes effectively for hydrogen-donating inactive analytes to improve the separation.

Acknowledgements

The authors thank Dr. Bunji Uno and Dr. Toshiyuki Tanaka for helpful discussions and suggestions.

References

[1] B.L. Karger, A.S. Cohen and A. Guttman, J. Chromatogr., 492 (1989) 585.
[2] G.M. McLaughlin, J.A. Nolan, J.L. Lindahl, R.H. Palmieri, K.W. Anderson, S.C. Morris, J.A. Morrison and T.J. Bronzert, J. Liq. Chromatogr., 15 (1992) 961.
[3] C.A. Monnig and R.T. Kennedy, Anal. Chem., 66 (1994) 280R.
[4] C.J. Pedersen, J. Am. Chem. Soc., 89 (1967) 7017.
[5] C.J. Pedersen, J. Am. Chem. Soc., 92 (1970) 386.
[6] H.K. Frensdorff, J. Am. Chem. Soc., 93 (1971) 600.
[7] H.K. Frensdorff, J. Am. Chem. Soc., 93 (1971) 4684.
[8] T. Takeda and H. Goto, Bull. Chem. Soc. Jpn., 52 (1979) 1920.
[9] T. Takeda, Bull. Chem. Soc. Jpn., 53 (1980) 2393.
[10] T. Takeda and Y. Matsumoto, Bull. Chem. Soc. Jpn., 60 (1987) 2313.
[11] T. Takeda, Y. Kimura, Y. Kudo and H. Matsuda, Bull. Chem. Soc. Jpn., 62 (1989) 2885.
[12] Y. Kikuchi, N. Takahashi, T. Suzuki and K. Sawada, Anal. Chim. Acta, 256 (1992) 311.
[13] L.F. Lindoy and G.W. Walker, J. Am. Chem. Soc., 112 (1990) 3659.
[14] P.S.K. Chia, L.F. Lindoy, G.W. Walker and G.W. Evertt, J. Am. Chem. Soc., 113 (1991) 2533.
[15] Y. Esaka, Y. Yamaguchi, K. Kano, M. Goto, H. Haraguchi and J. Takahashi, Anal. Chem., 66 (1994) 2441.
[16] Y. Esaka, Y. Yamaguchi, K. Kano and M. Goto, J. Chromatogr. A, 652 (1993) 225.
[17] R.M. Silverstein, G.C. Bassler and T.C. Morrill, Spectrometric Identification of Organic Compounds, Tokyo Kagaku Dohjin, Tokyo, 5th ed. 1992, p. 170 (translation from the English edition, Wiley, New York, 1991).

ELSEVIER

Journal of Chromatography A, 711 (1995) 313–322

JOURNAL OF CHROMATOGRAPHY A

Comparison of separation selectivity in aqueous and non-aqueous capillary electrophoresis☆

Inga Bjørnsdottir, Steen Honoré Hansen*

Department of Analytical and Pharmaceutical Chemistry, Royal Danish School of Pharmacy, Universitetsparken 2, DK-2100 Copenhagen, Denmark

First received 15 February 1995; revised manuscript received 12 April 1995; accepted 28 April 1995

Abstract

The use of non-aqueous capillary electrophoresis in free solution in uncoated fused-silica capillaries was investigated and compared with capillary electrophoresis using aqueous systems. Cationic drug substances differing only in the amine functionallity or even having the same charge-to-mass ratio were used as test solutes. Some of these test substances are difficult to separate in plain aqueous buffers and even when using micellar electrokinetic chromatography or by adding cyclodextrins to the electrophoresis buffer it is difficult to obtain baseline separations. Very high separation selectivity may be obtained in non-aqueous capillary electrophoresis systems without adding surfactants or complexing agents to the electrophoresis medium. Major selectivity changes may be obtained using different organic solvents (formamide, N-methylformamide, N,N-dimethylformamide, N,N-dimethylacetamide, dimethyl sulfoxide, methanol and acetonitrile) for the electrophoresis medium, e.g., the relative electrophoretic mobilities of a primary, a secondary and a tertiary amine with otherwise identical structures are reversed on replacing acetonitrile with methanol as solvent.

1. Introduction

Improvement of separation selectivity is of fundamental importance and one of the main challenges in separation science. In capillary electrophoresis (CE), significant improvements in separation selectivity were obtained with the introduction of micellar electrokinetic chromatography (MEKC) [1,2], where the electrophoretic rate processes are combined with partitioning processes. Also, different kinds of complexation may be used in order to improve selectivity and this has found widespread application in the separation of mixtures of enantiomers [3].

Recently, considerable improvements in separation selectivity between cationic compounds with very similar structures and even with same charge-to-mass ratio were obtained [4,5] using either surfactants or cyclodextrins as additives to the electrophoresis buffer. However, these techniques suffer from a number of drawbacks: some of the additives may be fairly expensive, and the additives are often non-volatile and the separation systems are therefore not suitable for on-line coupling to a mass spectrometer.

☆ Presented in part at The 7th International Symposium on High-Performance Capillary Electrophoresis, Würzburg, Germany, Jan. 29–Feb. 2, 1995.

* Corresponding author.

0021-9673/95/$09.50
SSDI 0021-9673(27340)0000-0

A number of papers on the use of non-aqueous electrophoresis have been published, and in 1976, Korchemnaya et al. [6] reviewed the research that had been performed in that field until then. Since this review appeared, only a single investigation on the use of the non-aqueous mode has been reported [7]. However, recently the topic has gained renewed interest [8–12].

In this paper, it is demonstrated that high separation selectivity of very similar compounds may easily be obtained by using non-aqueous systems and a volatile salt as the electrolyte. In non-aqueous systems, changes in separation selectivity may be obtained that would be very difficult to achieve in capillary electrophoresis systems based on aqueous buffers.

2. Experimental

2.1. Capillary electrophoresis system

An HP^{3D} capillary electrophoresis system (Hewlett-Packard, Waldbronn, Germany) equipped with an on-column diode-array detector was used. A detection wavelength of 214 nm was used for all samples unless stated otherwise. The separation was performed in a fused-silica capillary (64 cm × 50 μm I.D.; 55.5 cm to the detector; for impurity testing a 64 cm × 100 μm I.D., 55.5 cm to the detector, capillary was used) (Polymicro Technologies, Phoenix, AZ, USA). The capillary was thermostated at 25°C with air. Samples were kept at ambient temperature in the autosampler and injected by applying a pressure of 5 kPa (50 mbar) for 3 s. A voltage of 25 kV was applied during analysis.

A Quanta 4000 capillary electrophoresis system (Waters, Milford, MA, USA) was used for studies with the surfactants in 0.05 *M* 6-aminocaproic acid buffer (pH 4.0). Detection was performed by measuring UV absorption at 214 nm. The separation was performed in a fused-silica capillary (60 cm × 75 μm I.D.; 56 cm to the detector) (Polymicro Technologies). Sample injection was accomplished by hydrostatic injection for 15 s. All analyses were performed using an applied voltage of 20 kV. Data collection was performed using Turbochrom version 3.3 software (PE Nelson, Cupertino, CA, USA).

Prior to use, the capillaries were rinsed with 1 *M* sodium hydroxide for 60 min, 0.1 *M* sodium hydroxide for 20 min, distilled water for 20 min and the final electrophoresis medium for 10 min. Between analyses, the capillaries were flushed with electrophoresis medium for 2 min.

2.2. Chemicals and reagents

Imipramine hydrochloride (IMP), desmethylimipramine (DMI), methylimipramine iodide (IMP-CH_3) and imipramine N-oxide hydrochloride (DINO) were obtained from Dumex (Copenhagen, Denmark), didesmethylimipramine hydrochloride (DDMI) from Ciba-Geigy (Basle, Switzerland), maprotiline hydrochloride (MAP), litracene hydrochloride (LIT), amitriptyline hydrochloride (AMI), nortriptylene hydrochloride (NOR) and protriptyline hydrochloride (PRO) from H. Lundbeck (Valby, Denmark), 6-aminocaproic acid (6-ACA) and polyoxyethylenesorbitan monolaurate (Tween 20) from Sigma (St. Louis, MO, USA), 3 - (N,N - dimethylmyristylammonium)propanesulphonate (MAPS) and N,N-dimethylacetamide (DMA) from Fluka (Buchs, Switzerland), acetic acid and N,N-dimethylformamide (DMF) were obtained from Riedel-de Häen (Seelze, Germany). Dimethyl sulphoxide (DMSO), HPLC grade acetonitrile and sodium acetate were obtained from Merck (Darmstadt, Germany). Ammonium acetate, formamide and N-methyl formamide (NMF) were obtained from Aldrich (Steinheim, Germany). The used methanol was of HPLC-grade and all chemicals were used without further purification.

2.3. Sample preparation

Mixed test sample I consisted of IMP, DMI, DDMI, IMP-CH_3 and DINO in methanol at concentrations of 0.06, 0.04, 0.02, 0.04 and 0.04 mg/ml, respectively, or at a concentration of 0.04 mg/ml each.

Mixed test sample II consisted of: AMI, NOR, PRO, MAP and LIT in methanol at a concentration of 0.04 mg/ml each.

When investigating formamide, NMF, DMF, DMA and DMSO, the mixed test sample was prepared in the respective organic solvent.

For testing the impurities in DINO, 5.1 mg/ml of this substance was dissolved in methanol.

Standard addition was performed by adding 10 μl of each of 0.05 mg/ml methanolic solutions of IMP-CH_3, IMP, DMI and DDMI to 300 μl of the DINO test solution.

3. Results and discussion

CE is normally performed using either aqueous buffers or buffers with the addition of only smaller amounts of organic solvents to regulate the electroosmotic flow and the selectivity. As many larger biomolecules are only compatible with aqueous buffers, the aqueous electrophoresis mode will also be the dominant technique in the future. However, using CE, especially smaller molecules such as pharmaceuticals may be separated in non-aqueous systems with increased separation selectivity. In this study, cationic drug substances differing only in the amine functionallity or even having the same charge-to-mass ratio were used as test substances (Fig. 1).

The separations of cationic drug substances using non-aqueous systems were compared with

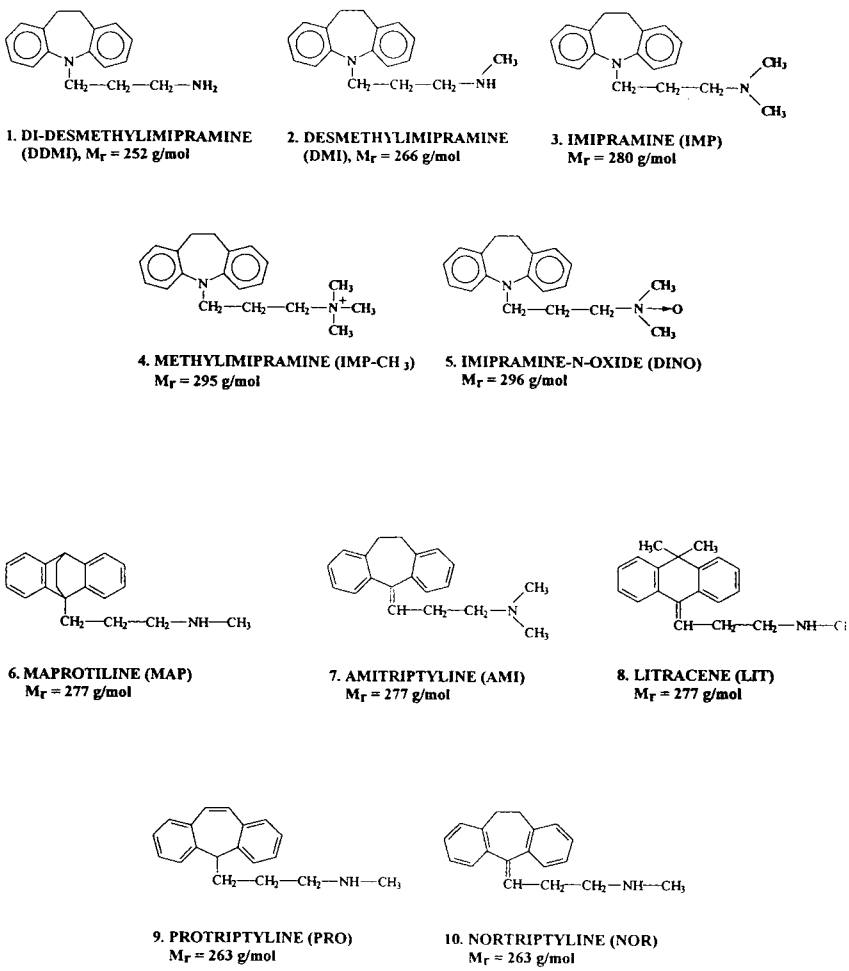

Fig. 1. Structures of the test substances.

respect to the nature of the organic solvent, the observed pH (pH*, see Section 3.2), the temperature and the water content in the electrophoretic medium.

It has been shown previously [4] that adding non-ionic and/or zwitterionic surfactants to the aqueous electrophoresis buffer may provide large increases in separation selectivity between test solutes (Fig. 2). However, instead of using large amounts of surfactants or complexing agents, similar or even better increments in separation may be obtained using "buffers" consisting of methanol, acetonitrile or other organic solvents with electrolytes added.

3.1. Organic solvent

A number of organic solvents were tested (Fig. 3) using mixed test sample I. Rapid and good separations were obtained using methanol and acetonitrile. When using DMF, DMA and DMSO, the analysis time increased owing to the slower electroosmotic flow (EOF). However, in formamide (not shown) no separation of IMP, DMI and DDMI was obtained and in NMF only small separation factors between these three test solutes were obtained. The relative electrophoretic mobilities of the primary, secondary and tertiary amines were reversed on replacing acetonitrile with methanol. The relative order of migration of the test solutes in DMF, DMA and DMSO was similar to that obtained in methanol whereas the relative order of migration in NMF resembled that in acetonitrile.

A more detailed study of the use of methanol and acetonitrile was performed. The gradual replacement of acetonitrile with methanol was studied (Fig. 4). On changing the solvent from 100% acetonitrile through 25% methanol in acetonitrile and 75% methanol in acetonitrile to 100% methanol, the mixed test sample I with imipramine and its derivatives exhibited major changes in selectivity. At 50% methanol in acetonitrile (not shown) no separation of the primary, secondary and tertiary amines could be observed. With the mixed test sample II it was primarily the migration of the tertiary amine (AMI) that changed relative to the four secondary amines. Smaller changes in selectivity were seen between the four secondary amines. These changes in selectivity may be ascribed to the "basicities" of the amines in the various solvents and solvent mixtures and thus to the solvation of the test solutes. It is known that there are differences in the relative basicities of primary, secondary and tertiary alkylamines when determining them in water or in the gas phase [13].

It is also interesting to observe the change in the EOF on changing the organic solvent. However, in methanol, acetonitrile and mixtures thereof the electrophoretic migration ($\mu_{ep} = \mu_{ap} - \mu_{eof}$) remained virtually constant (about $2 \cdot 10^{-4}$ cm^2/V·s), although the electroosmotic migration increased by a factor of ca. 10 on changing from methanol to acetonitrile and was highest at acetonitrile–methanol (75:25, v/v). These changes in EOF are probably due primarily to changes in viscosity. The viscosity of methanol is decreased with the addition of acetonitrile owing to formation of monomeric methanol [14]. The viscosity reaches a minimum at about 80% acetonitrile in methanol. However, viscosity is not the only explanation, as DMSO has a higher EOF than methanol although DMSO has a relatively high viscosity [15]. Therefore, changes in dielectric constants of the solvents and the zeta potential at the inner capillary wall may also play a role.

Detection can be problematic in non-aqueous capillary electrophoresis. A significant limit of detection is obtained at lower wavelengths when using formamide, NMF, DMF, DMA and DMSO as the noise level increases owing to the high UV absorbance of the organic solvent at lower wavelengths. When using methanol or acetonitrile, a detection wavelength at 214 nm may be used without problems.

3.2. pH*

As pH is only defined in diluted aqueous solutions, it has no direct meaning in non-aqueous solvents. However, acidic or basic electrolytes will still exhibit a major influence on the separation selectivity when added to the organic

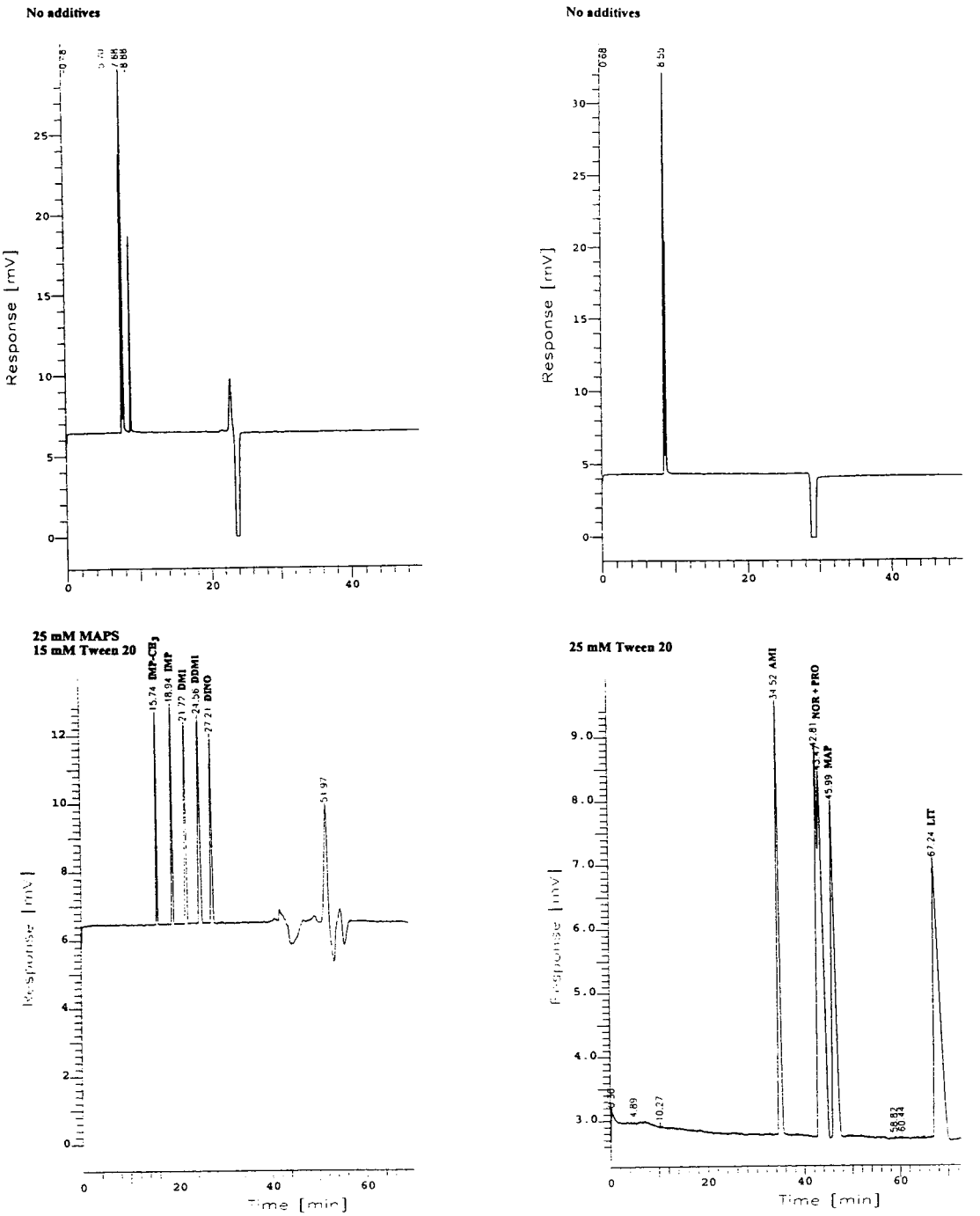

Fig. 2. Electropherograms of mixed test sample I (left) and mixed test sample II (right). Above, no addition of surfactants; below, addition of the surfactants MAPS and Tween 20 to the electrophoresis buffer. Apparatus: Waters Quanta 4000. Conditions: capillary, 56 cm to detector × 75 μm I.D.; temperature, 30°C; detection, 214 nm; buffer, 0.05 *M* 6-aminocaproic acid (pH 4.0); voltage, 20 kV; current, 62 μA. For peak identification, see Fig. 1.

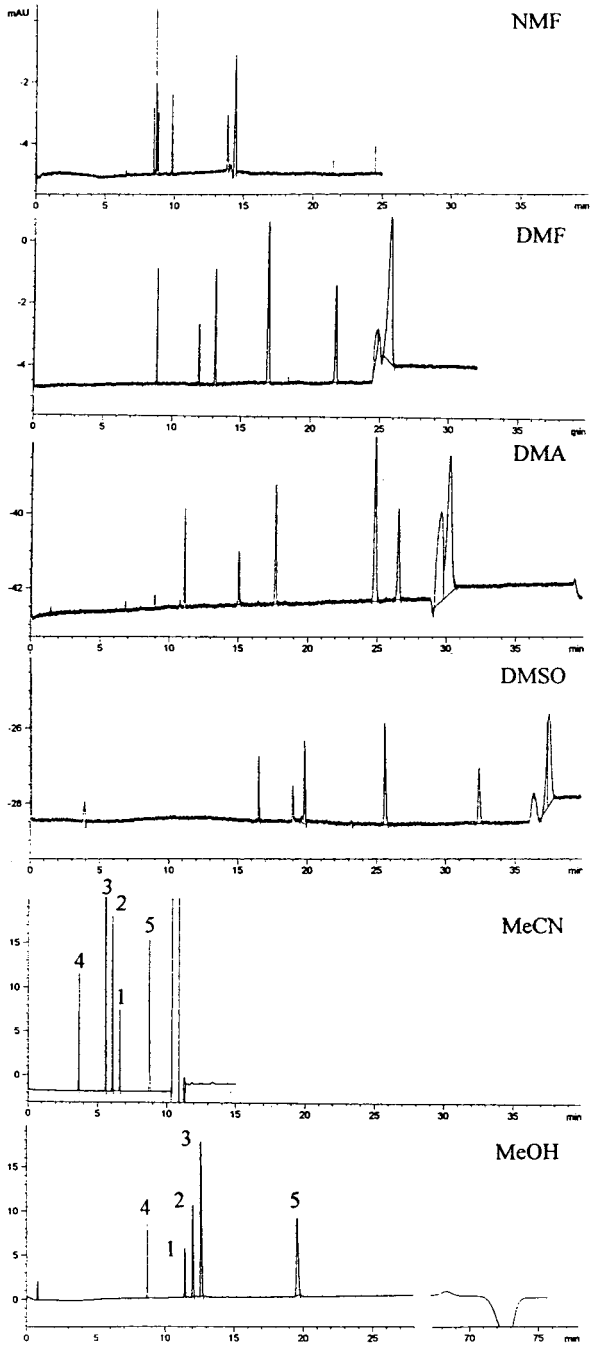

Fig. 3. Non-aqueous CE in NMF, DMF, DMA, DMSO, acetonitrile and methanol. Apparatus: HP^{3D} CE instrument. Conditions: capillary, 55.5 cm to detector × 50 μm I.D.; temperature, 25°C; detection, 214 nm; electrophoresis medium, 25 m*M* ammonium acetate–1 *M* acetic acid in the organic solvent; voltage, 25 kV; current, ca. 7 μA. For peak identification, see Fig. 1.

solvent used as electrophoresis medium. Fig. 5 shows electropherograms from an investigation where the electrolytes were changed from ammonium acetate–sodium acetate to ammonium acetate–acetic acid at different concentrations. As expected, selectivity changes occurred when acidic or basic salts were added to the electrophoresis medium. This also influences the electroosmotic flow, possible owing to changes in the zeta potential on the inner capillary wall.

3.3. Temperature

Changing the temperature surrounding the capillary is known to have an effect when using aqueous systems [5]. Temperature changes from 10 to 40°C had only a small effect on the mixed test sample I apart from a 25% increase in EOF. With the mixed test sample II an improvement of separation was seen only at 40°C, where all five test solutes were separated. However, a similar investigation on the influence of the temperature on the separation of opium alkaloids (which do not have similar chemical structures) in similar non-aqueous systems showed that major changes in selectivity could be introduced [11].

3.4. Water

On changing the electrophoresis medium from a 100% non-aqueous to a 100% aqueous system, most of the separation is gradually lost. This was to be expected as it is difficult to separate these test solutes (Fig. 2) in aqueous buffers [4].

4. Application

The loadability of the non-aqueous CE system was tested by using the system for drug purity testing. Imipramine-N-oxide (DINO) was investigated for its content of impurities, and a 0.5% solution was loaded to the capillary without any problems (Fig. 6). The limit of detection (defined as a signal three times the baseline noise) is about 1 μg/ml, corresponding to 10 ppm impurity in the drug substance. This is

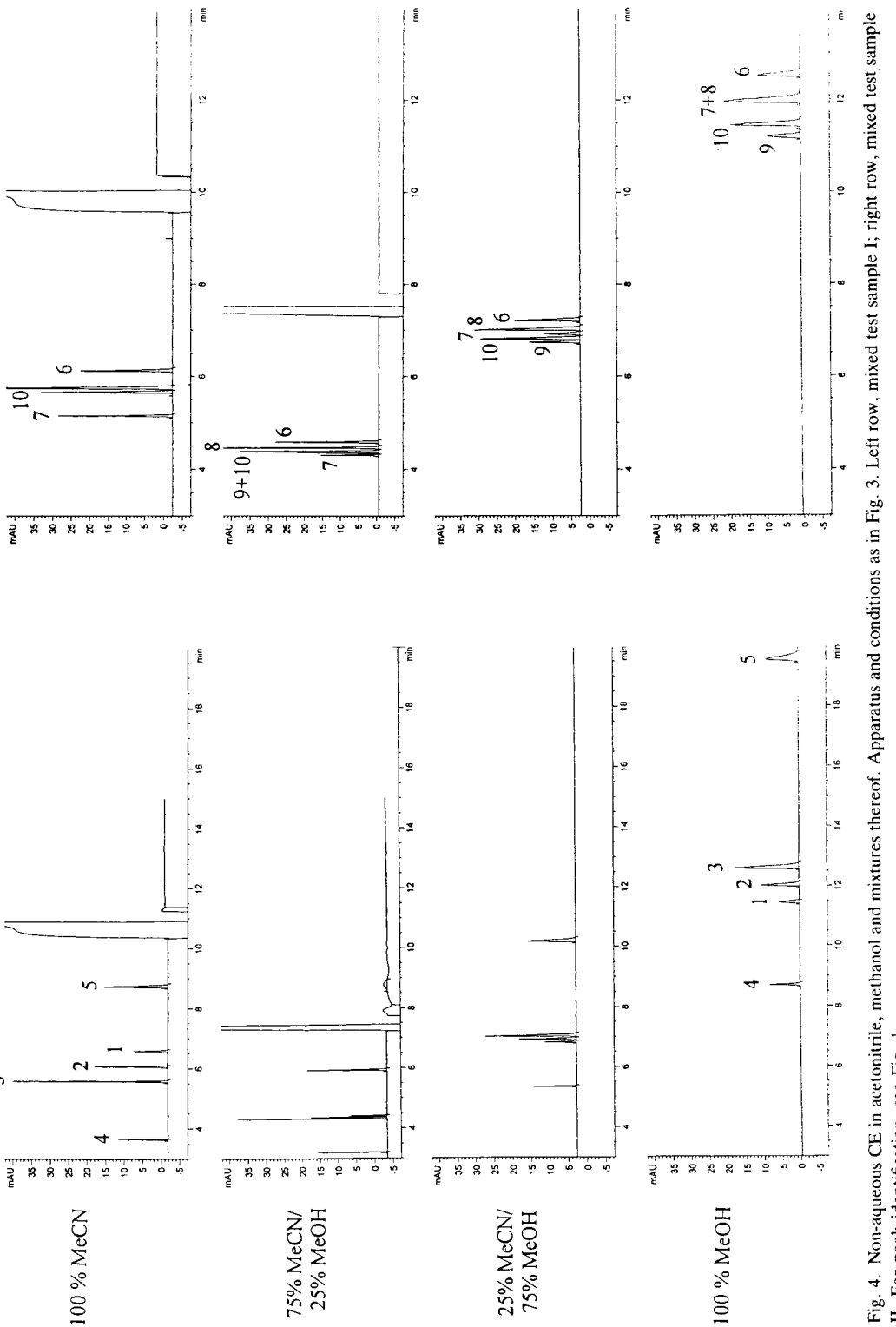

Fig. 4. Non-aqueous CE in acetonitrile, methanol and mixtures thereof. Apparatus and conditions as in Fig. 3. Left row, mixed test sample I; right row, mixed test sample II. For peak identification, see Fig. 1.

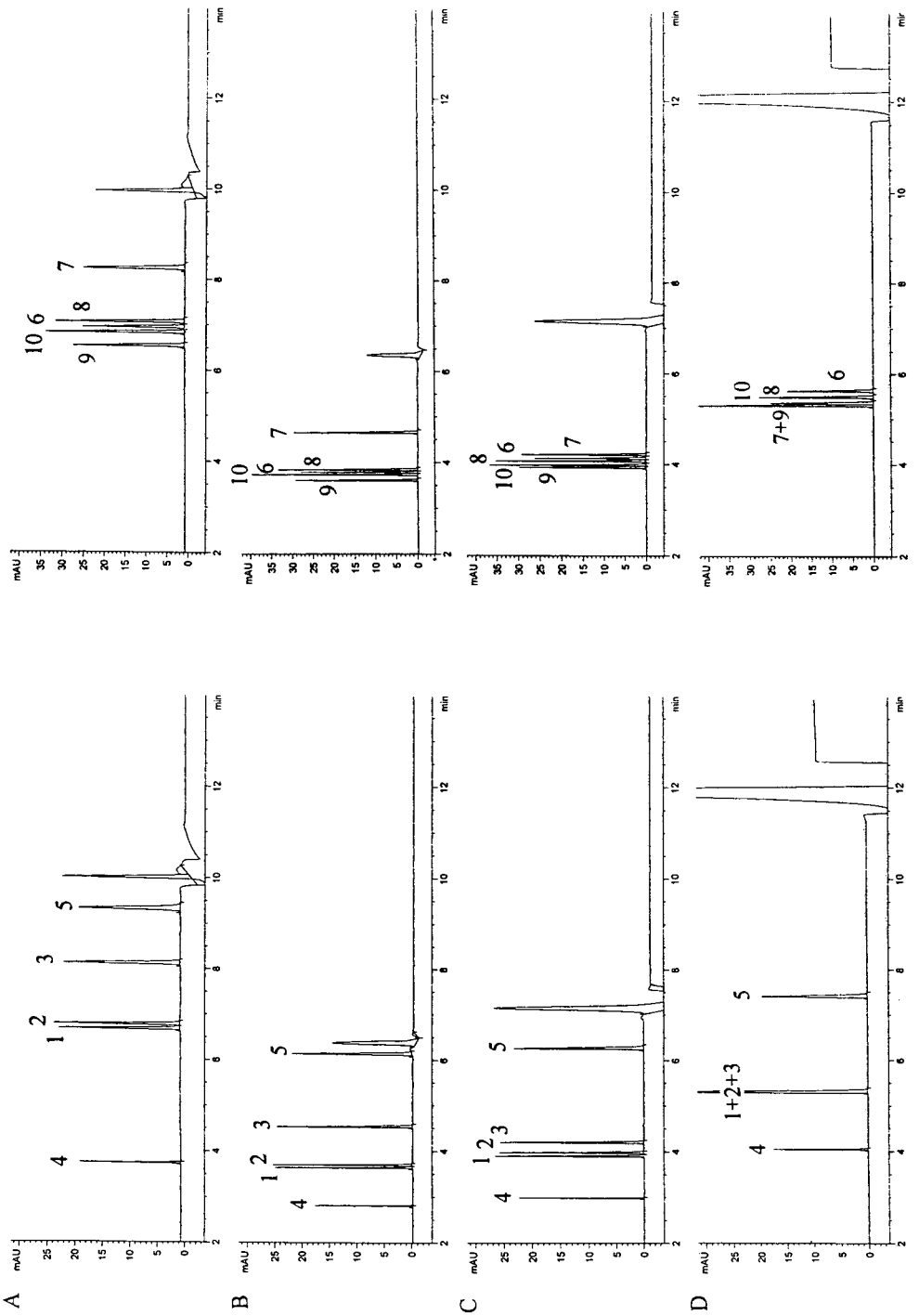

Fig. 5. Non-aqueous CE using basic and acidic electrolytes in acetonitrile–methanol (1:1, v/v). Apparatus, capillary, temperature, detection and voltage as in Fig. 3. Electrophoresis medium [all in acetonitrile–methanol (1:1, v/v)]: (A) 25 m*M* ammonium acetate–100 m*M* sodium acetate; (B) 25 m*M* ammonium acetate; (C) 25 m*M* ammonium acetate–100 m*M* acetic acid; (D) 25 m*M* ammonium acetate–1 *M* acetic acid. Left row, mixed test sample I; right row, mixed test sample II. For peak identification, see Fig. 1.

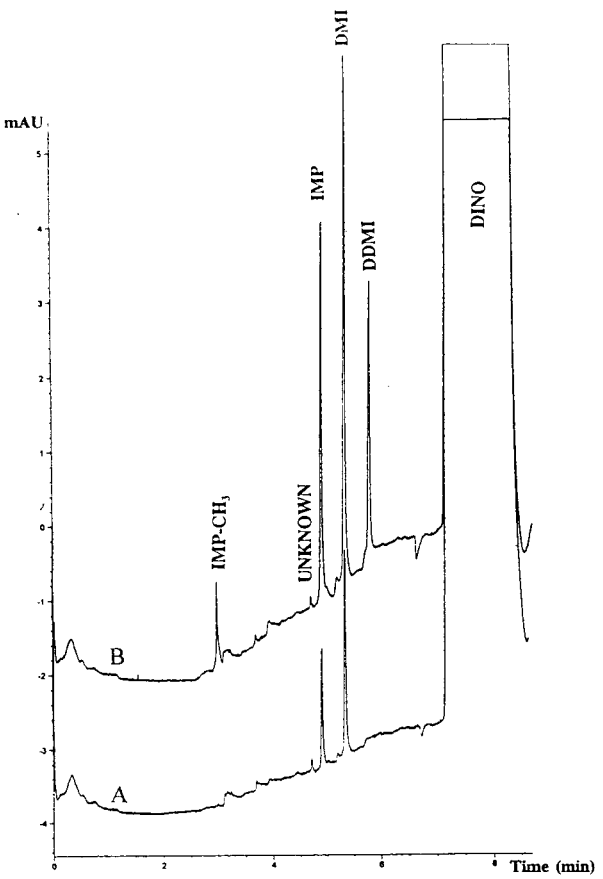

Fig. 6. Drug purity testing of DINO using non-aqueous CE. (A) 5.1 mg/ml sample of DINO in methanol and (B) standard addition of 10 μl of 0.05 mg/ml IMP, DMI, DDMI and IMP-CH_3 dissolved in methanol to 300 μl of DINO sample. Apparatus: HP^{3D} CE instrument. Conditions: capillary, 55.5 cm to detector × 100 μm I.D.; temperature, 25°C; detection, 214 nm; buffer, 25 m*M* ammonium acetate–1 *M* acetic acid in acetonitrile; voltage, 25 kV; current, 30 μA. For peak identification, see Fig. 1.

comparable to what has been obtained previously when using aqueous buffers [4]. A further advantage of the non-aqueous system is that owing to the low current (ca. 30 μA in a 100 μm I.D. capillary using 25 m*M* ammonium acetate in organic solvent) it is possible to use capillaries with a larger internal diameter, which again may provide higher loadability and thus lower limits of detection.

5. Conclusion

Non-aqueous capillary electrophoresis is a powerful tool for increasing and changing the separation selectivity of smaller molecules, and separation selectivities that would be very difficult to obtain in aqueous buffers may be introduced. Increased possibilities for changing the relative electrophoretic mobility of very similar compounds are obtained. On changing the organic solvent from a solvent with properties for both donating and accepting hydrogen bonds to a solvent which only is an acceptor for hydrogen bonding, major selectivity changes for primary and tertiary amines are observed. The technique is very suitable for drug purity testing but may also be useful for the determination of drugs and metabolites in biological fluids after concentration by solid-phase extraction and elution from the extraction column with organic solvents.

Acknowledgements

This work was supported by the Lundbeck Foundation, Denmark, by a grant to I. Bjørnsdottir, and by Hewlett-Packard through the donation of the HP^{3D} CE instrument. Waters is acknowledged for the donation of a Quanta 4000 instrument.

References

[1] S. Terabe, K. Otsuka, K. Ichikawa, A. Tsuchiya and T. Ando, Anal. Chem., 56 (1984) 111–113.
[2] S. Terabe, T. Katsura, Y. Okada, H. Ishihama and K. Otsuka, J. Microcol. Sep., 5 (1993) 23–33.
[3] T.L. Bereuter, LC-GC Int., 7 (1994) 78–93.
[4] S.H. Hansen, I. Bjørnsdottir and J. Tjørnelund, J. Pharm. Biomed. Anal., 13 (1995) 489–495.
[5] I. Bjørnsdottir and S.H. Hansen, J. Pharm. Biomed. Anal., 13 (1995) 687–693.
[6] E.K. Korchemnaya, A.N. Ermakov and L.P. Bochkova, J. Anal. Chem. USSR (1976) (Engl. Transl.), 33 (1978) 635–639.
[7] Y. Walbroehl and J.W. Jorgenson, J. Chromatogr., 315 (1984) 135–143.

[8] A.J. Tomlinson, L.M. Benson and S. Naylor, LC·GC, 12 (1994) 122–130.
[9] A.J. Tomlinson, L.M. Benson, J.W. Gorrod and S. Naylor, J. Chromatogr. B, 657 (1994) 373–381.
[10] R.S. Sahota and M.G. Khaledi, Anal. Chem., 66 (1994) 1141–1146.
[11] I. Bjørnsdottir and S.H. Hansen, J. Pharm. Biomed. Anal., submitted for publication.
[12] C.L. Ng, H.K. Lee and S.F.Y. Li, J. Liq. Chromatogr., 17 (1994) 3837–3857.
[13] C. Reichardt, Solvents and Solvent Effects in Organic Chemistry, VCH, Weinheim, 2nd ed., 1990, pp. 89–91.
[14] H. Sneider in J.F. Coetzee and C.D. Ritchie (Editors), Marcel Dekker, New York, 1969, pp. 301–342.
[15] E. Kenndler, in N.A. Guzman (Editor), Capillary Electrophoresis Technology, Marcel Dekker, New York, 1993, pp. 161–186.

ELSEVIER

Journal of Chromatography A, 711 (1995) 323–329

JOURNAL OF CHROMATOGRAPHY A

Monitoring of the poly(D,L-lactic acid) degradation by-products by capillary zone electrophoresis

Carole Vidil, Christian Braud*, Henri Garreau, Michel Vert

C.R.B.A.-URA CNRS 1465, Faculté de Pharmacie-UM1, 15, avenue Charles Flahault, 34060 Montpellier, France

First received 22 March 1995; revised manuscript received 28 April 1995

Abstract

Capillary zone electrophoresis (CZE) is presented as a new tool to resolve and analyze the ultimate degradation products of poly(D,L-lactic acid) aliphatic polyesters, namely water-soluble oligomers with a degree of polymerization lower than 8. The investigated oligomers were those present in a concentrated commercial D,L-lactic acid solution and those obtained by concentration of the same solution under vacuum. The repeatability of peak migration time was increased by introducing a relative migration factor aimed at minimizing the run-to-run peak shifts which depend on the experimental conditions, especially on the capillary and even on the instrument. Ring-opening of D,L-lactide was used to assign CZE peaks due to lactoyllactate and lactate. The rate constant and the activation energy of lactoyllactate hydrolysis were determined by monitoring the formation of lactate by CZE.

1. Introduction

Degradation of degradable and biodegradable polymers is usually monitored through indirect phenomena like oxygen consumption and CO_2 production, in the case of outdoor degradation, and by water absorption, mass loss and molecular mass decreases for both in vivo and outdoor degradations. To obtaining information at the molecular level, size exclusion chromatography (SEC) or high-performance liquid chromatography (HPLC), both in organic solvents or in mixtures of water with organic solvents, are very well suited. Hydrolytic degradation of polymeric biomaterials typically occurs in aqueous media and thus analytical tools compatible with water or polar solvents are required. Generally, hydrolysable polymers, such as aliphatic polyesters, lead to degradation by-products which bear ionic groups at one chain end, at least. Ultimate degradation by-products are thus water-soluble or water-dispersable. This makes high-performance capillary electrophoresis (HPCE) of interest for monitoring the final stage of hydrolytic degradation, and of biomediated degradation as well.

Capillary zone electrophoresis (CZE), which is the simplest HPCE technique, has been successfully used to separate oligomers of natural [1–4] and synthetic [5] origin.

Poly(β-malic acid), a water-soluble degradable polyester of the polycarboxylic type is now well-known as a hydrolytically degradable polymer [6,7]. Oligomer production during in vitro ageing was monitored by aqueous SEC using Biorad P2 gel. However, this technique, which is

* Corresponding author.

0021-9673/95/$09.50
SSDI 0021-9673(95)00517-X

able to separate only the five smallest oligomers is rather time-consuming since it requires several hours. CZE appeared much more efficient as it allowed easy separation of the fifteen smallest oligomers within 15 min [6].

In the case of poly(lactic acids), which are of increasing surgical and pharmacological interest [8], it has been demonstrated that slow release of lactic acid [9] and of lactoyllactic acid [10] reflects the last states of the hydrolytic degradation processes. However, the frontier between water-insoluble and water-soluble oligomers is still unknown. This lack of information originates from analytical difficulties to detect low-molecular-mass compounds especially in aqueous environments, and in the presence of high-molecular-mass polymers.

In the present paper, we report the results of a CZE monitoring of poly (D,L-lactic acid) oligomers which are formed in lactic acid concentrated solutions or during concentration of commercial D,L-lactic acid aqueous solutions under vacuum. Assignment of the ultimate oligomers was done on the basis of D,L-lactide hydrolysis.

2. Experimental

2.1. Materials

Commercial D,L-lactic acid (85% w/w aqueous solutions) and D,L-lactide were obtained from Sigma and Purac respectively and were used without further purification. All other chemicals were of analytical grade.

2.2. Synthesis

Oligo(D,L-lactic acid)

Commercial D,L-lactic acid solution (200 g) was introduced in a round-bottom flask (1000 ml) and heated at 85°C under vacuum for 2 h and then heated at 120°C for 9 h. The reaction medium was kept under argon atmosphere during the experiment.

Sodium D,L-lactoyllactate

D,L-lactide (500 mg) was dispersed in 50 m*M* sodium phosphate buffer adjusted to pH 6.8 (100 ml). As the reaction proceeded, the initial pH value was maintained by adding 1 *M* NaOH. After 3 h at room temperature, no lactide crystals remained in the medium. The buffered solution was then filtered on a 0.22-μm Millipore filter for sterilization. The resulting sodium D,L-lactic-lactoyllactate was stored in solution.

2.3. Methods

CZE was carried out using either 3D-CE (Hewlett-Packard) or a P/ACE 5000 (Beckman) instrument equipped with UV detection at 205 nm and 200 nm, respectively. Fused-silica capillaries of different sizes were filled with running buffer (0.1 *M* sodium borate adjusted to pH 8.9 with 1 *M* NaOH). Before each run, the capillary was rinsed, first for 2 min with 0.1 *M* HCl, second for 2 min with 0.1 *M* NaOH, and third for 1 min with water. Separation was performed at 25°C with an applied voltage of 30 kV. All the lactic acid derivatives ($C \approx 0.3\%$) which were analyzed by CZE, were initially dissolved in 0.05 *M* sodium phosphate buffer adjusted to pH 6.8. About 20 nl were injected in the capillary by the hydrostatic pressure method. Experiments were also performed by using 0.05 *M* sodium phosphate buffer at pH 6.8 and at a voltage of 20 kV with similar rinsing procedure.

SEC was carried out on 1% tetrahydrofuran (THF) solutions, using a chromatograph (Spectra-Physics SP 8810) equipped with two PL gel columns (50 Å + 100 Å; 5 μm gel beads; 300 × 7.5 mm I.D.). Separation was performed at a flow-rate of 0.6 ml min^{-1}. Refractometric detection was monitored by a Spectra-Physics SP 430 detector.

Potentiometric titration was performed on acid solution [500 mg of lactic acid oligomers dissolved (or dispersed) in 50 ml of pure water] which was neutralized with 1 *M* NaOH using a 665 Dosimat (Metrohm). pH values were recorded at 25.0°C with a TC-III combined electrode (Taccusel) connected to an ionoprocessor II (Taccusel) in order to determine the free acidity in the sample. Back titration was performed with 1 *M* HCl after addition of an excess alkali.

3. Results and discussion

3.1. D,L-lactic acid condensation

It is well-known that concentrated aqueous solutions with more than 80% (w/w) of lactic acid are composed of mixtures of monomer, dimer and higher oligomer species [11]. By heating such a solution under vacuum, it is possible to obtain polycondensates [low-molecular-mass polylactic acid (LMWPLA)] with molecular mass ranging up to a few thousands [12] which exhibit solubilities similar to those of high-molecular-mass poly(D,L-lactide). The most common solvents are then chlorinated hydrocarbons dioxane, THF, acetone. In contrast, water and alcohols are non-solvents.

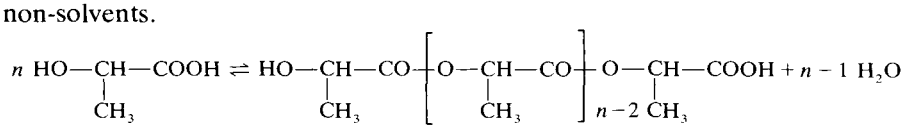

In order to obtain the very first oligomers, mild polycondensation has been performed. First, the commercial D,L-lactic acid solution was heated for 2 h at a relatively low temperature (85°C) to slowly remove water. Then, the mixture was maintained at 120°C for 9 h. The resulting oligomeric mixture was referred to as oligo(D,L-lactic acid).

The value of the number-average degree of polymerization of oligomers present in the commercial lactic acid solution and of oligo(D,L-lactic acid) were respectively 1.16 and 2.10 as determined by potentiometric titration. This result showed that oligo(D,L-lactic acid) was composed of a very small oligomers.

An aliquot of the lactic acid commercial solution was dissolved in THF and analyzed by SEC in THF. Four peaks were observed (Fig. 1a). However, this chromatographic separation was carried out in an organic medium, the carboxyl groups being non-ionized. Aqueous SEC with a Biorad P2 gel was successfully used for the separation of the sodium salt form of poly(β-malic acid) oligomers [4]. In the case of commercial lactic acid solution, resolution was too poor for proper separation. In contrast, CZE showed four well separated peaks (O1, O2, O3 and O4 in Fig. 2a) within 6 min in 0.1 *M* borate buffer (pH 8.9).

The SEC traces of oligo(D,L-lactic acid) (Fig. 1b) revealed the formation of new oligomers within the heated lactic acid commercial solution, as shown by comparing with traces of Fig. 1a. Oligo(D,L-lactic acid) was soluble in methanol. It was also soluble in water provided the -COOH end groups were ionized by adding sodium hydroxide in such a way that pH values remained under 6.8. Above this value, the oligomers progressively degraded to yield sodium lactate.

Fig. 2b shows the electrophoregram of oligo(D,L-lactic acid). Comparison of Figs. 2a and 2b

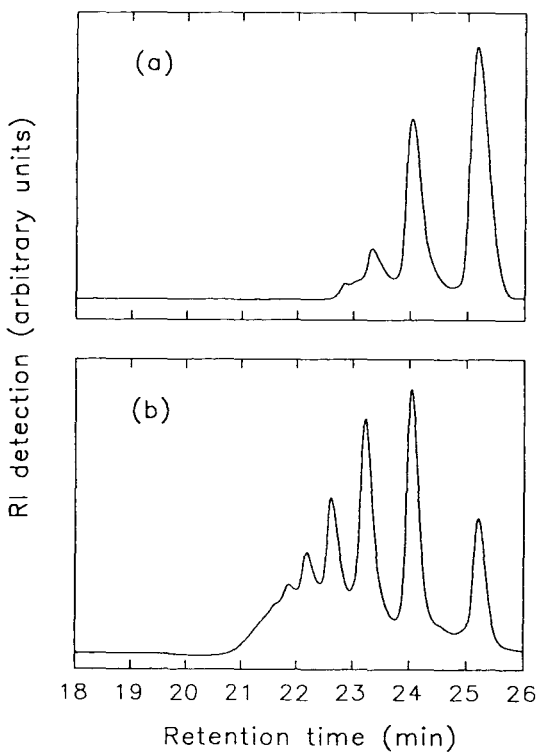

Fig. 1. SEC traces in DMF of commercial D,L-lactic acid solution (a) and of oligo(D,L-lactic acid (b).

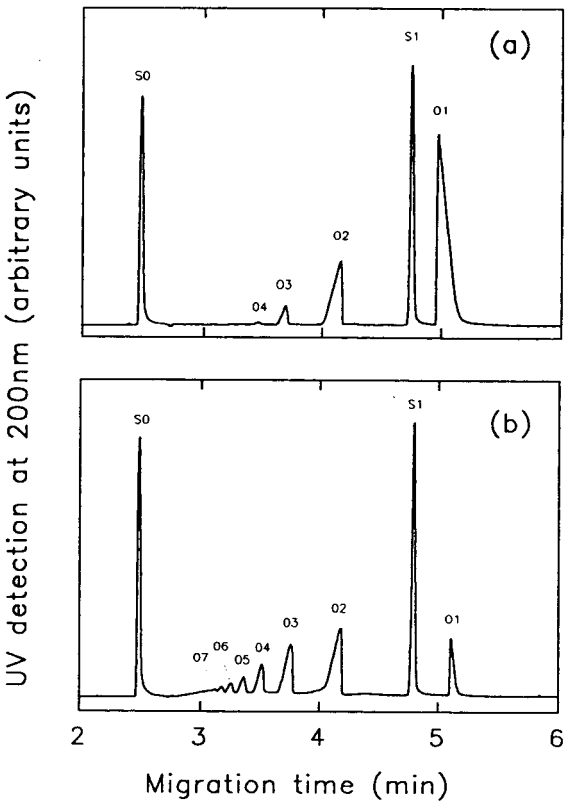

Fig. 2. Electropherograms of the sodium salt forms of commercial D,L-lactic acid solution (a) and of oligo(D,L-lactic acid) (b) [recorded on Beckman instrument with a fused-silica capillary ($\phi_{int} = 75$ μm, $L_T = 57.0$ cm); 0.1 M sodium borate buffer at pH 8.9; 25°C; for peak assignment see the text].

showed that O3 and O4 peaks were enlarged. Moreover, O5, O6, O7 peaks were now detected. These peaks can be reasonably assigned to tri-, tetra-, penta-, hexa- and heptamers, as polycondensation leads normally to a continuous distribution of degrees of polymerization.

The relative high pH value of the borate buffer did not affect the stability of oligo(D,L-lactic acid) since the electropherograms recorded by using 0.05 M phosphate buffer at pH 6.8 showed also seven peaks comparable to those of Fig. 2b. It must be noted that the running time was higher in the phosphate buffer (~20 min) than in the borate buffer. This longer time was due to the lower voltage (20 kV) imposed by the higher conductivity of the phosphate ions. Therefore, all further analyses were performed in borate buffer.

3.2. Electrophoretic characteristics of CZE peaks

In order to avoid the effects of a progressive deviation of peak migration time after several consecutive runs, two internal standards (S0, benzyl alcohol which reveals the electroosmotic flow [13] and SI, benzoic acid, a negatively charged standard molecule) were added to the tested solutions. The peak of an oligomer i was thus defined by the relative migration factor:

$$RMF_i = (T_i - T_{S0})/(T_{S1} - T_{S0})$$

where T_i, T_{S0} and T_{S1} are the migration time of the oligomer i and those of the added standards, respectively. T_i values were deduced from the middle of the width of the peak at half-height.

The reproducibility of RMF_i values (Table 1) was checked by comparing data obtained from the same instrument equipped with different capillaries and from different instruments whose characteristics are listed in Table 2. When RMF_i values are plotted versus i (Fig. 3), it clearly appears that the capillary electrophoretic separation was limited to oligomers smaller than $i = 8$

Table 1
Electrophoretic characteristics of O_i peaks observed in Fig. 2b

i	RMF_i
1	1.13 ± 0.02
2	0.71 ± 0.02
3	0.54 ± 0.01
4	0.44 ± 0.01
5	0.38 ± 0.01
6	0.34 ± 0.01
7	0.31 ± 0.01

Table 2
Physical characteristics of the differents capillaries used to determine intrinsic parameters of the two internal standards with fresh buffer solutions

Origin	ϕ_{int} (μm)	L_T (cm)	L_D (cm)	I (μA)	t_{EO} (min)	t_{benz} (min)	$\mu_{benz} \cdot 10^4$ ($cm^2\ V^{-1}\ s^{-1}$)
Hewlett-Packard	50	65.0	57.0	29	3.23	6.49	−3.20
Beckman	50	49.0	42.4	38	1.72	3.24	−3.15
Beckman	75	57.0	50.4	74	2.49	4.79	−3.08

ϕ: internal diameter; L_T: total length; L_D: distance between the inlet and the detector; EO: benzyl alcohol; benz: benzoic acid, applied voltage, 30 kV giving intensity I.

since RMF_i values levelled off at 0.3 when the oligomer length increased.

3.3. Kinetics of lactoyllactate hydrolysis

Peaks O1 and O2 in Figs. 2a and 2b were unambiguously assigned to lactate and lactoyllactate respectively from D,L-lactide (I) hydrolysis. The D,L-lactide ring opened in sodium phosphate buffer at pH 6.8. Under this condition, only sodium lactoyllactate (II) was formed as shown by the unique peak observed in Fig. 4a and characterized by a RMF value of 0.71. When the resulting solution was allowed to age, the dimer was progressively transformed into sodium lactate (III).

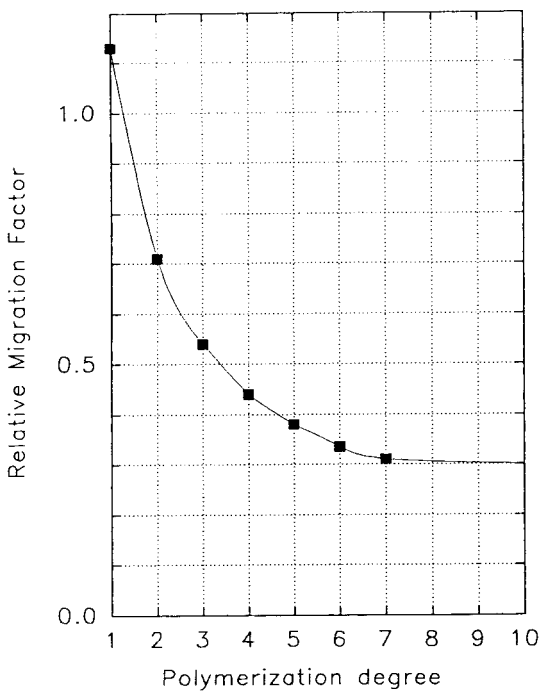

Fig. 3. Plot of relative migration factor (RMF) as a function of the degree of polymerization from data of Table 1.

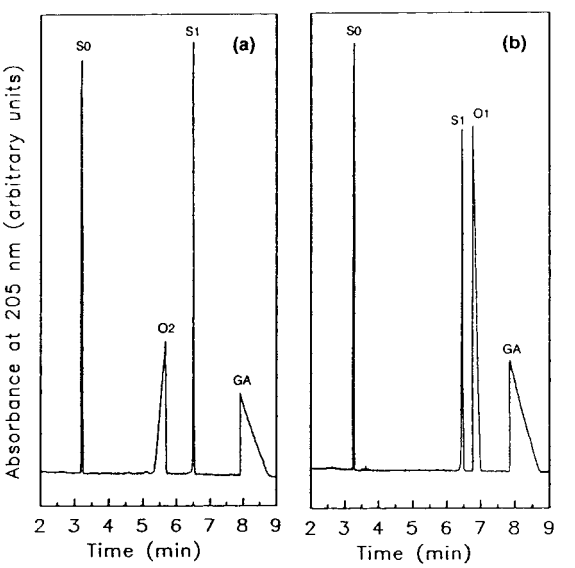

Fig. 4. Electropherograms of sodium D,L-lactoyllactate (a) and of sodium D,L-lactate (b) in the presence of 0.066 M glycolic acid used as internal reference [recorded on Hewlett-Packard instrument with a fused-silica capillary ($\phi_{int} = 50$ μm, $L_T = 65.0$ cm); 0.1 M sodium borate buffer at pH 8.9; 25°C; for peak assignment see the text].

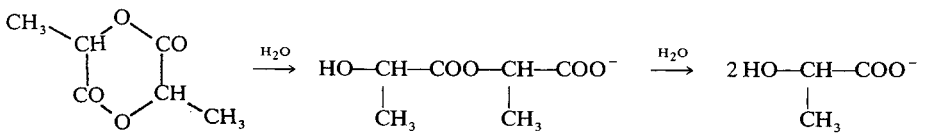

(I) (II) (III)

The peak at RMF = 0.71 progressively disappeared and a second peak (RMF = 1.13) appeared which was assigned to lactate (Fig. 4b).

The relative concentrations of the two species were deduced from the electropherograms recorded for different reaction times in the presence of an internal standard, glycolic acid. This allowed the determination of the kinetics parameters of the reaction:

$$\text{Dimer} + H_2O \rightarrow 2\ \text{Monomer} \quad (1)$$

Let us define the molar concentration $[X]^t$ and the measured area $(A_X)^t$ where X is either the dimer (Di), the monomer (Mono) or the internal standard (GA) and t is the time. These parameters are linked by the relation:

$$(A_X)^t = K\varepsilon_X[X]^t \quad (2)$$

where K is a constant depending on the detector and ε_X the molar extinction coefficient of species X.

According to the conservation law:

$$2[\text{Di}]^0 = 2[\text{Di}]^t + [\text{Mono}]^t = [\text{Mono}]^\infty \quad (3)$$

The degree of conversion, $p = [\text{Mono}]^t/[\text{Mono}]^\infty$ is then:

$$p = [\text{Mono}]^t/(2[\text{Di}]^t + [\text{Mono}]^t) = 1/(1 + 2[\text{Di}]^t/[\text{Mono}]^t) \quad (4)$$

Experimentally, (A_{Di}), (A_{Mono}) and (A_{GA}) were measured as a function of t. Data allowed calculation of:

$$(\%A_{\text{Mono}})^t = 100(A_{\text{Mono}})^t/[(A_{\text{Mono}})^t + (A_{\text{Di}})^t] = 100/[1 + (A_{\text{Di}})^t/(A_{\text{Mono}})^t] \quad (5)$$

Glycolic acid being an internal standard, one has:

$$(A_{\text{Gly}})^0 = (A_{\text{Gly}})^\infty \quad (6)$$

If we define:

$$R_{\text{Mono}} = (A_{\text{Mono}})^\infty/(A_{\text{GA}})^\infty \quad (7)$$

$$R_{\text{Di}} = (A_{\text{Di}})^0/(A_{\text{GA}})^0 \quad (8)$$

Eqs. 6, 7, 8 and 3 lead to:

$$R_{\text{Mono}}/R_{\text{Di}} = (A_{\text{Mono}})^\infty/(A_{\text{Di}})^0 = (\varepsilon_{\text{Mono}}[\text{Mono}]^\infty)/(\varepsilon_{\text{Di}}[\text{Di}]^0) = 2\,\varepsilon_{\text{Mono}}/\varepsilon_{\text{Di}} \quad (9)$$

and combination of Eqs. 5 and 2 leads to:

$$(A_{\text{Di}})^t/(A_{\text{Mono}})^t = 100/(\%A_{\text{Mono}})^t - 1 = \varepsilon_{\text{Di}}[\text{Di}]^t/(\varepsilon_{\text{Mono}}[\text{Mono}]^t)$$

and

$$[\text{Di}]^t/[\text{Mono}]^t = \varepsilon_{\text{Mono}}/\varepsilon_{\text{Di}}\ \ (100/(\%A_{\text{Mono}})^t - 1) \quad (10)$$

Using Eqs. 9 and 10, Eq. 4 can be written:

$$p = 1/[1 + (R_{\text{Mono}}/R_{\text{Di}})\ \ (100\%A_{\text{Mono}})^t - 1)] \quad (11)$$

Figs. 4a and 4b show respectively the electropherograms which were obtained for $p = 0$ and $p = 1$. From these figures, $R_{\text{Di}} = 0.68$ and $R_{\text{Mono}} = 0.85$ can be determined. Introducing these values in Eq. 11, one could plot experimental values of the degree of conversion vs. time (Fig. 5). Experimental data obeyed Eq. 12 which is typical of a pseudo first order reaction, water being in large excess:

$$1 - p = e^{-K'.t} \quad (12)$$

as shown by the good fit between experimental and calculated data (Fig. 5).

Furthermore, data in Fig. 5 were used to show that constant K' obeyed the Arrhenius law $K' = A\,e^{-E/RT}$ with $A = 6.8 \cdot 10^{11}\ h^{-1}$ and $E = 87.4$ kJ.

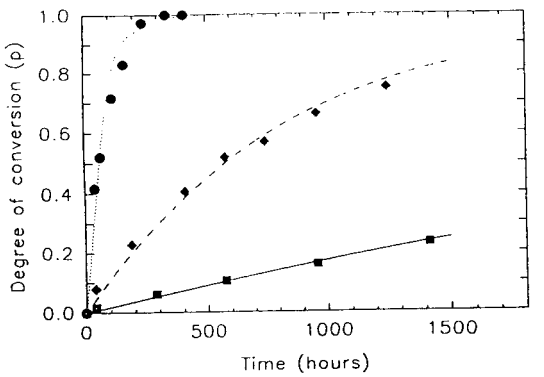

Fig. 5. Degree of conversion of ester bond scission of sodium D,L-lactoyllactate in 0.05 *M* sodium phosphate buffer (pH 6.8) at different temperatures (○: 60°C; ◆: 37°C; □: 21°C). Data were fitted with $K_{60} = 14.10^{-3}$ h^{-1} (-----), $K_{37} = 12 \cdot 10^{-4}$ h^{-1} (– – –), and $K_{21} = 19 \cdot 10^{-5}$ h^{-1} (———) by using Eq. 12.

4. Conclusions

This study showed that HPCE can easily detect oligomers of D,L-lactic acid in the salt form in aqueous systems. Monomer and dimer peaks were unambiguously assigned. In aqueous media at neutral pH, i.e. when –COOH groups are ionized, oligomers with a degree of polymerization smaller than 8 were detected. Therefore, CZE can be considered as a tool for monitoring the late stages of the hydrolytic degradation of HMWPLA. It is of interest to note that CZE appears to be a helpful complement of SEC in organic media which is used to monitor the early states of HMWPLA degradation.

Acknowledgements

The authors wish to thank Prof. Michel Audran (Faculty of Pharmacy, Montpellier) and Dr. Alain Rousseau (E.N.S.C.M., Montpellier) for their helpful contribution to the collection of experimental data on Hewlett-Packard 3D-CE and SEC machines, respectively.

References

[1] W. Nashabeh and Z. El-Rassi, J. Chromatogr., 514 (1990) 57.
[2] J.B.L. Damm, G.T. Overklift, B.W.M. Vermeulen, C.F. Fluitsma and G.K. van Dedem, J. Chromatogr., 608 (1992) 297.
[3] J.T. Smith and Z. El-Rasssi, J. High Res. Chromatogr., 15 (1992) 573.
[4] C. Chiesa and C. Horvath, J. Chromatogr., 645 (1993) 337.
[5] J. Bullock, J. Chromatogr., 645 (1993) 169.
[6] C. Braud and M. Vert, Polym. Bull., 29 (1992) 177.
[7] C. Braud and M. Vert, Trends Polym. Sci., 3 (1993) 57.
[8] C.G. Pitt, in M. Vert, J. Feijen, A. Albertsson, G. Scott and E. Chiellini (Editors), Biodegradable Polymers and Plastics, The Royal Society of Chemistry, Cambridge, 1992, pp. 7–19.
[9] S.M. Li, H. Garreau and M. Vert, J. Materials Sci.: Materials in Medicine, 1 (1990) 123.
[10] S.P. Sawan and J.J. Barry, A.C.S. Polym. Prept., 29 (1988) 299.
[11] C.H. Holten, Lactic Acid – Properties and Chemistry of Lactic Acid and Derivatives, Verlag Chemie, Weinheim, 1971.
[12] J. Mauduit, N. Bukh and M. Vert. J. Controlled Release, 23 (1993) 209.
[13] R. Kuhn and S. Hoofsteter-Kuhn, Capillary Electrophoresis: Principles and Practice, Springer-Verlag, Berlin, 1993.

ELSEVIER

Journal of Chromatography A, 711 (1995) 331–337

JOURNAL OF CHROMATOGRAPHY A

Gel electrophoretic analysis of cellular and secreted proteins from resting and activated rat alveolar macrophages treated with pentamidine isethionate

James K. Selkirk*, C. He, B.A. Merrick

Laboratory of Molecular Carcinogenesis, National Institute of Environmental Health Sciences, Research Triangle Park, NC 27709, USA

First received 28 June 1994; revised manuscript received 1 August 1994; accepted 19 May 1995

Abstract

Pneumocystic carinii pneumonia, which is a major cause of death among patients suffering from acquired immunodeficiency syndrome, has often been treated successfully with pentamidine isethionate. This study examines pentamidine effects on cellular and secreted proteins from rat alveolar macrophages by two-dimensional gel electrophoresis and computerized image analysis. Over 100 secreted proteins were detected by fluorography. Fluorography showed pentamidine diminished tumor necrosis factor and interleukin-1 release along with other proteins. Effects of combined bacterial lipopolysaccharide and pentamidine were more pronounced on secreted versus cellular proteins in protein amount and pattern difference. Thus pentamidine exhibited a general repressive effect on cellular and secreted protein expression in resting and activated macrophages.

1. Introduction

Pentamidine isethionate [1,5-di(4-amidinophenoxy)pentane], was first used against protozoan infection in 1938 [1]. Although many other structural analogues were screened as trypanocides, pentamidine was the compound adopted for clinical use, although with caution due to its high toxicity. However, despite pentamidines' numerous deleterious side effects including nephrotoxicity, hepatotoxicity and hypotension, it was used with great success against epidemics of African trypanosomiasis in the post World War II period [2]. The drug was shown to be effective in infantile pneumocyctis carinii pneumonia (PCP) outbreaks in Europe, reducing the mortality rate from 50 down to 3.5%. However, it did not gain wide acceptance for general clinical use because of its multifocal toxicity, and also because subsequent occurrence of PCP was quite rare until the advent of acquired immunodeficiency syndrome (AIDS) which has now reached worldwide significance and is threatening to become a pandemic phenomenon. Since PCP has been shown to be one of the most common life-threatening infections in AIDS patients, pentamidine has again become prominent as one of the major drugs of choice for PCP infection.

Until recently, the long-term risks associated with the mechanisms of pentamidine toxicity had not received great emphasis because of the high

* Corresponding author.

0021-9673/95/$09.50
SSDI 0021-9673(95)00607-9

lethality of AIDS. However, as the longevity and survival of AIDS patients increase and the use of pentamidine becomes more common, adverse actions and long-term side effects of this drug will become increasingly important. It is already known that pentamidine interferes with numerous metabolic pathways and therefore has the potential for broad-based cytotoxicity. Originally pentamidine was administered only parenterally, either intramuscularly or intravenously, which resulted in deposition of the drug in virtually all organs and tissues in the body. Also, pentamidine has a slow turnover rate since treatment is followed by a relatively slow release from the body with the chemical present in urine up to eight weeks after cessation of therapy [3]. Although the lung is the site of PCP infection, pulmonary distribution after parenteral administration of pentamidine is relatively low as compared to the rest of the body. This observation led to adoption of an aerosolized route for pentamidine where high concentrations could be reached by direct deposition into the lungs [4], and with the hope of reducing severe systemic side effects. Subsequently, clinical studies did show that a daily dosage of 600 mg by inhalation resulted in general clinical improvement and survival [5]. However, more recent studies comparing parenteral and aerosol administration suggest that, while the aerosol route works well with mild infection, moderate or heavy infections are less successfully treated with this modality [6,7]. Currently, there is no adequate biochemical explanation as to why heavier infection of PCP should be less sensitive to pentamidine via direct deposition into the lungs.

In addition to its antimicrobial effects, aerosol-borne pentamidine may produce adverse effects upon resident alveolar macrophages which are essential components of the immunologic response to pulmonary infection and disease. Phagocytosis, recruitment and cytokine production are primary functions of macrophages which are activated by infectious organisms as a major line of defense in the pulmonary system. Activation of macrophages in in vitro culture can also be experimentally elicited by exposure to bacterial lipopolysaccharide (LPS) as the inducing agent. Since macrophage response to pentamidine may alter normal cellular biochemistry and therefore cytokine defense mechanisms may be impacted, we have evaluated electrophoretic patterns from both cellular and secreted proteins, as well as determined the presence of tumor necrosis factor (TNFα) and interleukin-1 (IL-1α) from isolated rat alveolar macrophages under resting and activated conditions using Western blotting with polyoclonal antibodies, two-dimensional polyacrylamide gel electrophoresis and computerized image analysis.

2. Experimental

2.1. Cell culture and radiolabeling

Rat alveolar macrophage cultures obtained after pulmonary gavage of female F344 rats (12–16 weeks old), were washed and plated to remove non-adherent cells [8]. Cells were resuspended in RPMI 1640 medium supplemented with glutamine, penicillin and streptomycin. For electrophoresis and immunoblotting experiments, macrophages were plated at 10^6 cells/ml in 100-mm plates. After 1 h for attachment, cells were exposed to pentamidine solubilized in water for 0.5 h prior to bacterial LPS at 1 μg/ml. Immediately after exposure to LPS, [^{35}S]-methionine was added at 100 μCi/well. Cells were incubated for 24 h at 37°C in a plastic enclosure gassed with a mixture of oxygen–carbon dioxide (95:5). Log orders of pentamidine concentration were selected up to a limit of 10 μM in which cellular viability was maintained without cytotoxicity.

At harvest, culture medium was removed and cells were scraped, washed in phosphate-buffered saline (PBS), pelleted and stored at −80°C until electrophoretic analysis. Radiolabeled secreted proteins in the supernatant were dialyzed with PBS containing 0.2 mM phenylmethylsulfonyl fluoride (PMSF) and concentrated with Amicon centrifugal membranes (M_r cut-off 10 000), and lyphophylized prior to storage at −80°C.

Incorporation of [^{35}S]-methionine into macrophage protein was evaluated in 12 well plates at

10^6 cells/well. Under the conditions described above, cells were incubated at 0, 0.1, 1.0 and 10.0 μM pentamidine with and without LPS for 24 h. Cold carrier bovine serum albumin was added to each cell sample which was washed with 10% trichloroacetic acid until only background ^{35}S counts appeared in the supernatant. Excess ^{35}S was removed from secreted proteins by centrifugal dialysis. Protein was dissolved in 0.1 M NaOH, neutralized with acetic acid and counted in Aquasol.

2.2. Two-dimensional gel electrophoresis, fluorography and immunoblotting

Immediately prior to analysis, whole cells or secreted proteins were dissolved in urea-based lysis buffer [8]. Cellular protein was electrophoresed at 250 000 dpm of acid-precipitable radioactivity or as 125 000 dpm of secreted protein. Protein samples were subjected to two-dimensional gel electrophoresis according to O'Farrell [9]. Isoelectric focusing was in a pH gradient ranging from pH 4 to 8. Protein separation according to M_r by sodium dodecyl sulfate–polayacrylamide gel electrophoresis (SDS–PAGE) used a 10–16% acrylamide gradient. Gels with ^{35}S-labeled proteins were impregnated with fluor (Amplify, Amersham, Arlington Heights, IL, USA), dried, then exposed to preflashed XAR-5 film (Kodak, Rochester, NY, USA) for one to two weeks at −80°C. Film was developed using a Konica processor.

Two-dimensional gels were electroblotted onto poly(vinylidene diflouride) membranes and blocked with gelatin (Norland) for 2 h. Blots were incubated overnight with murine polyclonal antibody for IL-1α and TNFα (Genzyme, Cambridge, MA, USA). Secondary antibody detection for IL-1 used alkaline phosphatase and peroxidase for TNF, respectively. Murine rTNF (Genzyme) was electrophoresed, separated, electroblotted and stained with colloidal gold (Bio-Rad).

2.3. Image analysis

Films were digitized with an Optronics Model P-1000 densitometry scanner and analyzed on an International Imaging Systems workstation. Digitized images were subjected to smoothing and background subtraction algorithms in order to reduce each 1536×1536 pixel image into numerical data [10]. Every protein on each image was numerically described by x,y coordinates, the center point, and peak and total integrated densities (0 to 256 gray value range), and also sigma x,y diameters for an elliptical spot shape. Initial computer generated images were edited for artifacts and then modeled with a bi-gaussian algorithm on a Trace Multiflow computer to apportion protein spot density. Data from 3–5 gels for each treatment were registered and compared, and subsequently compiled into one master image [10]. Similarly, master images from each treatment were constructed from replicate images and qualitatively compared in order to determine common and unique proteins.

3. Results and discussion

While the typical response of macrophages to treatment with LPS is an increase of approximately 35% over the control with regard to incorporation of [^{35}S]methionine into protein, Fig. 1 shows pentamidine slowed this effect when macrophages were activated with LPS. While pentamidine (10 μM) itself had little effect upon [^{35}S]methionine incorporation into macrophage protein, the expected LPS induction of ^{35}S labeling was depressed between 10 μM and 1 μM. When [^{35}S]methionine labeling was measured in secreted protein (see inset), the greatest effect of pentamidine was at 10 μM which depressed the LPS-induced increase in ^{35}S labeling of macrophage protein from 65 down to 17% above the control value. In contrast to cellular protein labeling, 10 μM pentamidine alone gave a decrease in secreted protein labeling of 15%.

Treatment with pentamidine did not greatly affect the relative distribution of cellular macrophage proteins as compared to the control pattern. The labeling time used in these experiments resulted in more than 700 proteins showing incorporation of radiolabel. The more prominent quantitative changes are noted in Fig. 2.

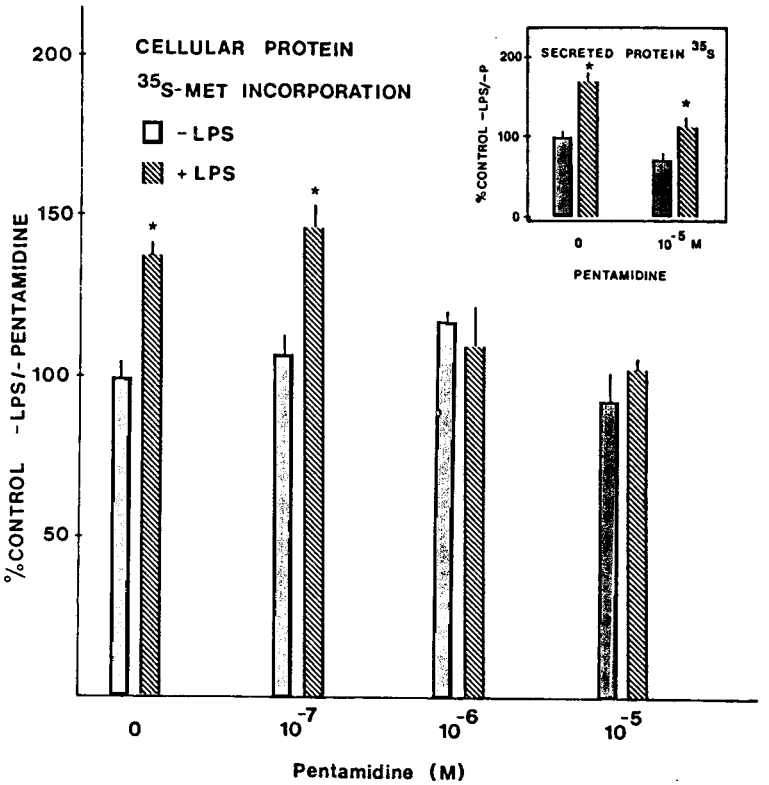

Fig. 1. Effect of bacterial lipopolysaccharide (LPS) and pentamidine on protein synthesis in rat alveolar macrophages. The histogram shows incorporation of [^{35}S]methionine for 24 h with increasing concentrations of pentamidine. Asterisks indicate significant differences at $p > 0.5\%$ from controls without LPS or pentamidine.

Those proteins with more than five-fold density difference are noted by letters (A–K). There were also five proteins that pentamidine either induced or sufficiently down-regulated to absence (solid triangles) which were modulated in the presence and absence of LPS. This indicated a specific pentamidine effect. The more prominent quantitative changes were seen in proteins A (M_r 63 000), C, D (52 000), E (37 000), F (29 000), J (26 000) and K (11 000). Two proteins were induced by LPS since both the M_r 69 000 and 11 000 proteins were missing in the pentamidine/−LPS panel. However, treatment with LPS also down-regulated two basic M_r 75 000 proteins as well as an acidic M_r 88 000 protein. The occurrence of both induction and down-regulation of proteins suggest a complex pattern of protein modulation by treatment with pentamidine.

Since macrophages secrete TNFα as well as IL-1α, which are both prominent in the general immune response, it was important to determine if pentamidine treatment altered the usual formation of these proteins by the LPS antigen. Fig. 3 shows the effect of pentamidine in the presence and absence of LPS. The left panel shows a small constitutive amount of TNFα while the right panel shows a considerable induction of TNFα as well as a small quantity of IL-1α. It would appear therefore that pentamidine does not specifically inhibit the formation of these important protective proteins during macrophage activation by LPS. In addition there was a considerable LPS-induced increase of a low-mo-

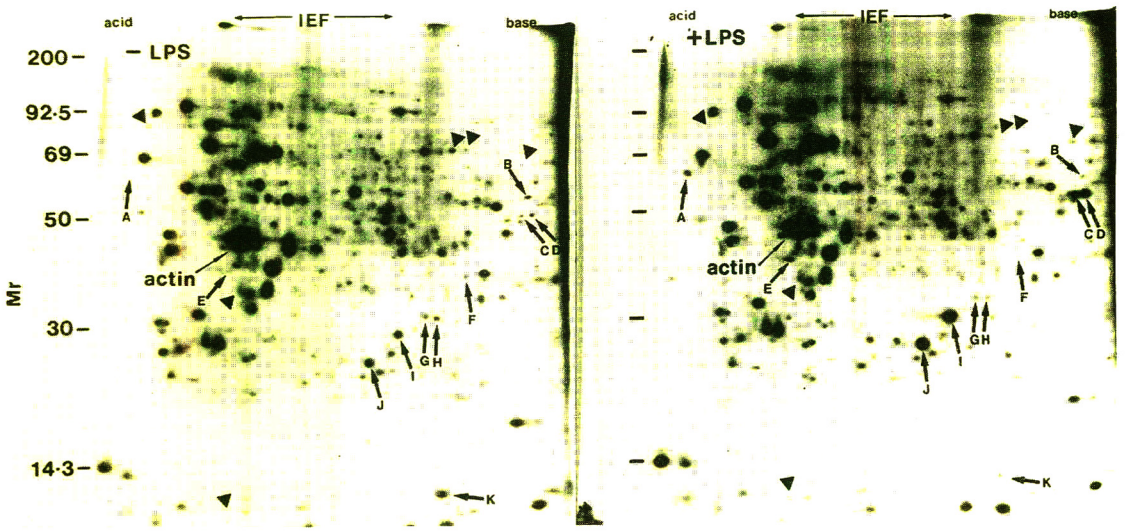

Fig. 2. Fluorographs from [^{35}S]methionine labeling of cellular proteins from pentamidine-treated rat alveolar macrophages after 24-h incubation with 10 μM pentamidine and with or without LPS. The presence (+) or absence (−) of LPS is indicated on the figure. Quantitative changes are indicated by arrows, while qualitative changes are marked triangles. M_r values $\times 10^{-3}$.

lecular-mass protein (M_r 13 500) which has not yet been identified. Identification of TNFα and IL-1α was previously confirmed by immunoblotting with specific antibodies [8].

The overall modulation of secreted proteins was assessed using image analysis as seen in Fig. 4. Treatment with LPS showed the majority of secreted proteins (128, shaded spots) to be unchanged with 8 proteins (+) down-regulated and 53 proteins (○) induced by LPS. The addi-

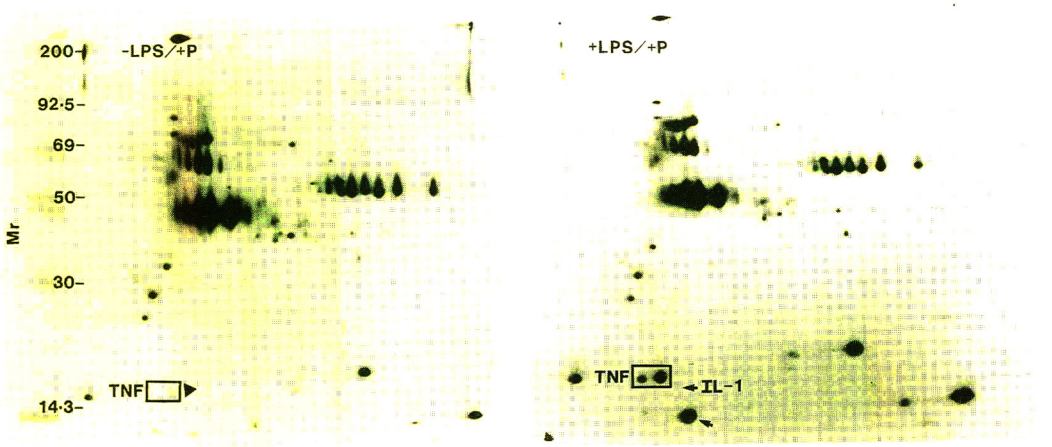

Fig. 3. Fluorographs from [^{35}S]methionine-labeled secreted proteins from rat alveolar macrophages after 24-h incubation with or without LPS. Immunoblotting confirmed the presence of TNFα and IL-1α. P = Pentamidine. M_r values $\times 10^{-3}$.

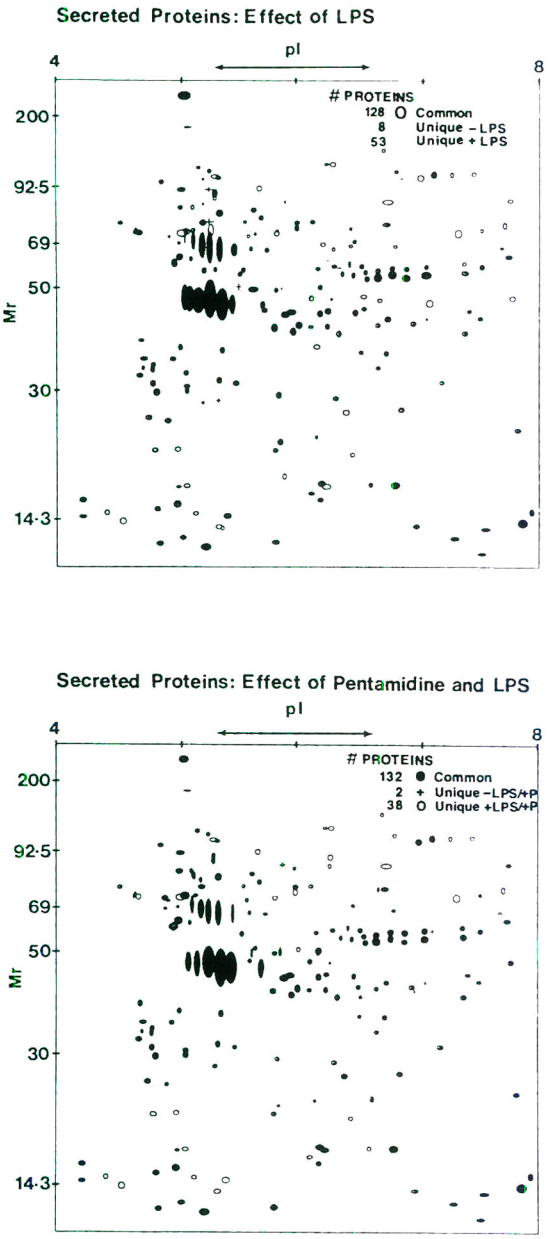

Fig. 4. Computerized comparison of secreted proteins from alveolar macrophages as affected by 10 μM pentamidine (P) and bacterial LPS for 24 h. [^{35}S]Methionine-labeled proteins secreted into culture medium were concentrated and subjected to two-dimensional polyacrylamide gel electrophoresis. Fluorographs were scanned and analyzed by image analysis algorithms. Master composite images as shown above represent shared (common) and different (unique) proteins with and without LPS in the absence or presence of pentamidine.

tion of pentamidine caused relatively little qualitative change in the protein profile under these conditions with 132 proteins common with and without LPS. Only 2 proteins were down-regulated below the resolution of analysis, although pentamidine did reduce the inductive effect of LPS with only 38 proteins up-regulated.

Pentamidine isethionate is structurally categorized in the aromatic diamidine family of compounds that are extensively used as trypanocides [11]. The mechanism of action of pentamidine is still uncertain, although it appears to inhibit dihydrofolate reductase and deplete folic acid [12]. It also binds to DNA in a non-intercalative way, and is known to preferentially attach to the kinetoplast in trypanosomes [13]. Pentamidine also inhibits proteases [14], oxygen consumption in cells [14], RNA polymerase [15], nucleic acid, protein and phosopholipid synthesis [16,17], all of which supports the concept of this drug being a multifocal cellular toxicant. This wide range of toxicity against normal cellular processes is probably the reason that pentamidine is lethal to non-dividing cells and also serves as evidence that interaction with DNA is not the only mode of action [18].

The striking similarity of control and pentamidine-treated protein patterns observed in this study also supports the concept that this compound is functioning as a general cell toxicant which attacks numerous metabolic pathways although pentamidine also stimulated the production of a number of specific proteins (Figs. 2 and 4), whose structure and function have yet to be determined. Furthermore, it was clear that LPS caused a significant induction of TNFα and a small induction of IL-1α, both of which were to some degree reduced by the presence of pentamidine. However, TNFα and IL-1α are still secreted (Fig. 1, inset), suggesting that these important cytokines are still produced and this part of the signaling pathway for pulmonary defense is still intact. These cytokine results also suggest pentamidine to be an overall cellular toxicant, rather than a specific inhibitor of these two particular cytokines. Although visible on the gel and confirmed by immunoblotting, IL-1α was too light for densitometric quantitation. Since

these cytokines are important to the immune response it is important that they are not inhibited, and that a patient's treatment regime of pentamidine be so designed that perturbation of normal cellular biochemistry is minimized while the efficacy of the drug is maximized.

Comparative image analysis of the secreted proteins showed a complex series of biochemical changes mostly through stimulation by LPS, although a few proteins were induced by the presence of pentamidine alone.

With the growth of the number of AIDS patients, the clinical literature on the health effects and efficacy of pentamidine for treatment of PCP has presented a broad spectrum of physiological effects. The results of this study are the first presentation of cellular protein patterns of alveolar cells treated with pentamidine. The combination of two-dimensional gel electrophoresis and computerized image analysis has shown specific protein perturbations against a broad background of shared proteins by both normal and pentamidine-treated cells. There appears to be a combination of organ toxicity, which probably accounts for the numerous side effects seen in vivo, coupled with a modulation of a separate subset of proteins some of which are induced and several of which are down-regulated. At the present time, the function of these proteins is unknown. It is, however, important that they be isolated and identified in order to determine their placement in their respective biochemical pathways and to formulate a generalized mechanism of pentamidine cytotoxicity.

Acknowledgements

The authors would like to thank Dr. Gary Rosenthal and Dr. Michael Luster from the Laboratory of Biochemical Risk Analysis, NIEHS for their assistance in the technique for harvesting rat alveolar cells.

References

[1] H. King, E.M. Lourie and W. York, Ann. Trop./Med. Parasitol., 32 (1938) 177.
[2] G. Ivady and L. Paldy, NCI Monographs, 43 (1976) 201.
[3] T.P. Waalkes, C. Denham and V.T. DeVita, Clin. Pharmacol. Ther., 11 (1970) 505.
[4] R.J. Debs, R.M. Straubinger and E.N. Brunette, Am. Rev. Respir. Dis., 135 (1987) 731.
[5] A.B., Montgomery, R.J. Debs and J.M. Luce, Chest, 95 (1989) 747.
[6] J.E. Conte, D. Chernoff, D.W. Feigal, P. Joseph, C. McDonald and J.A. Golden, Ann. Rev. Intern. Med., 113 (1990) 203.
[7] G.W. Soo Hoo, Z. Mohesenifar and R.D. Meyer, Am. Rev. Intern. Med., 113 (1990) 195.
[8] B.A. Merrick, C. He, W.A. Craig, G.C. Clark, E. Corsini, G.J. Rosenthal, B.K. Mansfield and J.K. Selkirk, Appl. Theor. Electrophoresis, 2 (1992) 177.
[9] P. O'Farrell, J. Biol. Chem., 258 (1975) 4007.
[10] B.K. Mansfield, R.C. Mann and J.K. Selkirk, Cancer Res., 48 (1988) 1110.
[11] R. Heathcote, Int. J. Trop. Med. Hyg., 44 (1946) 1.
[12] T.P. Waalkes and D.R. Makalu, NCI Monographs, 43 (1976) 171.
[13] J. Williamson, Pharmacol. Ther., 7 (1979) 445.
[14] R.D. Pearson and E.L. Hewlett, Ann. Intern. Med., 103 (1985) 782.
[15] M.J. Waring, Mol. Pharmaxol., 1 (1965) 1.
[16] W.E. Gutteridge, J. Protozool., 16 (1969) 306.
[17] R.S. Bornstein and J.W. Yarboro, J. Surg. Oncol., 2 (1970) 393.
[18] M. Sands, M.A. Kron and R.B. Brown, Rev. Infect. Dis., 7 (1985) 625.

ELSEVIER

Journal of Chromatography A, 711 (1995) 339–346

JOURNAL OF CHROMATOGRAPHY A

Validation of a capillary electrophoresis method for the determination of cephradine and its related impurities

Paola Emaldi*, Stefano Fapanni, Anna Baldini

Laboratory of Quality Control, ACS Dobfar, viale Addetta, 6, 20067 Tribiano (Milan), Italy

First received 17 November 1994; revised manuscript received 28 April 1995; accepted 28 April 1995

Abstract

A method validation is reported for the determination of the β-lactamic antibiotic cephradine and its main impurity, cephalexin, by micellar electrokinetic chromatography (MEKC) with UV photometric detection. The validation was carried out in compliance with the analytical performance parameters required by the USP XXII. The capillary electrophoresis (CE) method was statistically compared with the HPLC method used in quality control laboratories; the analysis of variance showed no significant difference between the results obtained by the two methods, demonstrating CE to be a suitable alternative technique to HPLC in routine quality control.

1. Introduction

Capillary electrophoresis (CE) is a relatively new but a very promising technique, which was first developed in biological (proteins and nucleic acids) separations, as an evolution of classical electrophoresis. Its importance has grown in recent years in different fields, mainly owing to its advantages over the more commonly used chromatographic techniques, such as high efficiency and selectivity in a short run time, reduced use of organic solvents and ease and low cost of operation.

Although in the last few years many studies of CE applications, using both free solution capillary electrophoresis (FSCE) and micellar electrokinetic chromatography (MEKC), in pharmaceutical analysis have been published [1–4], there have been few investigations on validated methods for routine analysis [5–8].

Pharmaceutical quality control needs analytical methods for the determination of the active component and its related impurities in a matrix which might be relatively complex. We found two interesting separation conditions that have been reported [7,8] for the quantitative analysis of a mixture of cephalosporins by MEKC. When such conditions were applied to the analysis of our bulk products (a powder containing 65% cephradine and 35% arginine or 70% cephradine and (30% sodium carbonate), it was found the migration time was not reproducible on repeated injections. A mixed micellar system was then investigated.

The method reported in this paper for the determination of cephradine and cephalexin was validated following the analytical performance parameters required by the USP XXII; it shows linearity in the range of concentrations consid-

* Corresponding author.

0021-9673/95/$09.50
SSDI 0021-9673(95)00520-X

ered, with a correlation coefficient of 0.999, good precision under repeatable conditions [repeatability (R.S.D. of seven successive injections of a 1 mg/ml standard solution of cephradine) = 0.37%], good day-to-day reproducibility (expressed by the R.S.D. obtained in a recovery trial, which was performed by analysing three pairs of sample solutions at different concentrations on three days; R.S.D. = 0.88%) for UV response, good precision of migration time (R.S.D. = 0.4%) and perfect correspondence with HPLC data, demonstrating CE to be a valuable alternative in pharmaceutical quality control.

2. Experimental

2.1. Instrumentation

Experiments were carried out on a P/ACE System 2050 instrument (Beckman Instruments, Fullerton, CA, USA) equipped with a 30-kV power supply, a UV spectrophotometric detector connected to a data collection system and able to perform both hydrodynamic injection and voltage injection. The detection wavelength was 214 nm.

Separations were performed in a fused-silica capillary (57 cm × 0.075 mm I.D., 50 cm effective length) (Beckman), thermoregulated at 25°C by a liquid coolant (Beckman), with a voltage of 20 kV applied. Hydrodynamic injection was performed at 0.5 p.s.i. for 5 s (corresponding to an injection volume of about 5 nl).

2.2. Standards and reagents

Working standards of cephradine monohydrate and cephalexin were prepared by purification of our products and assayed against the corresponding USP standard.

Disodium hydrogenphosphate was purchased from Merck (Merck-Bracco, Milan, Italy), boric acid from Sigma (Sigma Aldrich, Milan, Italy) and sodium dodecyl sulphate (SDS) and polyoxyethylene lauryl ether (Brij 35) from Merck.

Water used to prepare standard solutions, sample solutions and run buffer was obtained from a Millipore system (Millipore, Vimodrone, Milan, Italy).

Working standard solutions of cephradine and cephalexin were prepared dissolving 50 mg of cephradine monohydrate (potency 93.3%, cephalexin content 2.52%) in 50 ml of deionized water; sample solutions were prepared by dissolving 50 mg of sample powder in 50 ml of deionized water; run buffer solution was prepared by dissolving 122 mg of boric acid, 284 mg of disodium hydrogenphosphate, 1.442 g of SDS and 100 mg of Brij 35 in 100 ml of deionized water.

3. Results and discussion

3.1. Separation of cephradine by MEKC

In order to develop a method for the determination of cephradine, we first tried to resolve a cephradine–cephalexin mixture (cephalexin being the main impurity of cephradine) by FSCE. Using 0.1 *M* borate buffer we could not achieve complete separation either by varying the buffer pH in the range of 6–10 or modifying the applied voltage from 10 to 30 kV.

The great similarity between the two cephalosporin structures (Fig. 1) is responsible for their very similar electrophoretic mobilities, making it very difficult to achieve a satisfactory separation in the FSCE operating mode.

We then applied the conditions suggested by

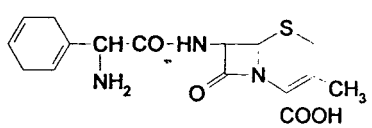

Cephradine

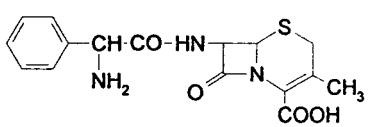

Cephalexin

Fig. 1. Structures of cephradine and cephalexin.

Nishi et al. [7] for the separation of nine cephalosporins by MEKC, i.e., 0.02 *M* borate–phosphate buffer (pH 9) containing 0.15 *M* SDS. Under these conditions, the selectivity was very good.

A very good separation of cephradine and cephalexin was also obtained applying the conditions reported by Sciacchitano et al. [8], who studied the separation of five cephalosporins by MEKC, using a higher concentration (0.2 *M*) of SDS in the buffer (0.02 *M* buffer).

The separation of such similar compounds when a micellar buffer is employed is achieved by the specific partitioning of the analytes between the hydrophobic micelles and the aqueous run buffer (chromatographic effect), resulting in an increased difference in relative mobilities, which improves the separation.

Such high SDS concentrations in the buffer (0.1–0.2 *M*) resulted, of course, in very good selectivity with good repeatability of migration time on repeated injections when a cephradine standard solution was analysed, as shown in Fig. 2. Similar conditions are unsuitable, however, for routine analysis when our products (cephradine buffered with arginine and cephradine buffered with sodium carbonate) are to be analysed.

When repeated injections of a buffered cephradine solution were made, a dramatic drift of the migration times was noticed, with a corresponding broadening of peak width. There was no similar problem when a cephradine standard solution was injected several times. This effect on migration time was interpreted as being due to some interaction between a component of either the buffer (SDS) or the sample (carbonate or arginine) or both and the silica capillary surface, interfering with the separation process. For this reason, the column was rinsed three times between each run with 0.1 *M* NaOH, water and buffer solution to protect the capillary surface from modifications, in compliance with the study of Smith et al. [9], although the rinsing procedure was not effective in improving the reproducibility of migration times, as shown in Fig. 3.

To obtain reproducibility of migration times, fresh buffer should be used in each run, making in impossible to use the autosampler in a routine analysis sequence. We sought to overcome the poor reproducibility by searching for a suitable mixed micellar system (ionic plus non-ionic surfactants) in order to decrease the SDS concentrations without losing selectivity.

Cephradine and cephalexin and all the related impurities were baseline resolved (the resolution factor between cephradine and cephalexin is 2.05), as shown in Fig. 4, when using 0.02 *M* borate–phosphate buffer containing 0.05 *M* SDS and 0.1% Brij 35. The repeatability of migration times is good for up to ten injections, after which the buffer in the run vials must be replaced with some of the buffer previously prepared and stored for this purpose.

3.2. Method validation

We validated our CE method in compliance with the analytical performance parameters required by the USP XXII for HPLC method validation. The following parameters were evaluated: selectivity, migration time precision, area precision, linearity and range, accuracy and comparison with HPLC results for cephradine, precision, linearity, detection limit and quantification limit for cephalexin.

Selectivity

Selectivity is correlated with the resolution factor, defined as

$$R_s = 2 \cdot \frac{t_2 - t_1}{W_2 + W_1}$$

where t = migration time of peaks 1 and 2 and W = width of the peaks measured on the baseline in time units. The resolution factor for cephradine and cephalexin, as already mentioned, was 2.05.

Accuracy and reproducibility

Accuracy and reproducibility were measured by recovery trails, according to the following method. Six standard solutions (St) and six sample solutions (S) of the same batch, two for each of concentrations $a/2$, a and $3/2a$, where a

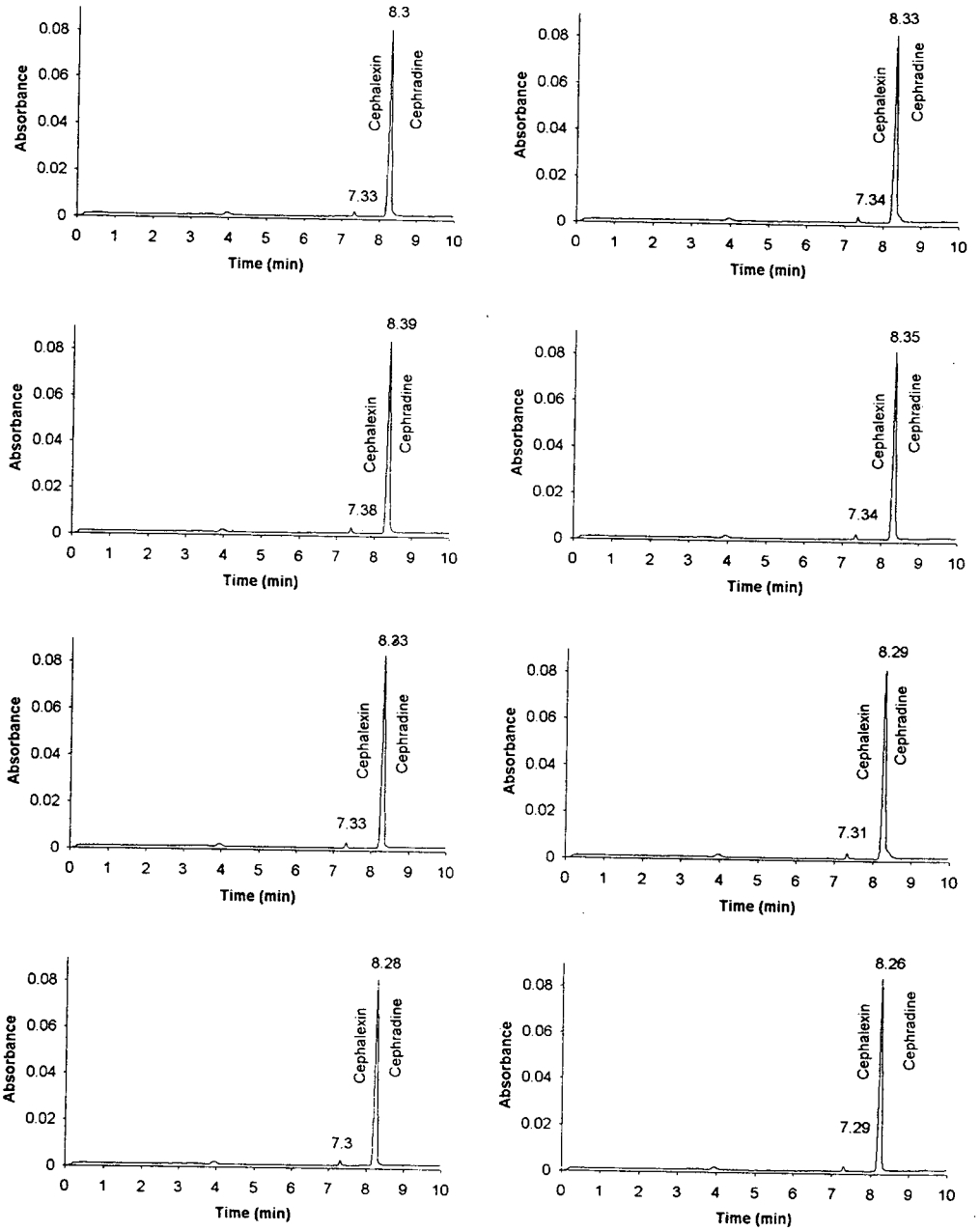

Fig. 2. Chromatogram for repeated injections of cephradine standard solution (1 mg/ml). CE conditions: 0.02 *M* borate–phosphate buffer (pH 9) containing 0.15 *M* SDS, 20 kV, 214 nm.

is the working concentration (1 mg/ml), were prepared on three days and analysed by three analysts with different buffer solutions, in the following orders: $a/2$, St_1–S_1–St_2–S_2; a, St_3–S_3–St_4–S_4; and $3/2a$, St_5–S_5–St_6–S_6. The results are summarized in Table 1 together with the results of the recovery trial.

Accuracy, defined as

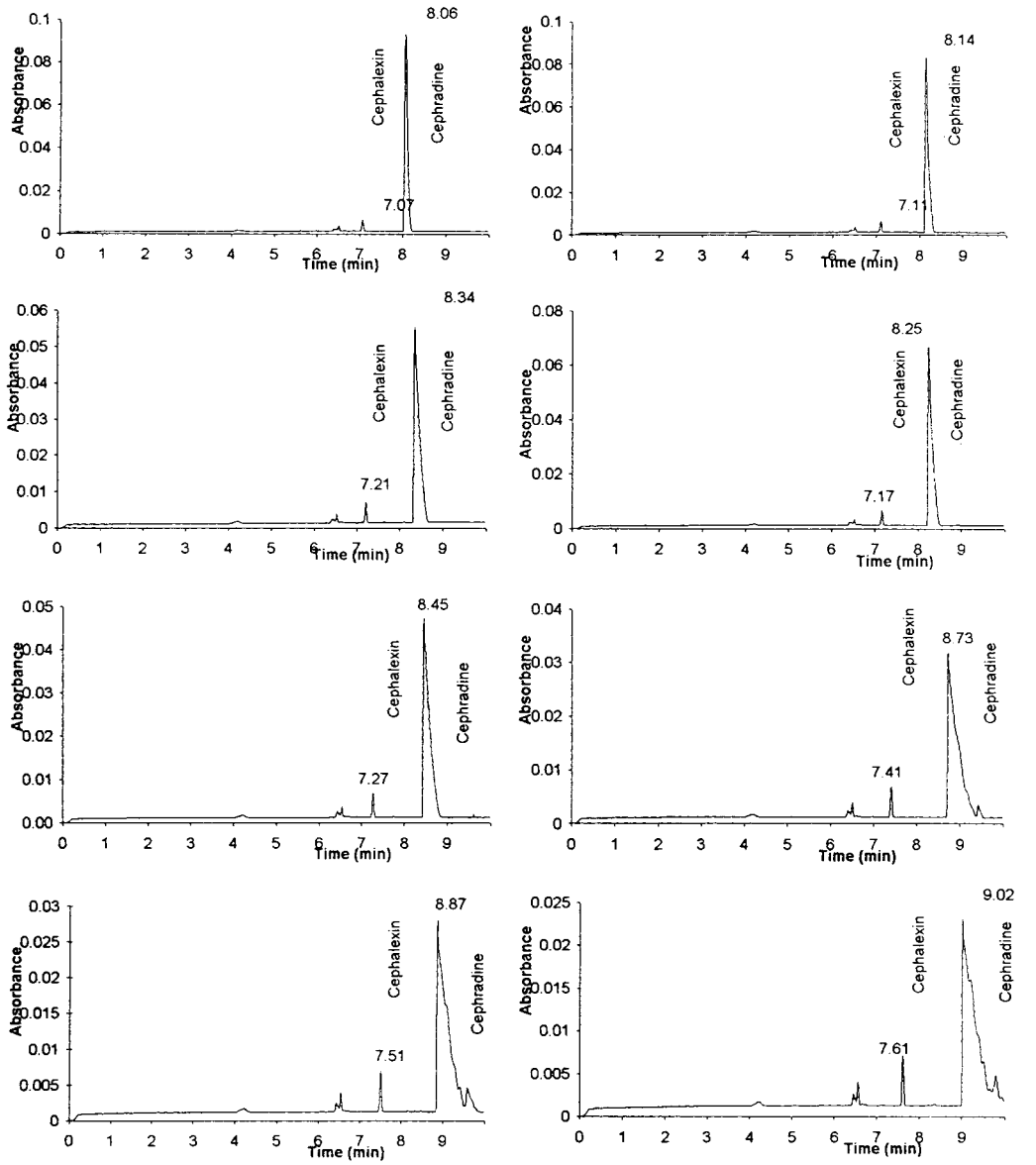

Fig. 3. Chromatogram for repeated injections of cephradine sodium carbonate solution (1 mg/ml), showing the migration time drift and the progressive broadening of cephradine peak. Conditions as in Fig. 2; rinsing between each run.

$$\text{Accuracy} = M \pm (\text{S.D.}/\sqrt{n})t$$

is 70.2 ± 0.31, where M is the mean potency value from recovery testing and Student's t is

$$t(0.05,17) = 2.11$$

The validation was made analysing 18 samples by the t-test so the Student's t is relative to $18 - 1 = 17$ determinations ($P = 0.05$).

The statistical analysis of the means and of the variances showed the homogeneity of the values within the confidence limits of 95%.

The reproducibility is defined by the relative standard deviation (R.S.D.) characteristic of the

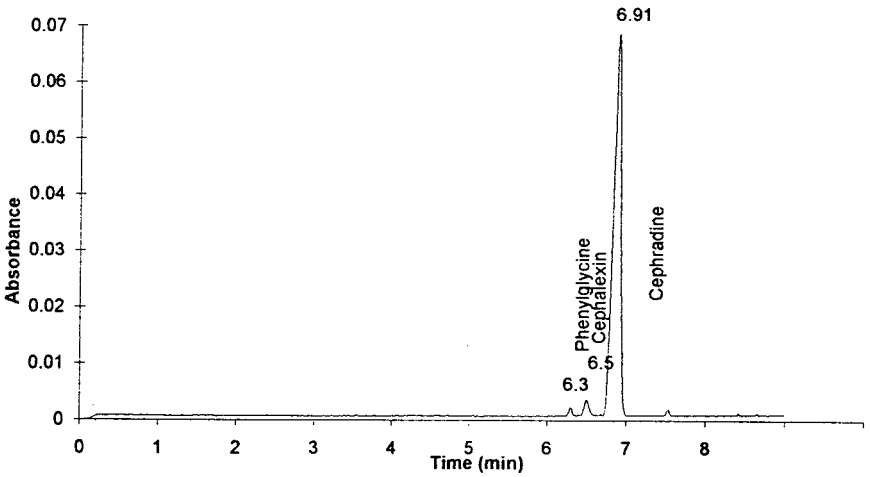

Fig. 4. Chromatogram for a chosen batch of cephradine (1 mg/ml). CE conditions: 0.02 *M* borate–phosphate buffer containing 0.05 *M* SDS and 0.1% Brij 35.

method; the R.S.D. was obtained from the recovery trial and was found to be 0.88%.

Linearity and repeatability

To evaluate the linearity, three solutions of cephradine were prepared and analysed. A solution having the working concentration (1 mg/ml) was prepared; this solution was named *a*. Three solutions having concentrations of 1.5*a*, *a* and *a*/2 were prepared.

Each of these solutions was injected seven times starting from the least to the most concentrated. Successively, the area values obtained were analysed using EXCEL software to evaluate the correlation coefficient (*r*), standard deviation (S.D.) within solutions, sensitivity (slope), intercept, limit of detection (LOD) and limit of quantification (LOQ). The same operations as used to evaluate cephradine linearity were repeated for cephalexin, but the concentrations of the solutions were in this case 2.52% of the working concentration *a* (1 mg/ml of cephradine), 1.26% *a* and 3.75% of *a*. The results are given in Table 2.

The detection limit [signal-to-noise ratio (S/N) = 3] for cephalexin is 0.526 μg/ml and the quantification limit (S/N = 10) is 1.752 μg/ml. Detection limit is defined by LOD = S.D. (area

Table 1
Reproducibility, accuracy and results of recovery tests

Sample concentration	Potency (%)					Average recovery (%)
	Day 1	Day 2	Day 3	Average	R.S.D. (%)	
a/2	70.91	69.18	70.27	70.1	1.0476	99.8
a/2	70.10	69.27	70.79			
a	69.98	70.37	70.88	70.3	0.7221	100.2
a	69.50	70.63	70.62			
3/2*a*	70.90	69.59	69.68	70.3	0.8623	100.1
3/2*a*	69.86	70.53	70.90			
Pooled				70.2	0.8773	100.03

Reproducibility = 0.88%; accuracy = 70.2 ± 0.31%.

Table 2
Repeatability and linearity regression data for cephradine and cephalexin

Product	Repeatability		LOD (μg/ml)	LOQ (μg/ml)	Linearity			
	Area R.S.D. (%)	Migration time R.S.D. (%)			Slope	Correlation coefficient	Range (mg/ml)	Intercept
Cephradine	0.37	0.4			8.99	0.9996	0.5–1.5	0.091
Cephalexin	0.56		0.526	1.752	15.33	0.9993	0.01–0.04	−0.001

corresponding to the lower concentration of the range − blank area) · 3/slope. The quantification limit is defined by LOQ = S.D. (area corresponding to the lower concentration of the range − blank area) · 10/slope.

The R.S.D. of the areas was calculated for the three concentrations. The repeatability value which is characteristic of the method is that relative to solution *a* and was found to be 0.37% for cephradine and 0.56% for cephalexin.

The R.S.D. of the migration time was measured for 23 repeated injections of cephradine buffered with sodium carbonate and was found to be ·0.4%. Fresh buffer was used after each sequence of ten injections.

Comparison with HPLC results

Nine batches of cephradine buffered with sodium carbonate were analysed by both the traditional HPLC method and MEKC. In both methods a working standard solution (1 mg/ml) was injected first, followed by a sequence of a maximum of five sample solutions (1 mg/ml) and the series of analyses was repeated twice. The results are reported in Table 3.

From these data, the mean and the R.S.D.

Table 3
Comparison of HPLC and CE assays for cephradine buffered with sodium carbonate, with results of the variance analysis

Day	Batch No.	HPLC: Mean potency (%)	CE				Difference, HPLC–CE (%)
			Determination I	Determination II	Mean potency (%)	Difference, I − II (%)	
1	057/4	73.46	72.96	74.05	73.51	−1.48	−0.05
2	064/4	74.17	72.39	72.23	72.31	0.22	1.86
2	065/4	73.20	72.47	71.71	72.09	1.05	1.11
2	066/4	73.57	72.23	71.80	72.02	0.60	1.55
2	067/4	72.49	73.23	72.80	73.02	0.59	−0.53
3	055/4	75.25	74.04	73.49	73.77	0.75	1.49
3	058/4	71.80	71.17	71.22	71.20	−0.07	0.61
3	059/4	74.0	72.22	73.56	72.89	−1.84	1.11
3	060/4	70.40	69.21	70.37	69.79	−1.66	0.61
Mean		73.15			72.29		0.86
S.D.		1.43			1.23		
R.S.D.		1.95			1.70		
Variance		2.0336			1.5128		
F (calc.)		0.74					
F (tab.)		4.45					
t (calc.)		1.370					
t (tab.)		2.11					

were calculated and an analysis of variance was performed, showing no significant difference (at the 95% confidence limits) between the results obtained with the two methods, with t (calculated) $< t$ (tabulated) and F (calculated) $< F$ (tabulated).

4. Conclusions

CE was evaluated to determine its suitability for β-lactam antibiotic analysis in routine quality control. The method reported for the determination of cephradine by MEKC was validated in compliance with the USP XXII analytical performance parameters. All required statistical parameters were respected. The resolution between the main peak and the related impurities was greater than 2. The detector response was linear in the considered range (correlation coefficient 0.999). The R.S.D. was less than 2% (0.4% for both areas and migration times).

The values obtained with our CE method and those obtained by the validated HPLC method were not significantly different. This validation demonstrates that CE may be a valuable alternative technique to HPLC in pharmaceutical quality control.

References

[1] S. K. Yeo, H.K. Lee and S.F.Y. Li, J. Chromatogr., 585 (1991) 133–137.
[2] C.X. Zhang, Z.P. Sun, D.K. Ling and Y.J. Zhang, J. Chromatogr., 627 (1992) 281–286.
[3] M.T. Ackermans, J.L. Beckers, F.M. Everaerts and I.G.J.A. Seelen, J. Chromatogr., 590 (1992) 341–353.
[4] M. Heuermann and G. Blaschke, J. Chromatogr., 648 (1993) 267–274.
[5] K.D. Altria, A.R. Walsh and N.W. Smith, J. Chromatogr., 645 (1993) 193–196.
[6] K.D. Altria and J.L. Chanter, J. Chromatogr. A, 652 (1993) 459–463.
[7] H. Nishi, N. Tsumagari, T. Kakimoto and S. Terabe, J. Chromatogr., 477 (1989) 259–270.
[8] C.J. Sciacchitano, B. Mopper and J.J. Specchio, J. Chromatogr. B, 657 (1994) 395–399.
[9] S.C. Smith, J.K. Strasters and M.G. Khaledi, J. Chromatogr., 559 (1991) 57–68.

ELSEVIER

Journal of Chromatography A, 711 (1995) 347–352

JOURNAL OF CHROMATOGRAPHY A

Short communication

Separation of sulfur containing chemical warfare related compounds in aqueous samples by micellar electrokinetic chromatography

Richard L. Cheicante[a], John R. Stuff[a,*], H. Dupont Durst[b]

[a]*EAI Corporation, 1308 Continental Drive, Abingdon, MD 21009, USA*

[b]*Army Material Command Treaty Laboratory, Edgewood, MD 21005, USA*

First received 27 December 1994; revised manuscript received 29 March 1995; accepted 1 May 1995

Abstract

A method is described in which micellar electrokinetic chromatography (MEKC) is used to separate thiodiglycol, 2,2′-sulfinyldiethanol, 1,4-dithiane, 1,4-thioxane, O-isobutyl methylphosphonothioic acid and O-ethyl methylphosphonothioic acid in aqueous samples. Detection limits range from 1 to 10 μg/ml and the calibration curves are linear over two orders of magnitude. The compounds are separated in under 10 min. The method fulfills our requirements for a rapid, on-site screening technique for these compounds.

1. Introduction

A treaty to ban the use, production and storage of chemical warfare (CW) agents is currently under review by many countries [1]. The treaty calls for destruction of all stockpiles within ten years of ratification. There are also provisions within the treaty for challenge inspections including allegations of use, production, storage and monitoring of destruction. These provisions will require on-site analytical methods for the verification of treaty-related activities. Methods for the detection of CW agents, precursors, manufacturing byproducts and degradation products will be required. Several of these compounds, thiodiglycol, 2,2′-sulfinyldiethanol, 1,4-dithiane, 1,4-thioxane, O-isobutyl methylphosphonothioic acid and O-ethyl methylphosphonothioic acid, contain a sulfur atom which makes them amenable to direct detection with UV spectroscopy.

Our current on-site method [2] for the detection of these compounds in aqueous samples uses a methylene chloride extraction followed by a concentration step or solid-phase extraction/elution and derivitization. The samples are then analyzed by gas chromatography–mass spectrometry (GC–MS). This preparation and analysis are time-consuming. The current goal of our research is to be able to identify these compounds in aqueous samples at a level of 10 μg/ml. Quantitation is not a requirement for on-site analysis, but is used in other work being conducted in our laboratory. One focus of our research is to develop on-site screening methods which are fast and require little sample prepara-

* Corresponding author.

0021-9673/95/$09.50
SSDI 0021-9673(95)00524-2

tion. Screening methods alone do not provide definitive compound identification which is a requirement for treaty-related inspections. During an inspection, time is the limiting factor. Screening methods are used to prioritze samples for further analysis by GC–MS. Among the options being explored are ion chromatography, micro high-performance liquid chromatography and capillary electrophoresis. Capillary electrophoresis is unique because it requires little sample volume, produces fast, high efficiency separations, is flexible in terms of various types of separation techniques which can be performed and used to identify different types of compounds (e.g. free zone, gel and MEKC), generates little waste and can be easily transported. The use of capillary electrophoresis for the separation of some CW-related compounds has been reported [3–5].

MEKC was first described by Terabe and coworkers [6–8]. MEKC is a branch of capillary electrophoresis in which a surfactant is added, above its critical micelle concentration, to the running buffer. The formation of micelles allows the separation of both neutral and charged species. Compounds partition between the micelles and the buffer solution contained within a capillary column. Negatively charged micelles migrate towards the anode under the influence of an electric field which is produced when a voltage is applied across the capillary. The bulk flow, called the electroosmotic flow (EOF), is a consequence of surface charge on the interior wall of the capillary. The direction of the EOF is towards the cathode and is generally greater than the migration velocity of the micelles. Therefore, the net movement of species is towards the cathode. Migration times for neutral species are based upon the amount of time analytes spend partitioned into the micelles. Recent reviews of MEKC have been published [9–11].

This study focuses on the application of MEKC to the separation of thiodiglycol (TDG), 2,2′-sulfinyldiethanol (TDGO), 1,4-dithiane, 1,4-thioxane, O-isobutyl methylphosphonothioic acid (IBMPSA) and O-ethyl methylphosphonothioic acid (EMPSA) in aqueous samples with direct UV detection.

2. Experimental

2.1. Chemicals

Boric acid, β-cyclodextrin, acetonitrile, monobasic sodium phosphate, methanol, thiodiglycol, 1,4-dithiane, 1,4-thioxane and 2,2′-sulfinyldiethanol were obtained from Sigma-Aldrich (Milwaukee, WI, USA). Sodium dodecylsulfate (SDS) was obtained from Fluka (Ronkonkoma, NY, USA). O-Isobutyl methyl-phosphonothioic acid and O-ethyl methylphosphonothioic acid were obtained from Edgewood Research, Development and Engineering Center (Edgewood, MD, USA). Distilled, deionized water (18 MΩ was generated internally from a Barnstead (Dubuque, IA, USA) Nanopure system.

2.2. Apparatus

MEKC experiments were performed using a P/ACE 2100 system (Beckman, Columbia, MD, USA), at 15 kV. The temperature was thermostated at 25°C. A fused-silica capillary with an effective length of 50 cm, total length 57 cm, and 75 μm I.D. was used for all separations. Injections were hydrodynamic for 3 s. Detection was by a single-wavelength UV (deuterium lamp) detector set at 200 nm.

2.3. Procedures

The most significant separation problem was the resolution of the closely related species, TDG and TDGO. Composition of the buffer system was optimized in terms of concentration of SDS, borate, organic modifier (methanol), cyclodextrin and use of another buffer system, phosphate, in order to achieve baseline resolution and best detection of these components. The initial buffer composition chosen was 10 m*M* borate and 50 m*M* SDS at pH 9. The buffer was prepared by dissolution of boric acid and SDS in 18 MΩ, distilled, deionized water. The pH of the solution was adjusted to 9 with 10% (w/w) NaOH.

3. Results and discussion

In order to optimize the separation of TDG and TDGO, we added methanol as an organic modifier. Kaneta et al. [12] showed that acetonitrile and dimethylformamide were effective modifiers for improving the resolution of hydrophobic species, while methanol was better for less hydrophobic compounds. Methanol increases the viscosity of the solution, thus slowing the electroosmotic flow and extending the elution range of the buffer system. Janini et al. [13] showed that the electroosmotic mobility is mainly influenced by buffer viscosity and that other factors such as dielectric constant, zeta potential, and modifier–capillary wall interactions are significant at trace levels of modifier, but diminish as the concentration of modifier increases. In our system, we found that as the methanol concentration increased, the elution times for TDG and TDGO also increased, as expected, but the resolution decreased. The addition of the organic modifier not only affects the elution range, but can also alter the distribution of analytes between the micelles and buffer solution. The addition of MeOH to our system enhances the concentration of the analytes in the buffer relative to the micelles thereby lowering the resolution. A more detailed discussion of the addition of organic modifiers is given in Refs. [12,13].

The addition of other modifiers, such as acetonitrile and β-cyclodextrin, did not enhance the resolution or detection of these compounds.

The last variable changed was the concentration of the surfactant. The optimum resolution occured at an SDS concentration of 100 mM. Concentrations above 125 mM SDS produced too high a current which leads to increased Joule heating.

The use of phosphate (pH 7, 100 mM SDS, 10 mM phosphate) as the buffer did not enhance

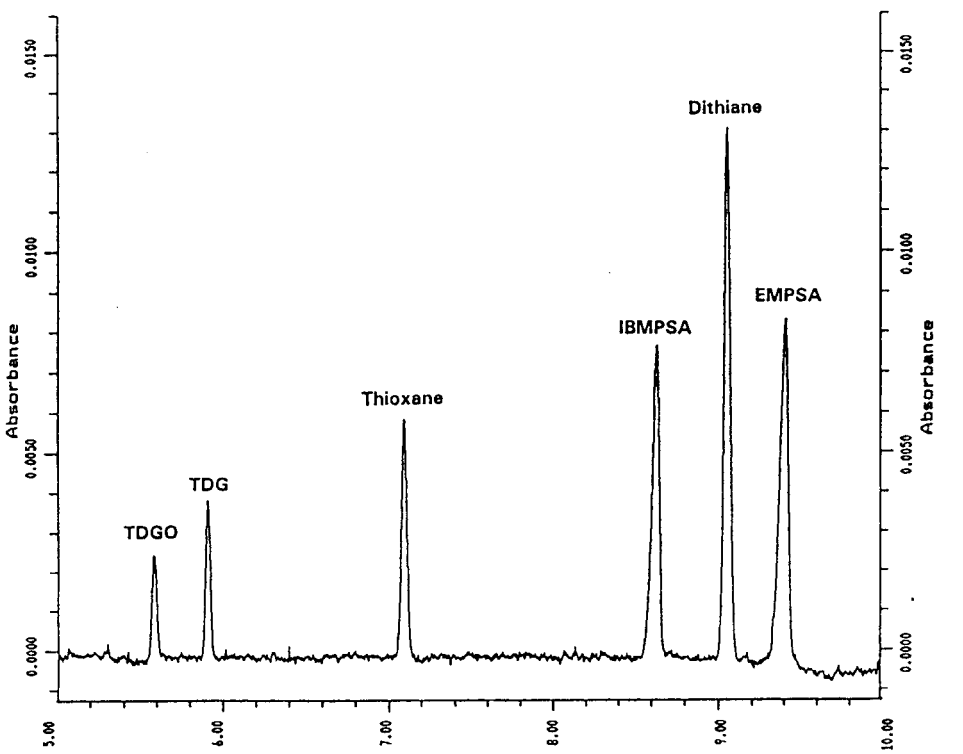

Fig. 1. Electropherogram of the six analytes at 50 μg/ml. Buffer is 10 mM borate/100 mM SDS at pH 9.0. Separation at 25 kV and 25°C.

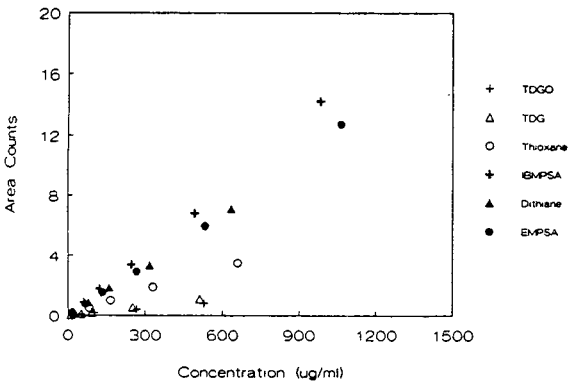

Fig. 2. Calibration curves for the six analytes.

the separation and led to a decrease in the response of the analytes.

An electropherogram of the six compounds of interest is shown in Fig. 1. The compounds are all baseline resolved. Calibration curves for the six compounds are shown in Fig. 2. The plots are linear over two orders of magnitude with correlation coefficients of 0.999 or better. The precision of the method, in terms of area count and migration time reproducibility, along with limits of detection are given in Table 1. The precision for migration times and area counts are all less than 5% except for IBMPSA which is 6.6% (area count). The detection limits, based on a signal-to-noise ratio of 3:1, are well within our goal of 1–10 ppm for this method.

The separation of the neutral species is based on a partitioning between the micelles and the buffer solution. Those compounds which are most hydrophobic spend more time in the micelles. The negatively charged micelles migrate towards the anode against the EOF, however, their net movement is towards the cathode since the magnitude of the EOF is greater than their mobility. Therefore, the more hydrophobic the compound, the longer the migration time. This is shown in Fig. 1 as the order of elution for the neutral species is TDGO, TDG, 1,4-thioxane, and 1,4-dithiane. The separation of ionic compounds, like IBMPSA and EMPSA, is based on a combination of free zone and micellar mechanisms [9].

Environmental samples were collected from the Edgewood Area of Aberdeen Proving Ground, MD, USA. They were spiked and run by MEKC. Fig. 3 shows typical electropherograms of a blank and a spiked sample. All six compounds are easily identified.

4. Conclusion

Micellar electrokinetic chromatography with UV detection serves as a useful screening method for the separation of sulfur-containing chemical warfare related compounds. The method is rapid and sensitive (meets our requirement of 10 μg/ml), requires little or no sample preparation, uses little sample volume and generates minimal waste. The method could easily be adapted to on-site analysis. Currently, we are using this method in the laboratory to screen aqueous samples and aqueous extracts of soils and other

Table 1
Statistical data

Compound	Correlation coefficient	Detection limit (μg/ml)	Precision[a] (area count)	Precision[a] (migration time)
TDGO	0.9999	10	3.2	0.21
TDG	0.9999	10	2.9	0.26
Thioxane	0.9985	8.0	3.6	0.18
IBMPSA	0.9997	1.7	6.6	0.24
Dithiane	0.9992	4.1	4.2	2.5
EMPSA	0.9995	2.5	3.8	2.7

[a] $n = 5$.

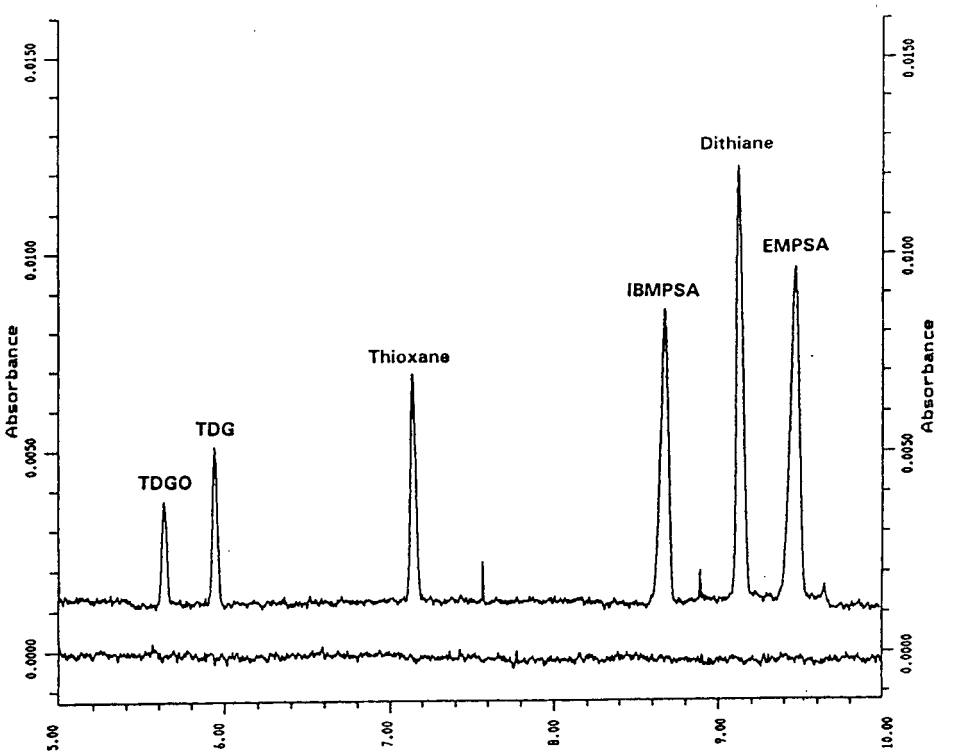

Fig. 3. Environmental water sample analysis using MEKC with sample blank (lower) and laboratory spiked sample (upper). Buffer is 10 m*M* borate/100 m*M* SDS at pH 9.0. Separation at 25 kV and 25°C.

solid samples for these compounds. Future research will be on making our CE instrumentation field portable.

Acknowledgements

The authors would like to thank Dennis Reutter and Lynn Hoffland of the Army Materials Command Treaty Laboratory for funding at ERDEC under contract #DAA15-91-0019.

References

[1] Convention on the Prohibition of the Development, Production, Stockpiling, and Use of Chemical Weapons and on their Destruction, United States Control and Disarmament Agency, Washington, D.C., 1993.

[2] On-Site Sample Preparation Method for Soil, Water, and Wipe Samples for the Qualitative Determination of Chemical Warfare (CW) Related Compounds, U.S. Army Chemical and Biological Defense Command, Treaty Assistance Directorate, APG, MD, USA, unpublished results.

[3] G.A. Pianetti, M. Taverna, A. Baillet, G. Mahuzier and D. Baylocq-Ferrier, J. Chromatogr., 630 (1993) 371.

[4] W.H. Robins and B.W. Wright, Capillary Electrophoresis Methods for the Determination of Chemical Warfare Agent Degradation Products, Pacific Northwest Laboratory, 1993.

[5] R.L. Cheicante, Capillary Electrophoretic Techniques Used in the 1st Provisional Technical Secretariat Interlaboratory Comparison Test, presented at Scientific Conference on Chemical and Biological Defense Research, APG, MD, November 1994.

[6] S. Terabe, K. Otsuka, K. Ichikawa, A. Tsuchiya and T. Ando, Anal. Chem., 56 (1984) 111.

[7] S. Terabe, K. Otsuka and T. Ando, Anal. Chem., 57 (1985) 834.

[8] Micellar Electrokinetic Chromatography, S. Terabe, Manual #266924, Beckman Instruments, Fullerton, CA, USA, 1992.

[9] S. Terabe, N. Chen and K. Otsuka, Adv. Electrophoresis, 7 (1994) 87.
[10] C.A. Monnig and R.T. Kennedy, Anal. Chem., 66 (1994) 280R.
[11] W. Kuhr and C.A. Monnig, Anal. Chem., 64 (1992) 389–407R.
[12] T. Kaneta, T. Yamashita and T. Imasaka, Electrophoresis, 15 (1994) 1276.
[13] G.M. Janini, K.C. Chan, J.A. Barnes, G.M. Muschik and H.J. Issaq, Chromatographia, 35 (1993) 497.

Author Index Vol. 711

PUBLICATION SCHEDULE FOR THE 1995 SUBSCRIPTION

Journal of Chromatography A and *Journal of Chromatography B: Biomedical Applications*

MONTH	1994	J–J[a]	A	S	O	N	D	
Journal of Chromatography A	Vols. 683–688	689–708/1	708/2 709/1 709/2 710/1	710/2 711/1 711/2	712/1 712/2			The publication schedule for further issues will be published later.
Bibliography Section		713		714/1			714/2	
Journal of Chromatography B: Biomedical Applications		663–669	670/1 670/2	671/1 + 2	672/1 672/2	673/1 673/2	674/1 674/2	

[a] Vol. 701 (Cumulative Indexes Vols. 652–700) expected in December.

INFORMATION FOR AUTHORS

(Detailed *Instructions to Authors* were published in *J. Chromatogr. A*, Vol. 657, pp. 463–469. A free reprint can be obtained by application to the publisher, Elsevier Science B.V., P.O. Box 330, 1000 AH Amsterdam, Netherlands.)

Types of Contributions. The following types of papers are published: Regular research papers (full-length papers), Review articles, Short Communications and Discussions. Short Communications are usually descriptions of short investigations, or they can report minor technical improvements of previously published procedures; they reflect the same quality of research as full-length papers, but should preferably not exceed five printed pages. Discussions (one or two pages) should explain, amplify, correct or otherwise comment substantively upon an article recently published in the journal. For Review articles, see inside front cover under Submission of Papers.

Submission. Every paper must be accompanied by a letter from the senior author, stating that he/she is submitting the paper for publication in the *Journal of Chromatography A* or *B*.

Manuscripts. Manuscripts should be typed in **double spacing** on consecutively numbered pages of uniform size. The manuscript should be preceded by a sheet of manuscript paper carrying the title of the paper and the name and full postal address of the person to whom the proofs are to be sent. As a rule, papers should be divided into sections, headed by a caption (*e.g.*, Abstract, Introduction, Experimental, Results, Discussion, etc.). All illustrations, photographs, tables, etc., should be on separate sheets.

Abstract. All articles should have an abstract of 50–100 words which clearly and briefly indicates what is new, different and significant. No references should be given.

Introduction. Every paper must have a concise introduction mentioning what has been done before on the topic described, and stating clearly what is new in the paper now submitted.

Experimental conditions should preferably be given on a *separate* sheet, headed "Conditions". These conditions will, if appropriate, be printed in a block, directly following the heading "Experimental".

Illustrations. The figures should be submitted in a form suitable for reproduction, drawn in Indian ink on drawing or tracing paper. Each illustration should have a caption, all the *captions* being typed (with double spacing) together on a *separate sheet*. If structures are given in the text, the original drawings should be provided. Coloured illustrations are reproduced at the author's expense, the cost being determined by the number of pages and by the number of colours needed. The written permission of the author and publisher must be obtained for the use of any figure already published. Its source must be indicated in the legend.

References. References should be numbered in the order in which they are cited in the text, and listed in numerical sequence on a separate sheet at the end of the article. Please check a recent issue for the layout of the reference list. Abbreviations for the titles of journals should follow the system used by *Chemical Abstracts*. Articles not yet published should be given as "in press" (journal should be specified), "submitted for publication" (journal should be specified), "in preparation" or "personal communication".

Vols. 1–651 of the *Journal of Chromatography*; *Journal of Chromatography, Biomedical Applications* and *Journal of Chromatography, Symposium Volumes* should be cited as *J. Chromatogr.* From Vol. 652 on, *Journal of Chromatography A* (incl. Symposium Volumes) should be cited as *J. Chromatogr. A* and *Journal of Chromatography B: Biomedical Applications* as *J. Chromatogr. B*.

Dispatch. Before sending the manuscript to the Editor please check that the envelope contains four copies of the paper complete with references, captions and figures. One of the sets of figures must be the originals suitable for direct reproduction. Please also ensure that permission to publish has been obtained from your institute.

Proofs. One set of proofs will be sent to the author to be carefully checked for printer's errors. Corrections must be restricted to instances in which the proof is at variance with the manuscript.

Reprints. Fifty reprints will be supplied free of charge. Additional reprints can be ordered by the authors. An order form containing price quotations will be sent to the authors together with the proofs of their article.

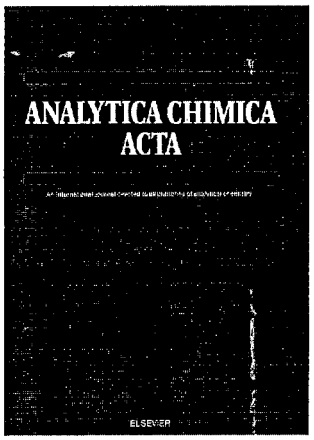

ANALYTICA CHIMICA ACTA

An International Journal Devoted to All Branches of Analytical Chemistry

Editors

Aims and Scope

Analytica Chimica Acta publishes the highest quality refereed research papers, reviews and preliminary communications covering all aspects of analytical science, and particularly those areas at the forefront of analytical development. **Full Author, Subject and Technique Indexes** are provided every 10 and 50 volumes.

Audience

Chemists (all disciplines) in academic institutions, industry, independent laboratories and consulting firms.

Abstracted/Indexed in

Aluminum Abstracts, Analytical Abstracts, BIOSIS, Biological Abstracts, Chemical Abstracts, Current Contents: Physical, Chemical & Earth Sciences, EMBASE, Engineered Materials Abstracts, Index Medicus, Mass Spectrometry Bulletin, Material Business Alert, Metals Abstracts, Science Citation Index.

1995 Subscription Data

Volumes 297-314 (in 54 issues)
Subscription price: Dfl. 6804.00 (US$ 3581.00)
ISSN 0003-2670

Elsevier Science B.V.
P.O. Box 211
1000 AE Amsterdam
The Netherlands
Fax: +31 (20) 485 3598

In the USA and Canada:
P.O. Box 945
New York
NY 10159-0945, USA
Fax: +1 (212) 633 3680

I would like ☐ a free sample copy of **Analytica Chimica Acta.**
☐ Instructions to Authors.
☐ to enter a subscription for 1995.
Please send me a Proforma Invoice.

Name .....
Address .....
.....
.....

The Dutch Guilder price (Dfl.) applies worldwide except in the Americas (North, Central and South America). US$ price quoted applies in the Americas only. Customers in the European Community should add the appropriate VAT rate applicable in their country to the price(s).